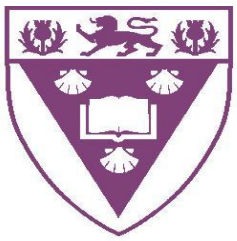

RHODES UNIVERSITY

Grahamstown • 6140 • South Africa

# GEOCHEMICAL EXPLORATION FOR COPPER - COBALT IN THE DEMOCRATIC REPUBLIC OF CONGO, CENTRAL AFRICAN COPPERBELT: A CASE STUDY ON PR851


By

**Paul Katombe Kisumbule**


A thesis submitted in fulfillment of the requirements for the degree of

MASTER OF SCIENCE
(Exploration Geology Coursework and Thesis)

Supervisor: Professor Dr. Stephen A. Prevec


MSc Exploration Geology Program in 2014
Geology Department
Rhodes University
P.O. Box 94
Grahamstown 6140
South Africa


31 October 2014

**DECLARATION**

I, Paul Katombe Kisumbule, declare that this thesis is my own work and any authors have been acknowledged accordingly. It is being submitted in fulfillment of the Degree of Master of Science in Exploration Geology at Rhodes University, Grahamstown, and has not been submitted before for the examination of any degree through any other tertiary institution or university.

**Signature of the candidate**……

Mr. Paul Katombe Kisumbule

Signed on the 31st day of October 2014 at Rhodes University, Grahamstown / Eastern Cape / Republic of South Africa

**ACKNOWLEDGEMENTS**

This scientific work was made possible by the support of First Quantum Minerals Ltd and the gracious authorization of the Zambia exploration manager Mr. Doug Jack. I would like to acknowledge the following people or group of people for their support towards the successful completion of this thesis:

My supervisor, Head of Exploration Geology Department Professor Stephen A. Prevec for his professional mentoring, advice, suggestions and comments. I hereby express my gratitude for bearing with me up to the approval of this thesis,

Mrs. Ashley Goddard for her necessary administrative and logistical supports when coming to Rhodes University and during my time in Grahamstown,

The entire academic staff in the Department of Geology at Rhodes University for their high standard lectures during the all coursework program,

All the CoMiSa SPRL Exploration teams including but not limited to the Former Democratic Republic of Congo Exploration Manager Mr. Michael John Parker and my fellow exploration geologists who contributed at all levels during the greenfield exploration campaign in the Democratic Republic of Congo together with myself to collect and make available some of the geoscientific data used in this thesis,

My lovely wife Marie Kayowa Katombe for her continuous prayers, words of encouragement and affection that showed sense of belonging,

My daughter Precieuse Bishimba Kisumbule for her unforgettable pure smiles that brighten my heart and pushed me moving extra miles forward,

My family, and in particular my deceased father Maurice Kasongo Kisumbule for the warm support, prayers and encouragement through the entire process of my study career since i started up to this level. Father i wish if you could be able to see this achievement of the hard work of education you started in my life. May your soul rest in peace,

And above all, the Source of my power, the Almighty God, the Creator of the entire universe.

**DEDICATION**

I dedicate this work to my wife Marie Kayowa Katombe, my first born Precieuse Bishimba Kisumbule and the rest of my family for their dedicated support and endurance during my absence while attending my MSc Exploration Geology course program at Rhodes University.

**ABSTRACT**

The PR851 licence area is located at about 80 km west from the town of Likasi in the district of Haut-Katanga and 175 km north-west of Lubumbashi, the capital city of Katanga Province in the Democratic Republic of Congo. The exploration licence was granted by the government of the Democratic Republic of Congo to First Quantum Minerals Ltd through its Congolese subsidiary Compagnie Minière de Sakania Sprl (CoMiSa Sprl) under certificate N° CAMI/CR/70/2003 on the 10th of October 2003 for a period of 5 years with a possibility of renewal for 3 years in respect to the new Congolese mining code.

The PR851 area lies on fragments of Mines Subgroup rocks of the Roan Group in the Congolese Copperbelt where most of the Cu-Co and stratiform-stratabound deposits such as Kipushi, Ruashi-Etoile, Kinsevere, Kipoi, Luishya, Luswishi, Shituru, Kamoya, Kambove, Tenke-Fungurume, Shinkolobwe, Swambo, Mindingi and Kamoto among others are found.

During the 20th century, the Union Minière du Haut Katanga (U.M.H.K.) undertook mineral exploration in the Congolese Copperbelt and numerous copper- and cobalt-occurrences were identified (for instance Kibamba copper occurrence in PR851 area).

From 2003, the Compagnie Minière de Sakania Sprl initiated a grassroots exploration program in PR851 area and geochemical exploration survey as one of the mineral exploration tools was implemented to aim at detecting copper and cobalt concentration in soil. The B horizon of the thick tropical soil in the area was sampled and soil samples were sent to Genalysis laboratories in Johannesburg, Republic of South Africa for main chemical analysis of Cu and Co only, whereas 10% of analyzed samples were dispatched to Perth, Western Australia for quality control analysis. Thresholds for anomalies of copper and cobalt were defined by literature comparison, standard deviations and spatial analysis. The anomalies were tested at a later stage by reverse circulation / diamond drilling during the year of 2005 to 2008 and the Cu-Co resources were estimated by Digital Mining Services of Harare, Zimbabwe in the year of 2008.

Geological logging of chips from reverse circulation and diamond drill cores revealed that copper mineralization is represented by malachite, chrysocolla, chalcopyrite and bornite whereas cobalt mineralization appeared in form of heterogenite.

The source of supergene mineralization remains unknown. Recommendations have been made to undertake more geological exploration work in order to fully investigate the geological setting and structural architecture of the region, which may result in a better understanding of the Cu-Co mineralization system and ore genesis. The latter has been no consensus up-to-date and different

theories have been proposed to discuss the ore genesis, including syn- and dia- genetic, synorogenic and sulphide remobilization to late-to-post- orogenic Cu-Zn-Pb Kipushi-type deposit. However, geological observations favored that the diagenetic and syngenetic models are applicable to numerous deposits in the Central African Copperbelt.

***Keywords:*** *PR851 area, Congolese Copperbelt, Cu-Co mineralization, Ore genesis, Geochemical exploration survey, Cu-Co assays, Cu-Co resource estimates*

**TABLE OF CONTENTS**

## LIST OF FIGURES

## LIST OF TABLES

# CHAPTER 1: INTRODUCTION

## 1.1. Background

The important world-class stratiform and stratabound deposits such as Cu, Co, Zn, Pb, U, Au and iron ore among others are hosted in the Neoproterozoic Katangan Belt wich sedimentation started in a continental Roan rift basin after ~ 880 Ma (Armstrong et al., 2005) and extends from eastern Angola, the Katanga Province in the South-East of the Democratic Republic of Congo to the North-West of the Republic of Zambia (Hitzman et al., 2012; Robert, 1956 and Mendelson, 1961). This belt is also known as the Central African Copper Belt which is about 800 kilometres long (Laznicka, P., 2010), almost 150 kilometres wide with 5km to 10km thick sediments (GECO Project, 2009). The rocks in the Neoproterozoic Katangan Belt are grouped as the Katangan Supergroup, comprising three Groups, namely from the bottom to the top (Cailteux, 2003):

- Roan Group, which includes initial rift-stage clastic rocks, postrift evaporitic carbonate rocks, second rifting-stage clastic rocks, mafic igneous flows and sills;
- Nguba Group, which includes at its base a regional marker, the glaciogenic Grand Conglomérat; and the
- Kundelungu Group, which commences with a glaciogenic unit as well, the Petit Conglomérat (Selley et al., 2005 cited by Hitzman, M. W. et al., 2012).

The Roan Group is the base of the Katangan succession and it has been subjected to more detailed studies on lithostratigraphy, petrography, geochemistry, metallogeny and others because of its economic value by hosting Cu-Co mineralization (Wendorff, 2000; Cailteux, 2003; Cailteux et al., 1994; Francois, 1987, 1993 and 1995 cited by Kampunzu et al., 1998), whereas the Nguba and Kundelungu Groups were poorly studied previously as a consequence of less economic interests. Nevertheless some researches and studies were undertaken on the Groups in places where Zn-Pb mineralization occurs such as at Kipushi, Kengere and Lombe (Intiomale et al., 1974; Intiomale, 1982, 1983) and also where the Kakontwe formation (Francois, 1973b) was mined for construction materials such as cements and limes. It is only recently with the presence of few economic deposits (Dikulushi, Lufukwe, Mwitapile and others) hosted in the Nguba and Kundelungu Groups and also the discovery of the giant worldclass Kamoa copper deposit hosted within the Grand Conglomerat unit of the Nguba Group, at the stratigraphic level above sediments hosting the major deposits in the Congolese Copperbelt to the east (Hitzman et al.,

2012; Cailteux et al., 2005) that exploration interests are increasingly growing and studies have been conducted in these two Groups of the Katangan Supergroup.

Sediments hosted copper deposits are extremely important sources of copper, cobalt and silver (Gustafson and Williams, 1981; Boyle et al., 1989; Hitzman et al., 2005), accounting for ~15% of the world's copper resource (Sillitoe, 2012). Also the global demand for base metal resources which continues to increase for the foreseeable future due to the continuing increase in global population and the desire and efforts to improve living standards worldwide are some of the drivers which dictate the aggressive ongoing exploration activities in the Central African Copperbelt; and numbers of exploration techniques have been undertaken in this area for the discovery of out-cropping deposits as well as those undercover. Meeting the increasing worldwide demand for minerals requires continued exploration and development of as yet undiscovered mineral deposits although the ability of the world community to meet this demand is increasingly affected by concerns about the impacts of exploration and mining on the environment, local communities and competing land uses.

With regards to mineral exploration in the Congolese Copperbelt, the government of the Democratic Republic of Congo implemented policies and regulations to acquire exploration rights over specific areas for a sustainable mineral exploration and development. However this mineral rights acquisition requires compliance with the mining law in place.

Geochemical techniques have been successfully applied over exploration leases in the Congolese Copperbelt with reference to recent copper deposit discoveries like Lonshi, Kamoa, and Frontier copper deposits in the Congo-Zambian Copperbelts and Sentinel Cu-Co deposit in the North Western Province of the Republic of Zambia based on the copper anomalies in soil (Hitzman et al., 2012; Broughton and Rogers, 2010). Furthermore soil geochemical surveys have been complimented by the application of other exploration techniques such as geophysical methods (Airborne, IP, EM, MAG, Titan*24*, etc.), structure and surface outcrop mapping, remote sensing, Global Lithospheric Architecture Mapping, reverse circulation and diamond drillings in the delineation of the above copper deposits (CoMiSa Sprl, 2008 (unpubl.)**.**

## 1.2. PR851 Exploration lease

The PR851 Exploration Lease (Figure 1) lies in a fragment of the Congolese Copperbelt and it is located in the district of Haut-Katanga, 80 km west of the town of Likasi, 70 km south-east of Kolwezi copper district and 175 km north-west of Lubumbashi, the provincial capital of Katanga Province in the Democratic Republic of Congo. The PR851 polygon area is relatively long in size (91.50 km long total perimeter) without good road access and infrastructures.

The average temperature remains fairly constant between 16 ˚C and 28 ˚C throughout the year and broadly two distinct seasons (Rain and dry seasons) are present in the area although a transition period between the two seasons can be remarkably distinguished during the year:

- Dry and cool season: from May to July
- Dry and hot season: from August to September
- Warm and wet season: October to April

Due to lack of cloud cover, rapid temperature drops occur after sunset during the dry season.

The site is characterized as mild, rainy, sub-tropical mid-latitude climate with dry winters and three seasons (dry, rainy and transitional seasons). The average annual rainfall is approximately 1,150 mm.

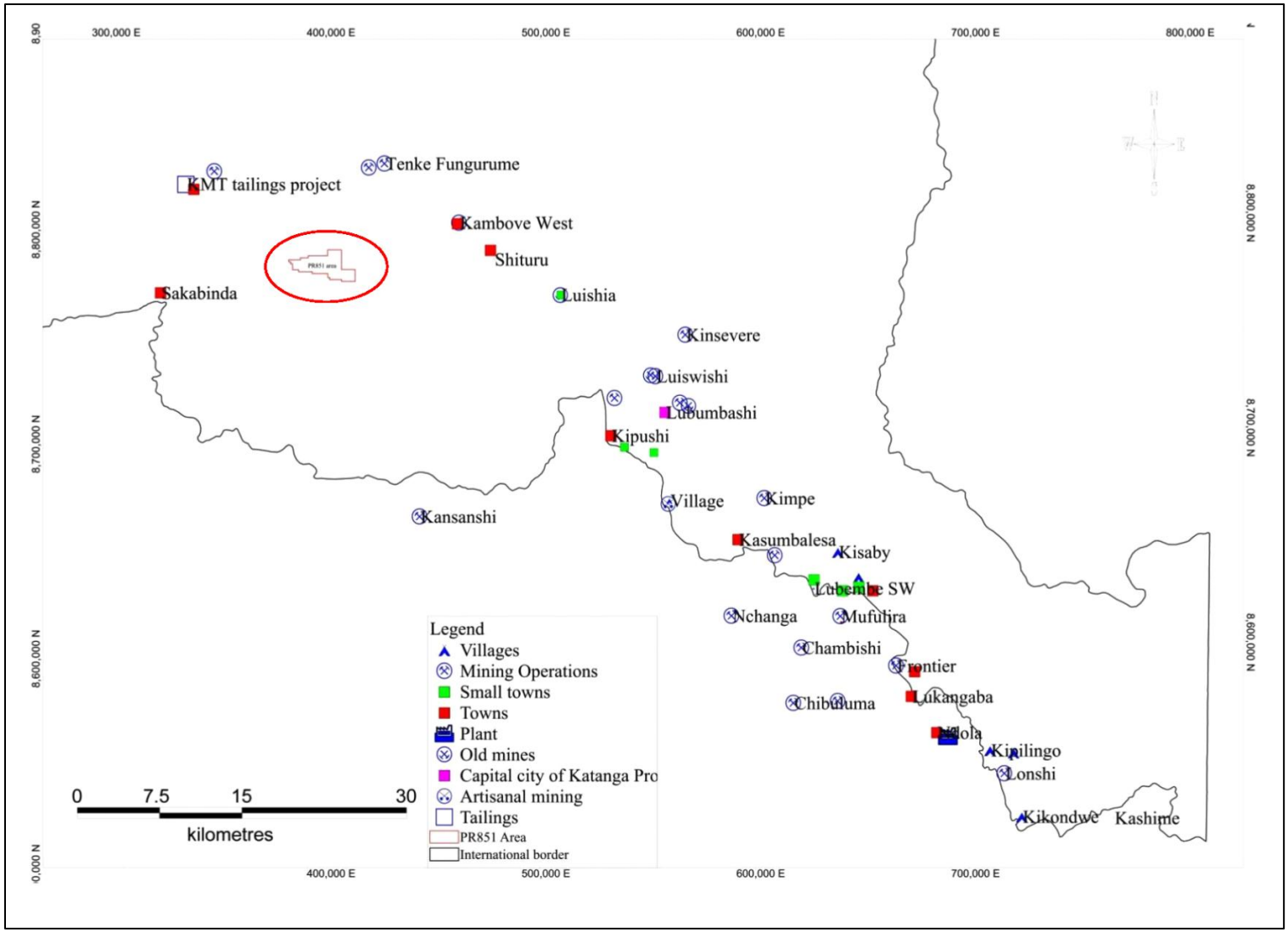


Figure 1: Location map of PR851 lease polygon outlined in red circle (modified after DRC Cadastre Minier 31/07/2010 from http://www.congomines.org/map/).

### 1.3. Previous work in the region

Since the colonial time in the 1960s to date, the Democratic Republic of Congo (former Republic of Zaire) has its economy mostly based on mineral resources and the Province of Katanga, economic pillar of the country, has been the major source of copper, cobalt as well as other commodities (such as uranium, lead, zinc and iron) contained in the Congolese Copperbelt.

The earliest author about mineral deposits of copper in the Katanga Province was Dr. Francesco Joe Maria de Lacerdas who completed the report dated 22nd March 1798. He was a Portuguese explorer and become governor of Rios de Sena in Mozambique. In his report it was stated that De Lacerdas contended that two years before, in 1796, a merchant had visited the great chief Cazembe who possessed copper and gold mines in the south of lake Moero and who was at war with a chief the land of whom was rich in 'latao' meaning 'yellow copper'. In 1806, two Portuguese also related that green stones existed in the land called 'Catanga' at the top of some hills from which copper was extracted and copper lingots bars were fabricated (Meuris, 2001 from http://www.africafederation.net/SCRAMBLE_KATANGA.htm).

After a succession of exploration events in the province of Katanga in the Democratic Republic of Congo before the 19th century, the Comité Special du Katanga (C.S.K.) was created on the 8th June 1900 which undertook mineral prospections in the Katanga area together with Tanganyika Concessions Ltd., the connection with Cecil Rhodes 'Chartered' (basically belgians and britishs).

At the beginning of the 20th century, the first 1:500,000 scale geological map of Katanga was made available by Cornet, Buttgenbach, and Studt (1908).

In 1901, some natives showed a certain Holland a mine in Kambove, one of the richest copper deposits in the world, which had been discovered sometimes ago by Jules Cornet in 1892. Kambove mine is located 65km north-east from the exploration lease PR851.

Before the independence of the country in the 1960s mineral prospection and exploitation rights were exclusively owned by the 'Union Minière du Haut Katanga (U.M.H.K.)'.

In 1967 the U.M.H.K. became respectively GECOMIN 'La Générale Congolaise des Minerais', GECOMINES 'La Générale Congolaise des Mines', then GECAMINES/EXPLOITATION 'La Générale des Carrières et des Mines-Exploitation' after nationalization which undertook mineral exploration based on localized regional mapping, pitting, trenching and shallow drilling following mineral outcrops.

In PR851 area, very few prospection works were done previously at a regional scale by the Democratic Republic of Congo State owned company Gécamines such as surface outcrops

description and digging of shallow pits of half a meter to 1m diameter up to nearly 15m deep with the aim to identify the *in-situ* rocks.

In 2003,First Quantum Minerals Ltd – a Canadian company listed on the Toronto Stock Exchange acquired the ownership of the exploration license PR851 via its Congolese subsidiary Compagnie Minière de Sakania SPRL (CoMiSa Sprl) which conducted detailed exploration works from grassroots to the discovery of the Kibamba Cu-Co deposit using different exploration techniques such as airborne geophysical survey, geological mapping, geochemical soil survey, trenching, reverse circulation and diamond drilling between 2004 and 2010.

Later from 2012 to 2013 Boss Mining SPRL, a listed company in the Virgin Islands, resumed exploration activities by doing few scattered diamond drilling in some other parts of the PR851 area. There are very limited to non-existent published detailed exploration geology reports on the PR851 area in universities and public libraries although some few records can be found in the Democratic Republic of Congo's Department of Geology website and in old First Quantum Minerals Ltd press releases.

### 1.4. Purposes of the study

The main objective of this study is to review geochemical exploration technique undertaken in the prospect area with emphasis on the use of soil sampling survey followed by drilling methods executed in the discovery of the Kibamba Cu-Co deposit. In the present case study soil sampling method has been proven to be very effective in mapping shallow sitted orebodies in the area. It can therefore be used to some extend as a very efficient tool in the exploration of sediments hosted Cu-Co in the world class Central African Copperbelt.

To achieve the purposes of the present work a review of available historical data from Gecamines Sarl on PR851 area coupled with real soil assays dataset compiled by CoMiSa Sprl was undertaken. This resulted in targets generation and prioritization for a later follow-up by reverse circulation and diamond drilling. Furthermore logging of all diamond cores and rock chips was done for drill section interpretation and resource estimates. Finally my personal experience in mineral exploration was considered after a total of twelve years of works to date in sediments hosted copper mineralization of the Central African Copperbelt in the Democratic Republic of Congo and Zambia including five consecutive dedicated working years (from 2003-2008) for Cu-Co exploration within PR851 area from Greenfield exploration to the discovery of Kibamba Copper-Cobalt deposit.

# CHAPTER 2: METHODOLOGY OF SOIL GEOCHEMICAL AND DRILLING EXPLORATION TECHNIQUES

## 2.1. Soil geochemical exploration

### 2.1.1. Literature review

The use of soil surveys as one of exploration tools in the search of Cu-Co deposits has been a successful prospection technique in the discovery of low to high grade deposits within the Central African Copperbelt and elsewhere in some parts of the world (Hitzman et al., 2012; Fleischer, 1984). Soil geochemical exploration is credited to have assisted significantly in the finding of suboutcropping and shallow buried Cu-Co deposits detected primarily through Cu anomalies in soil such as Lonshi, Frontier and Kamoa deposits in D.R. of Congo; Chibuluma and Sentinel deposits in the Republic of Zambia (Fleischer, 1984; Broughton and Rodgers, 2010; Hitzman et al., 2012) as well as the Bell Cu deposit of Central British Columbia (Carson et al., 1976 cited by Fletcher et al., 1986). Sillitoe (1995) cited by Sanfo (2006, unpubl.) argued that unlike many other methods applied in exploration, soil geochemical exploration remains one of the most efficient tools and proved to be directly responsible of a number of discoveries in different areas during the last past 25 years.

For a very successful exploration program a combinaison of soil geochemical exploration with the study of many other datasets like stratigraphy, topography, remote sensing, geophysics, geology (mineral associations, local dispersion processes, mineralization styles, weathering), climate, vegetation, site drainage, reverse circulation and/or diamond drilling is always recommended.

The PR851 area in the Congolese Copperbelt is mainly characterized by a type of brown-reddish tropical soils (Figure 2) as a result of deep weathering due to tropical climate.

The vegetation is thick and comprises grassland, typical tropical forest and swamps (locally called dambos) in a moderately flat landscape terrain with hills in places and anthills caused by termites which are known to transport material from down depths (60m or more below surface) up to surface. It is proven that these materials from termites reflect bedrock composition and/or the underlying regolith.

The drainage system in the area is more or less well developed and *in-situ* soils are developed in flat landscape whereas transported soils are observed at distance from high reliefs. Cu-Co mineralization (oxides and sulphides) is assuming to be located within the fragment of the Mines

Subgroup presenting a regular tabular, blanket-like shape. In this environment, copper as well as cobalt has both mechanical and hydromorphic dispersion which are highly considered in the implementation of geochemical survey.

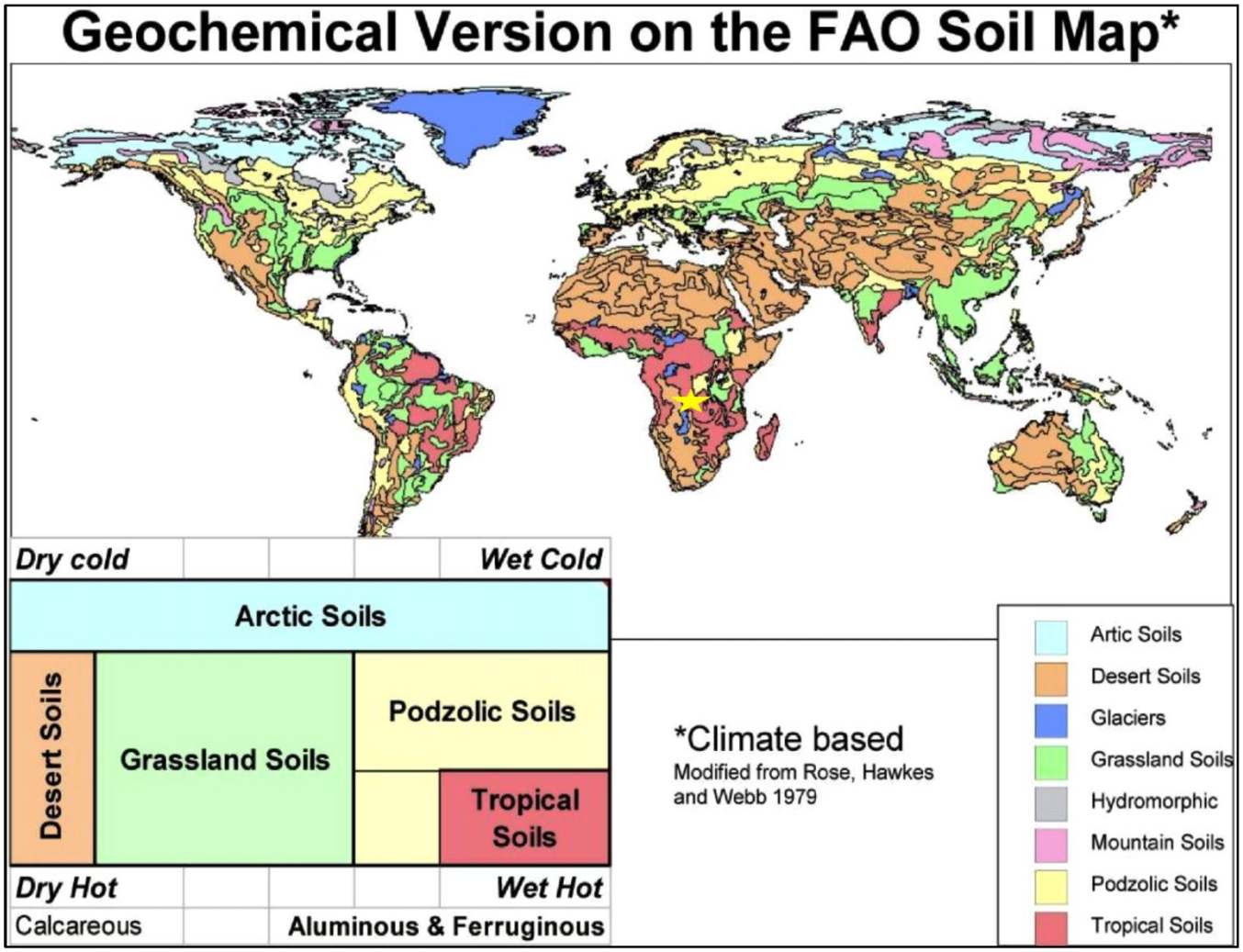


Figure 2: World soil map. Note yellow star showing location of PR851 area situated in tropical soils (modified after Dale, 2013 Unpubl.).

### 2.1.2. Sampling procedure

#### 2.1.2.1. Grid design and sampling overview

The regional soil sampling program in PR851 area consisted of 7000 planned samples (Figure 3) spaced at 100m intervals on 800m spaced east-west and north-south oriented lines for the first phase of reconnaissance in order to cover the entire license area. This was followed by a later detailed and localized soil sampling based on 400X100m and then 200X100m grids spacing (Figure 4) respectively on the second and third phases. Sampling lines were planned perpendicularly to the strike of the mineralization host rock units with at least two traverse lines and two to three soil samples being collected over the anticipated potential Cu-Co target. In the Congolese Copperbelt, most of the stratiform and stratabound economic Cu and / or Cu-Co ore deposits contained in the Katangan Supergroup extend along strike (e.g., Kamoa Cu deposit, Schmandt et al., 2013) than they do on width. Ideally soil geochemical survey following a rectangular grid is recommended.

The grid design and soil sampling strategies were dependent on many factors:

a. The First-Quantum Minerals Ltd through its CoMiSa Sprl subsidiary's very limited budget for personnel and sample analysis at the time of the present soil sampling program,

b. The topography of the area,

c. The anticipated size of the ore body buried at shallow depth,

d. The local Cu-Co dispersion processes,

e. The geology of the Katangan belt, more specifically of the Mines Subgroup within the prospect area,

f. The dimension (size) of the area under investigation, and

g. The favorability of the area to contain a Cu-Co ore deposit.

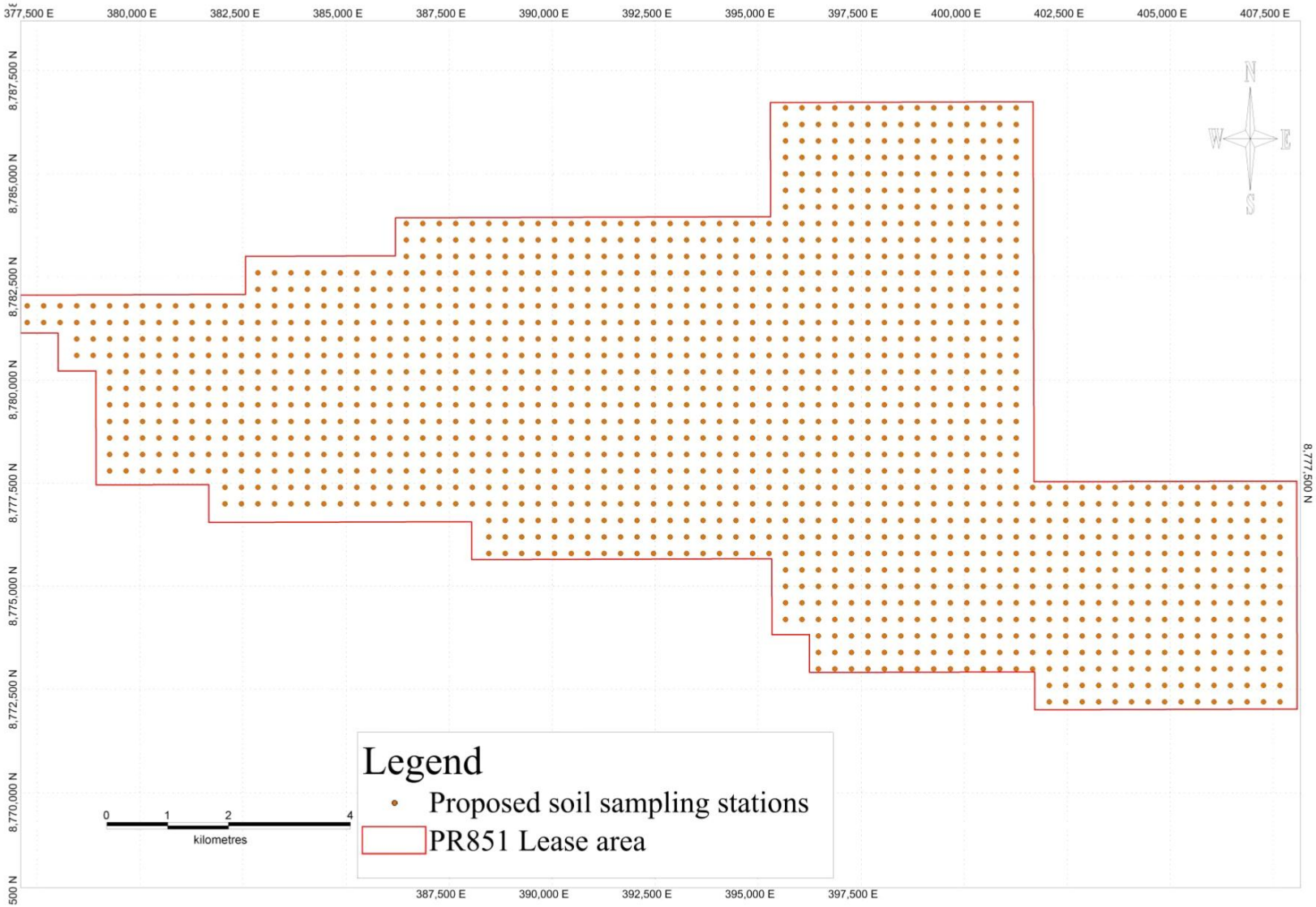


Figure 3: PR851area map of the proposed soil sample locations at the regional reconnaissance stage covering the entire license area (Katombe, 2005 Unpubl.)

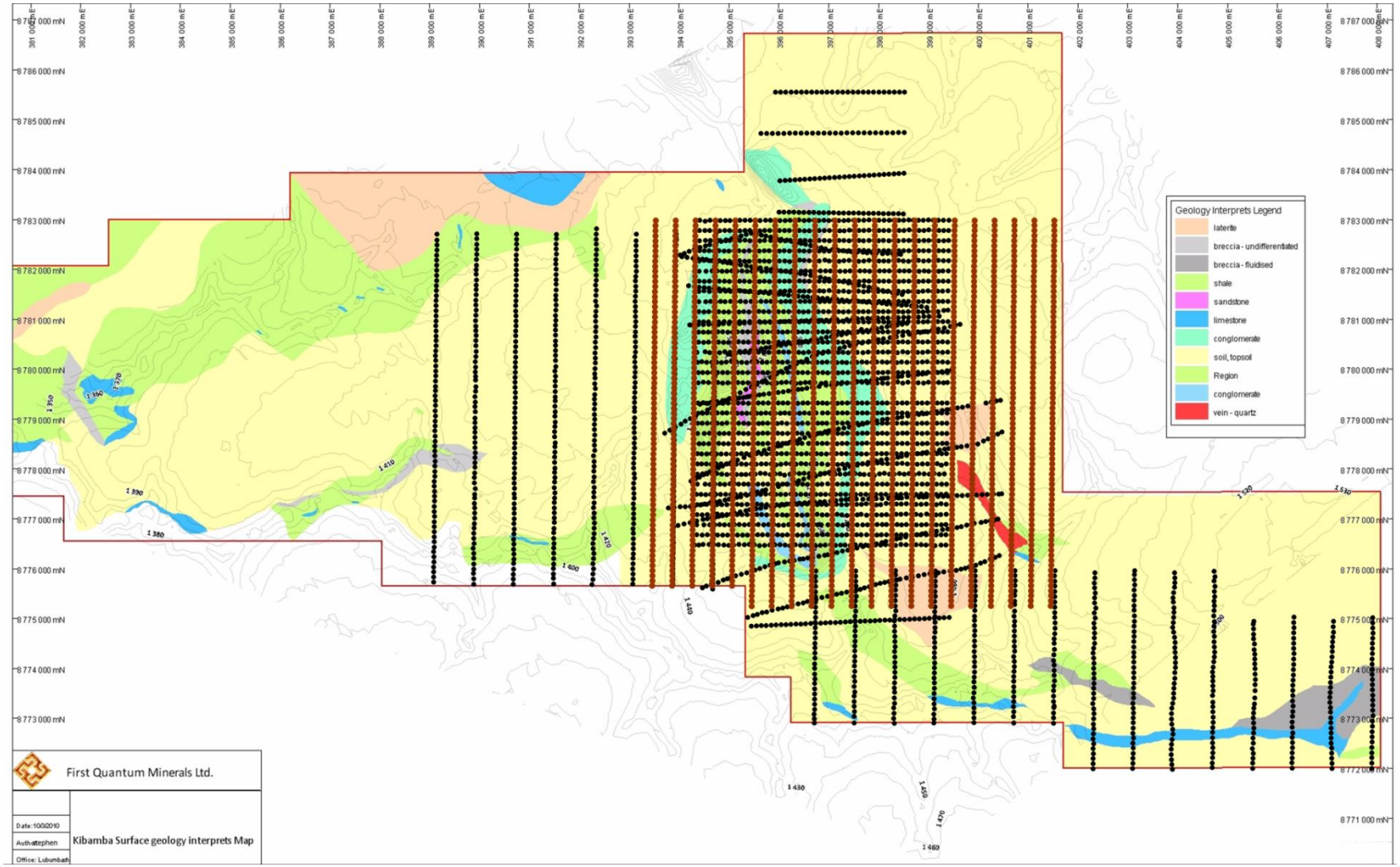


Figure 4: Different designed grids for soil sampling in the central part of PR851 area (with 800X100m Grid 1; 400X100 Grid 2 and 200X100m Grid 3). Note east-west lines offset from Grid 1 during sampling.

The sampling convention was conducted in an old-school ‘square grid’ and/or ‘rectangular grid’ method as opposed to a new-school ‘off-set grid’ which is believed to increase the sample search space and reduce the level of uncertainty (Figure 5).

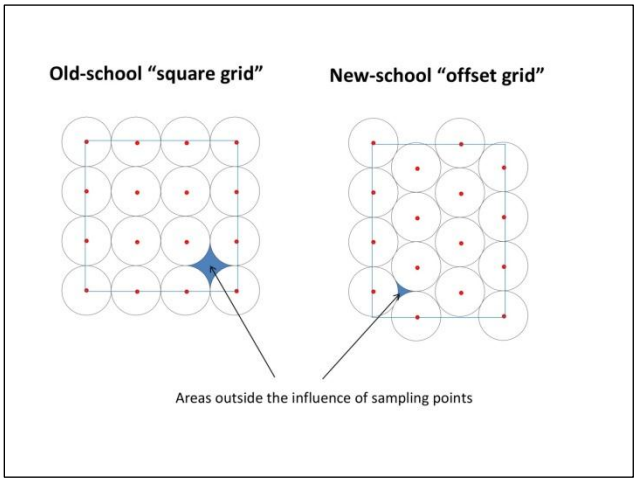


Figure 5: Illustration of an Old-school ‘Square grid’ as opposed to the New-school ‘Offset grid’ (source First Quantum Minerals LTD, 2014 unpubl.)

#### 2.1.2.2. Equipment

For a successful soil sampling program in PR851 area, a more detailed list of equipment included the followings:

- A topographic map for access, fences and obstacles location,
- Basic map of sampling area, with tracks, rivers, local hospitals and/or emergency medical care locations marked where possible and fuel stations in the vicinity of the sampling area,
- A geological map of the area,
- Appropriate well equipped all-terrain vehicles with enough fuel, winch cable, spare wheels,
- Paramedic first aid kit for safety containing supplies for cuts, scrapes, insect bites, appropriate snake bit kits for the area,
- A field rescue plan (with who is doing what and when in case of an emergency)
- Foods with different options including drinking water,
- Sunscreen and insect repellents,
- GPS with enough spare batteries,
- A laptop to load and download GPS coordinates,
- Magnetic compass (A cheap magnetic compass was invaluable if the GPS unit failed. Shouldn't bet safety on a couple of AA GPS batteries only),
- Satellite phones and/or mobile cellphones with their charging stations,
- Rucksacks to carry samples,
- Sample ticket books,
- Sampling sheets,
- Picks,
- Shovels,
- Sieves (180µm size),
- Scoops,
- Spatula,
- Polypropylene funnel,
- Slashes,
- Brushes and clothes for cleaning,
- Portable small compressors,
- Geochemical paper packets,

- Plastic sample bags,
- Plastic ziplock bags,
- Permanent markers, pens and pencils,
- Staplers and more than enough spare staples,
- Camping gears (tents, portable tables, chairs, kitchen utensils, and fridges),
- Petty cash box with money in it,
- List of contact numbers in case of any incident (This was helpful to call someone in the office each evening who knows what to do in case there was no call from the field).

**2.1.2.3. Field sampling**

Cu-Co geochemical signals can be detected in a wide variety of media (soil, termite, bedrock, plants and/or water from the drainage system or underground water) from which geochemistry is capable of targeting and extracts very important and meaningful information.

For a quick screening of PR851 area with expectations to delineate at least two to three single adjacent points anomalies, soil sampling was carried out by five teams, each composed of a trained CoMiSa SPRL geological technician plus three to four local labourers for digging and collecting soil samples under my own supervision as a junior geologist by the time of the sampling program. Field teams were supplied with coordinates of each single sampling location pre-loaded onto an assigned GPS and also printed onto A4 format sampling sheets. The sampling team leader had to navigate to the sampling point by using bearing and distance on the GPS instrument, aiming to be as close as possible to the planned location. Once on the location, a record of the actual GPS reading was taken even if at the planned location. In case a point was not accessible due to obstacles (geographical and artificial constraints such as river bed, termite mount, dense vegetation, graveyard etc…) the point was moved up to not more than 50m from the planned location and the coordinates of the new location noted on the sampling sheet. And if a case where the location couldn't be moved due to a huge obstacle the reason was recorded under the vegetation/land cover column of the sampling sheet (Figure 6) with respect to the sampling library code (Figure 7) and any extra information given in the comments column.

**LA COMPAGNIE MINIERE DE SAKANIA**

**COMISA sprl**

*Filiale de First Quantum Minerals Ltd*


SIEGE SOCIAL
1029, Boulevard KAMANYOLA
B.P 400 LUBUMBASHI
KATANGA, R.D CONGO

Tél:00-243-814000299
Fax:00-243-813010278


| | | Planned Position | | Actual Position | | | | | | | | | | | |
|---|---|---|---|---|---|---|---|---|---|---|---|---|---|---|---|
| Sample ID | QAQC Sample | UTM_Easting | UTM_Northing | UTM_Easting | UTM_Northing | RL (m) | Sampling Depth (cm) | Regolith type | Colour | Colour Tone | Vegetation or Land Cover | Moisture | Sampled by | Sampling Date | Comments |
| E0801 | | 394045 | 8776500 | 394045 | 8776520 | 1298 | 28 | TSO | RDBN | M | FOR | D | P.Katombe | 03/07/25 | Moved 20m south because of thick forrest |
| E0802 | | 394045 | 8776600 | - | - | - | - | - | - | - | - | - | P.Katombe | 03/07/25 | Falls In a large 'Dambo'. Not sampled |
| E0803 | | 394045 | 8776700 | 394050 | 8776700 | 1292 | 30 | CLY | GYBK | D | DAM | W | P.Katombe | 03/07/25 | Moved 5m East to the edge of the dambo |
| E0804 | | 394045 | 8776800 | | | | | | | | | | | | |
| E0805 | | 394045 | 8776900 | | | | | | | | | | | | |
| E0806 | | 394045 | 8777000 | | | | | | | | | | | | |
| E0807 | | 394045 | 8777100 | | | | | | | | | | | | |
| E0808 | | 394045 | 8777200 | | | | | | | | | | | | |
| E0809 | | 394045 | 8777300 | | | | | | | | | | | | |
| E0810 | FDP | 394045 | 8777400 | | | | | | | | | | | | |
| E0811 | | 394045 | 8777500 | | | | | | | | | | | | |
| E0812 | | 394045 | 8777600 | | | | | | | | | | | | |
| E0813 | | 394045 | 8777700 | | | | | | | | | | | | |
| E0814 | | 394045 | 8777800 | | | | | | | | | | | | |
| E0815 | | 394045 | 8777900 | | | | | | | | | | | | |
| E0816 | | 394045 | 8778000 | | | | | | | | | | | | |
| E0817 | | 394045 | 8778100 | | | | | | | | | | | | |
| E0818 | | 394045 | 8778200 | | | | | | | | | | | | |
| E0819 | | 394045 | 8778300 | | | | | | | | | | | | |
| E0820 | STD | | | | | | | | | | | | | | |
| E0821 | | 394045 | 8778400 | | | | | | | | | | | | |
| E0822 | | 394045 | 8778500 | | | | | | | | | | | | |
| E0823 | | 394045 | 8778600 | | | | | | | | | | | | |
| E0824 | | 394045 | 8778700 | | | | | | | | | | | | |
| E0825 | | 394045 | 8778800 | | | | | | | | | | | | |
| E0826 | | 394045 | 8778900 | | | | | | | | | | | | |
| E0827 | | 394045 | 8779000 | | | | | | | | | | | | |
| E0828 | | 394045 | 8779100 | | | | | | | | | | | | |
| E0829 | | 394045 | 8779200 | | | | | | | | | | | | |
| E0830 | BLK | | | | | | | | | | | | | | |
| E0831 | | 394045 | 8779300 | | | | | | | | | | | | |
| E0832 | | 394045 | 8779400 | | | | | | | | | | | | |
| E0833 | | 394045 | 8779500 | | | | | | | | | | | | |
| E0834 | | 394045 | 8779600 | | | | | | | | | | | | |
| E0835 | | 394045 | 8779700 | | | | | | | | | | | | |
| E0836 | | 394045 | 8779800 | | | | | | | | | | | | |
| E0837 | | 394045 | 8779900 | | | | | | | | | | | | |
| E0838 | | 394045 | 8780000 | | | | | | | | | | | | |
| E0839 | | 394045 | 8780100 | | | | | | | | | | | | |
| E0840 | FDP | 394045 | 8780200 | | | | | | | | | | | | |
| E0841 | | 394045 | 8780300 | | | | | | | | | | | | |
| E0842 | | 394045 | 8780400 | | | | | | | | | | | | |
| E0843 | | 394045 | 8780500 | | | | | | | | | | | | |
| E0844 | | 394045 | 8780600 | | | | | | | | | | | | |
| E0845 | | 394045 | 8780700 | | | | | | | | | | | | |

Figure 6: Illustration of a soil sampling spreadsheet for data capturing during soil sampling survey (after CoMiSa Sprl, 2005 unpubl.).

**Soil Sampling coding System**

| Regolith Overprint | | Colour | | Colour Tone | | Vegetation / Land cover | | Moisture | | QAQC Sample Category | | Sampled by | | Sampling Date |
|---|---|---|---|---|---|---|---|---|---|---|---|---|---|---|
| ALL | Alluvium | BE | Beige | D | Dark | CHU | Church | DY | Dry | BLK | Blank | P.Katombe | Paul Katombe | Day/Month/Year |
| CAL | Calcrete | BL | Black | L | Light | CIM | Cimetery | MT | Moist | FDP | Field Duplicate | D.Mota | Daniel Mota | |
| CLY | Clay | BR | Brown | M | Medium | CLA | Cultivated Land (Crops) | WT | Wet | STD | Standard | M.Kazadi | Marcel Kazadi | |
| FER | Ferricrete | CR | Cream | | | FAM | Farm | | | | | L.Mujinga | Liliance Mujinga | |
| FRO | Fresh rock | GY | Grey | | | FOR | Forrest (with trees) | | | | | P.Kasongo | Patrick Kasongo | |
| GOS | Gossan | KH | Khaki | | | GRS | Grassland | | | | | M.Kasongo | Maurice Kasongo | |
| GSO | Gravel Soil | LI | Lime | | | OFM | Old Farm | | | | | L.Musongela | Louis Musongela | |
| ISO | In Situ Soil | MI | Milky | | | ROD | Road | | | | | | | |
| ICA | Iron carbonate | OL | Olive | | | SCH | School | | | | | | | |
| LAT | Laterite | OR | Orange | | | VIL | Village | | | | | | | |
| LIM | Limonite | PK | Pink | | | WTR | Walking Track | | | | | | | |
| RUN | Regolith-undifferentiated | RD | Red | | | WDM | Waste Dam | | | | | | | |
| SAN | Sand | TN | Tan | | | WWA | Water Way | | | | | | | |
| SAP | Saprolite | WH | White | | | | | | | | | | | |
| TSO | Soil (Top Soil) | YE | Yellow | | | | | | | | | | | |
| TRS | Transported Soil | | | | | | | | | | | | | |

The following details should be noted:

* RL is read from the GPS by the sampler
* Regolith is the type of material collected
* Colour of the sampled material can be recorded as one code or a combination of two colour codes
* Vegetation / Land cover is the type of vegetation or land cover surrounding the sampling position
* QAQC STD are certified recognized standards

Figure 7: Soil sampling codes library model used in PR851 area sampling program (CoMiSa Sprl, 2005 unpubl.)

Small pits were dug into the top of the B horizon (Figure 8) between 25 to 30 centimeters below the surface or shallower in rocky areas away from the organic (humus) rich, dark-colored horizon. After sampling, the exact depth was recorded on the sampling sheet.

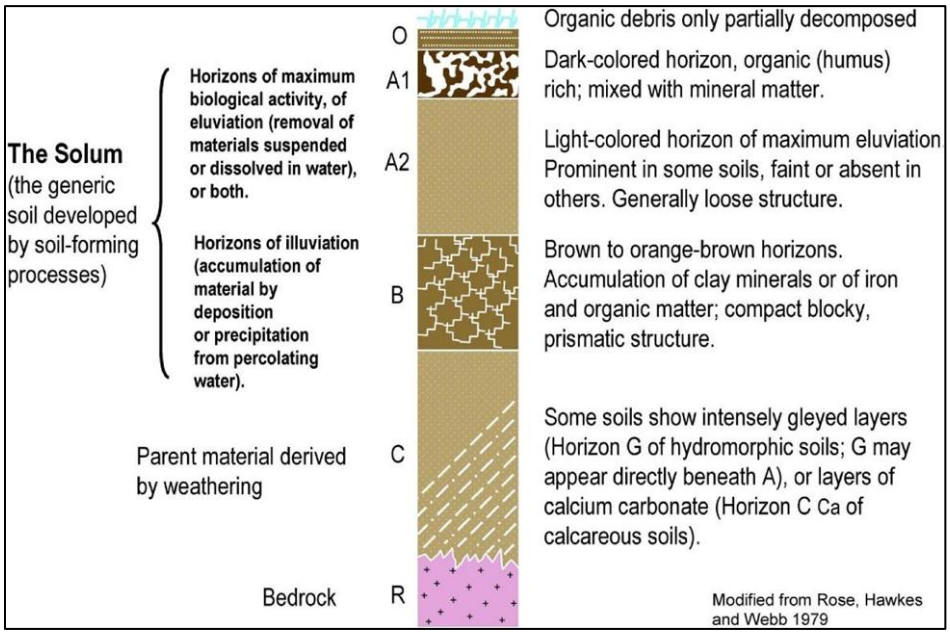


Figure 8: Illustration of B horizon from where soil samples should be collected (Dale, 2013 unpubl. Modified after Rose, Hawkes and Webb, 1979).

Briefly, in order to maintain consistency during field sampling, in-house clear sampling protocols and procedures were put in place:

- All soil sampling was conducted using the map datum of Arc 1950-35S in a Universal Transverse Mercator coordinate system. This was complimented by local grid coordinates (Figure 9) to easily locate sampling points by samplers in the field;
- Pitting /digging of small holes up to 25-30cm below surface or shallower in rocky areas away from the organic (humus) rich, dark-colored horizon was executed aiming at sampling material from the B horizon;
- 1.5 to 2kg of sample material was collected using a clean and not painted picks, shovels or scoops and washed hands to avoid contamination from which 100g of sample placed in a geochemical packet was collected from a first sieving and it was kept as a reference sample. The remaining material was sieved at 180µm from which two packs of sieved material 50g each were taken with one put in a second paper bag to be sent for laboratory analysis and the other one taken into a small clear ziplock plastic bag for hand-XRF analysis.
- Insertion of sample ticket into each sample packet from the sampling field. Sample number and coordinates location written on the outside of the packet as well as on the sampling sheet and in the sample ticket book on the appropriate page together with the junior geologist's name and the sampling date;
- Wearing of metals in any design (rings and/or bracelets) was prohibited during sampling collection and preparation exercise to avoid samples being contaminated;
- Suspected transported materials like soils from uphill and down slope was collected with precautions and related data results interpreted accordingly;
- Soil samples were transported by the personnel to the nearest point before being taken by an all-terrain vehicle due to lack of road network inside the exploration lease;
- Recording of observations around sampling locations such as topography, brief description of geology, ground morphology, soil characteristic (lateritic, clay…) was implemented. Description of samples consisted in capturing the sample ID, XYZ (with X: easting, Y: Northing and Z: Elevation), sampled by, color, grain size, texture, and alteration if any;
- Taking of actual coordinates at each sampling station. These real locations of soil samples were considered into the database for data processing. Note that between planned and actual sample coordinates, a deflection could occur due to GPS accuracy, user's knowledge and experience to operate

with the instrument, type of GPS and obstacles (rivers, hills, big trees, lake, village, road tracks, railways, tar-road, church, crops, swamps, waste dam…) during sampling.

- Pegging with flagged sticks from dead bush tree branches on each sampling station was done to physically materialize the grid for a near future follow-up;
- After sampling; each single pit was filled in, packed down and the ground rehabilitated as close as possible to its original condition in order to comply with environmental laws and regulations in place in the country;
- For safety reasons during sampling activities, sampling teams were carrying a well-equipped first aid kit. They were advised to take note of any tracks/paths, villages encountered so that an accurate quick exit and rescue could be gained in case of any emergency. Also they were required to have satellite phones and / or mobile cellphones with sufficient credit for any general contact or alert. A recommendation to call the office station was mandatory each single day after soil sampling was undertaken and in case of no feedback from the sampling field an action was taken by safety staff members.

So following the above in-house sampling protocols and procedures, a successful sampling survey has been conducted in PR851 area during nearly 3 years between 2005 and 2008 and a total of 6565 soil samples were collected from the field then taken for sample preparation and later sent for laboratory analysis to assay Cu and Co only rather than multi-elements analysis.

Field sampling report was sent to the CoMiSa SPRL senior exploration geologist for checking and filing.

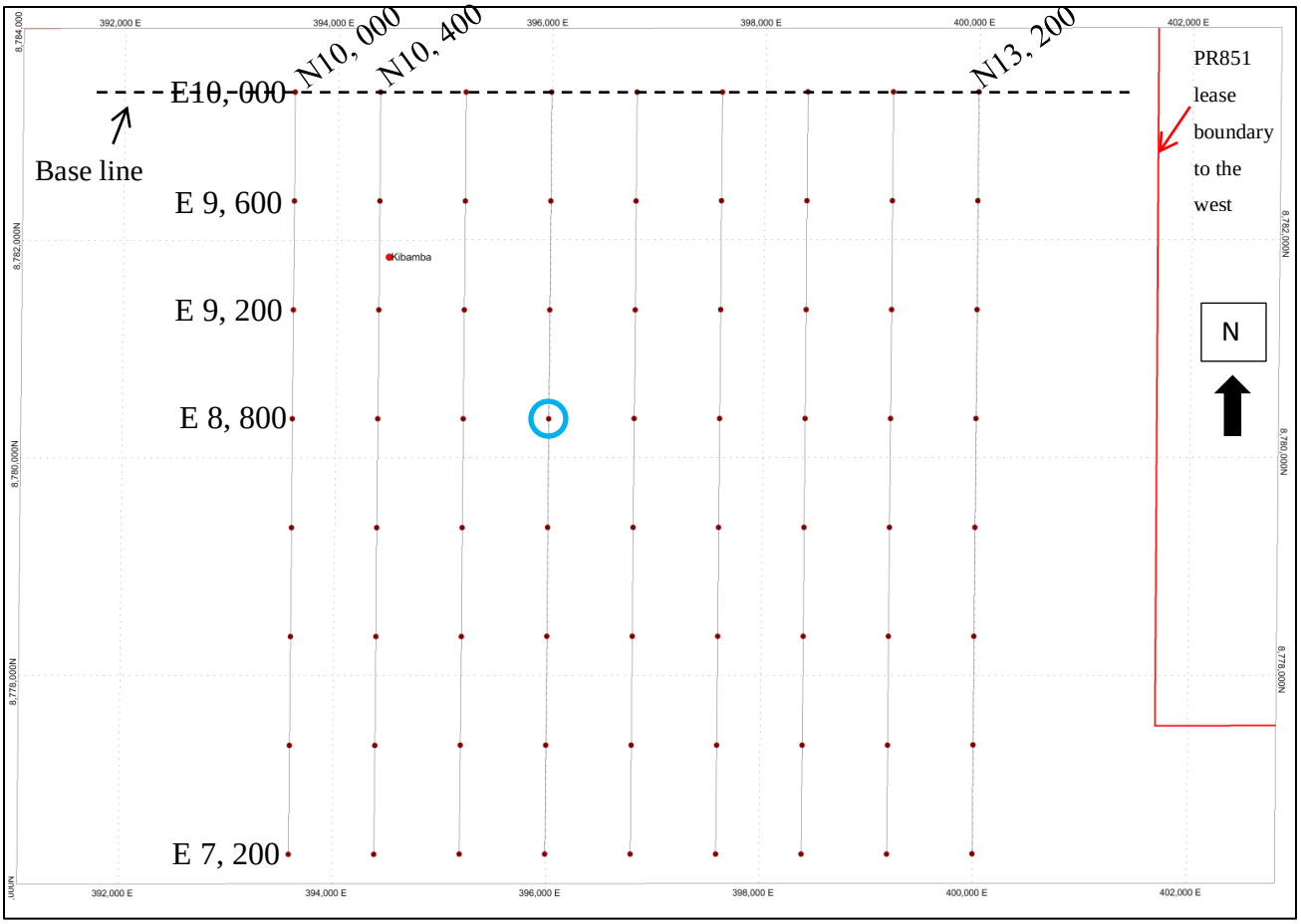


Figure 9: Illustration of a local grid labeling implemented in PR851 area. Note that the local coordinate of the circled sample in blue will be: N11200-E8800. This grid was designed and implemented by the author of the present thesis.

### 2.1.2.4. Preparation

After field sampling was undertaken, soil samples were properly packed and taken into a designated sample room for preparation. The sample preparation room was kept clean at all time with a floor washed regularly.

Munter (1988); Soltanpour et al. (1976), Elk and Gelderman (1988) argued that sample preparation steps, often taken for granted, have frequently been demonstrated to significantly affect qualitative and quantitative analytical results. Most of the time soil samples were received in an aggregated state and unsuitable condition for laboratory analysis. The volume of collected samples was larger than the required volume for analysis. Therefore because of the tendency of such bulk samples to fractionate by aggregate size, it becomes very important to thoroughly homogenize each sample by some sort of mixing before scooping and weighing a representative and suitable subsample.

In PR851 area, bulk soil samples from the field were dried, sieved, homogenized, subsampled and labeled accordingly prior to laboratory analysis.

*2.1.2.4.1. Drying method*

Each soil sample was spreading in thin layers over a plastic bag and layout under the sunlight to get dried (Figure 10). This was the recommended drying method in our case study as long as bulk samples from the field were most of the time in a moisture condition. Elk and Gelderman (1988) recommended that soil samples to be used for routine analyses not be dried at greater temperature than 36˚C. Thien et al. (1978) documented that microwave drying may alter the analytical results and should be avoided. In the sampling area, temperature does not exceed 36˚C either during winter period or wet season. Sampling was conducted before the hot season of the year and most of the time in dry season when temperatures are low.

The drying step was followed by some form of pulverization and/or grinding before sieving.


Figure 10: Illustration of soil sample layout under sunlight for drying.

*2.1.2.4.2. Sieving method*

Soil samples were passed through a 180-mesh screen (Figure 11) as required for Cu-Co analysis. During sieving process, stainless screen sieves were used to prevent any metal contamination. Cross-contamination between soil samples was avoided by minimizing soil-particle carryover on the sieving screen. Also a more thorough cleaning of sieving screen by brushing or washing with clean water and wiping between samples was required. During sieving basic precautions regarding safety and involving of common senses were followed. So wearing of dust masks to prevent respiration diseases was recommended.


Figure 11: Illustration of sieved soil sample using a 180-mesh screen

*2.1.2.4.3. <u>Subsampling and labeling methods</u>*

Following drying and sieving of samples, it was then possible to get representative subsamples for analysis (Figure 12). In PR851 area, sieved soil samples were thoroughly homogenized by mixing with a spatula. Subsamples were obtained from dip into the center of the homogenized bulk samples with a soil scoop. At this step, three subsamples were collected from the bulk sample and labeled identically as per the in-house clear sampling protocols and procedures.

After all subsamples were prepared a routine sample dispatch to laboratories for analysis was permanently conducted.

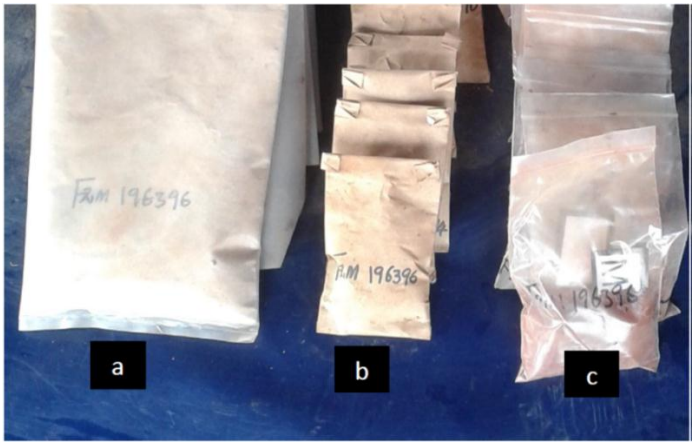


Figure 12: Illustration of representative subsamples for analysis (with a: Backup sample, b. Sample for laboratory analysis and c. Sample for hand-Niton/XRF analysis). Note that all three samples are labeled identically.

### 2.1.3. Dispatch

A routine sample dispatch was conducted when a bunch of 500 to 750 samples was attained.

Soil samples were put in boxes (Figure 13a) and sent conjointly to Genalysis Laboratory Services Pty South Africa and/or Australia for laboratory analysis, to Lubumbashi in the D. R. of Congo for hand-Niton/XRF analysis and lastly to the CoMiSa Sprl warehouse for storage (Figure 13b). Genalysis Laboratory Services Pty Ltd is an accredited laboratory (Table 1).


Figure 13: (a) Soil samples packed in boxes for dispatch, (b) Soil sample storage at the CoMiSa Sprl warehouse.

Table 1: Details of laboratories used for analysis of soil samples

| Name | Physical Address | Accreditation |
|---|---|---|
| Genalysis Sample Preparation Division | Unit 4a, 253 Dormehl Road, Middlepark, Anderbolt, Gauteng, South Africa 1459<br>Tel: +27 11 918 0869<br>Fax: +27 11 918 0879<br>Email: johannesburg@genalysis.com.au | NATA ISO/IEC 17025 |
| Genalysis Laboratory | 15 Davison Street, Maddington 6109, Western Australia<br>Tel: +61 8 9251 8100<br>Fax: +61 8 9251 8110<br>Email: genalysis@genalysis.com.au | NATA ISO/IEC 17025 |

Sample dispatch form (Figure 14) needed to be filled in and emailed to the senior exploration geologist for a final checkup before shipping soil samples abroad.

LA COMPAGNIE MINIERE DE SAKANIA

COMISA sprl

*Filiale de First Quantum Minerals Ltd*

Tél:00-243-814000299
Fax:00-243-813010278

SIEGE SOCIAL
1029, Boulevard KAMANYOLA
B.P 400 LUBUMBASHI
KATANGA, R.D CONGO

**Sample Dispatch Form**

| Date | Sample ID from | Sample ID to | Dispatched by | Received by | Lines | No. of samples | Comments |
|---|---|---|---|---|---|---|---|
| 03/08/20 | EO801 | EO850 | P.Katombe | M.Kasongo | 10 | 50 | |
| 03/08/20 | EO851 | EO900 | P.Katombe | M.Kasongo | 11 | 49 | EO879 not sampled |
| 03/08/20 | EO901 | EO950 | P.Katombe | M.Kasongo | 12 | 50 | |
| 03/08/20 | EO951 | EO1000 | P.Katombe | M.Kasongo | 13 | 50 | |
| 03/08/20 | EO1001 | EO1050 | P.Katombe | M.Kasongo | 14 | 47 | EO1003, EO1026 and EO104 |
| 03/08/20 | EO1051 | EO1100 | P.Katombe | M.Kasongo | 15 | 50 | |
| 03/08/20 | EO1101 | EO1150 | P.Katombe | M.Kasongo | 16 | 50 | |
| 03/08/20 | EO1151 | EO1200 | P.Katombe | M.Kasongo | 17 | 49 | EO1200 not sampled |
| 03/08/20 | EO1201 | EO1250 | P.Katombe | M.Kasongo | 18 | 50 | |
| 03/08/20 | EO1251 | EO1300 | P.Katombe | M.Kasongo | 19 | 50 | |

**Total No. Samples** 495

**Sender:**

**Receiver:**

Figure 14: Illustration of CoMiSa SPRL Soil Sample Dispatch Form used in PR851 area (after CoMiSa Sprl, 2005 unpubl.)

### 2.1.4. Laboratory analysis

#### *2.1.4.1. C/AAS – AX/AAS analytical methods*

Soil samples for geochemical analysis were analysed at Genalysis Laboratory Services PTY (LTD) in Johannesburg - South Africa and Perth – Western Australia (Table 1). Copper and cobalt were analyzed firstly by using C/AAS analytical method. This analytical technique was selected as it could offer a quick turnaround of laboratory results; it was very cost effective and for the first pass analysis only. At this level QAQC work was undertaken by using Genalysis Laboratory control samples.

At the follow up step, from C/AAS assay results all significant Cu-Co anomalies were re-assayed by using AX/AAS analytical method (four acid digestion- multi-acid attack including hydrofluoric, nitric, perchloric and hydrochloric acids in Teflon beakers Aqua regia digestion). For high precision ore-body evaluation, the above digest approach total dissolution for most minerals is one of the recommended analytical methods for Cu and Co respectively (Table 2).

Simultaneously Niton/XRF analyses were undertaken in CoMiSa Sprl laboratory based in Lubumbashi-D.R.of Congo for quick results. It appeared somehow a good close similarity or a positive correlation within a certain limit of tolerance between Cu analytical laboratory assays and results from the Niton/XRF handheld analyzer could have been established. However cobalt results indicated a deflection between laboratory and Niton/XRF results, and therefore required a specific calibration.

For both field and analytical analyses quality controls, QAQC (certified reference materials, standards, field duplicates and blank) samples were inserted at regular intervals to check the accuracy, precision, bias, and if there was any contamination before data validation and processing. In laboratories, extra QC samples (laboratory replicates and duplicates) to check the precision of the analytical work were also inserted and used.

Unfortunately as far as this work is concerned, historical QAQC data was not made available although the rest of the dataset shown in the following chapter remain real and true.

#### *2.1.4.2. $p^H$ analysis*

Systematic pH data were also taken from the first regional soil sampling. The pH values helped to identify which elements are likely to be stable in the soil and with the addition of hydrochloric acid to what degree $CaCO_3$ may be buffering soil acidity.

The understanding of acid-producing reactions like oxidation of a sulphide mineralization should interact with the overlying soil and generate a lower pH level. This information could have been used to show undercover mineralization in relation with conventional soil geochemical methods.

Table 2: Recommended analytical methods for low grade geological materials (from www.intertek.com | www.genalysis.com.au)

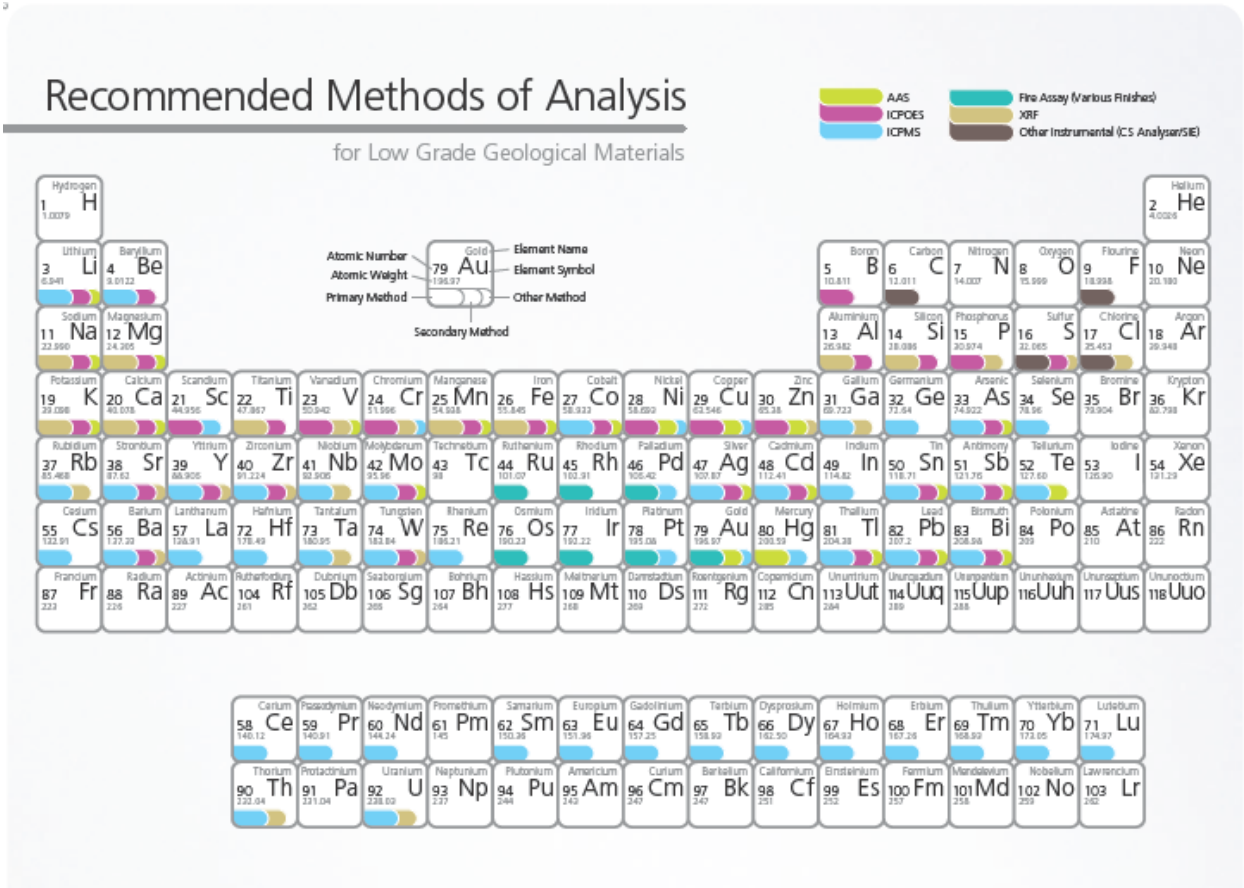


### 2.1.5. QA/QC

Quality control samples consisted of a series of blanks, field duplicates and certified standards and/or made up standards. These were inserted systematically into a batch of sample sequence at an interval of each tenth sample. QAQC samples were pre-assigned and printed onto sampling sheets and assigned sample tickets were put into the sample packs on which correct sample numbers were labeled accordingly. Sample packets were then filled with the indicated materials at the sample preparation room before dispatch.

### 2.1.6. Threshold

In order to prioritize a possible follow-up it will be necessary in this present work to define different 'orders' of anomalism (1$^{st}$ order, 2$^{nd}$ order and 3$^{rd}$ order). Therefore the anomaly threshold definition will be based on different principles such as literature comparison, standard deviations, spatial analysis and domaining.

### 2.1.7. Data processing and interpretation

Soil sampling data were collected on paper logs in the field, scanned and captured by hand into electronic excel spreadsheets and laboratory assay results were attached next to their soil sample ID's before being loaded and stored in an access database onto the server in CoMiSa Sprl Lubumbashi office. Data were then processed using MapInfo and Surpac softwares for statistical interpretations.

## 2.2. Drilling

Being one of the most expensive techniques, drilling in the present case study was conducted as part of an advanced exploration program and the choice of the method depends on the type of information sought. Marjoribanks (2010) discussed the indications, advantages and disadvantages of different exploration drilling methods (Table 3). Among all drilling methods reverse circulation and diamond were the drill techniques of choice in PR851 area.

Before drilling was implemented in the prospect area, the ground was firstly investigated by different exploration techniques (geophysical surveys, surface mapping, trenching and soil geochemical techniques). Even then target generation after integration of all available geological datasets was conducted prior to drilling.

Table 3: Comparison of drilling methods in mineral exploration (After Marjoribanks, 2010)

| Drill type | Indications | Advantages | Disadvantages |
|---|---|---|---|
| Hand auger | Geochemical sampling in upper few meters of unconsolidated material | Hand portable and operable. Unconsolidated sample, cheap | Poor penetration |
| Power auger (post-hole digger) | Geochemical sampling in upper few meters of unconsolidated material | Small lightweight machine vehicle mounted or hand operated. Better than hand auger. Quick and cheap | Poor penetration Sample contamination |
| Rotary air blast (RAB) | Geochemical sampling to base of regolith. Ideal regolith sampling tool | Large sample volume. No site preparation required. Quick and relatively cheap. Some rock chips give geological data | Poor penetration of hard rocks. Sample contamination, limited depth. No structural data. |
| Air core | Geochemical sampling where good characterization of bedrock required | Small rock core return, minimal contamination, relatively quick and cheap, can penetrate heavy clay/mud | Small sample size |
| Reverse circulation | Geochemical sampling hard and soft rocks to >200m, ore body proving above water table | Uncontaminated large volume sample, rock chip for geological data. Relatively quick and cheap comparing to diamond drilling | Large heavy rig may need access and site preparation, limited to no structural data, poor orientation control |
| Core diamond | Ore targeting and proving to >1,000m, high quality sample, the contents of known ore deposit and potential sites; Geological, structural, petrographic, mineralogical understanding, chemical assay | Maximises geological information, Uncontaminated, undisturbed high recovery sample, accurate hole positioning/control. | Large heavy rig may require access and site preparation, water supply needed, slow, and expensive. |

### 2.2.1. Reverse circulation drilling

Reverse circulation was used to assess undercover regolith and to test geochemical anomalies detected in soils on surface over a suspected potential causative body. It was carried out by Boart Longyear Inc of Zambia. This method is quicker and cost effective in comparison to diamond drilling. Nevertheless reverse circulation in PR851 area required access preparation and was hard to execute in the wet tropical environment conditions. Precautions were taken to avoid sample contamination by using compression air driven percussion hammar drill bit than rotary tricone bit.

Reverse circulation samples were collected, split, and ticketed at the drilling site on a meter by meter basis under my own supervision as a junior geologist at the time of drilling. After preparation, samples were then sent abroad to Genalysis laboratories for analysis and sample rejects stored and kept at the CoMiSa Sprl's in-house sample storage facility in Lubumbashi, Democratic Republic of Congo.

For optimization drill holes were implemented over a selected zone of maximum geochemistry. Figures 15a and 15b illustrate a successful drilling section test over soil geochemical anomaly at RSF area.

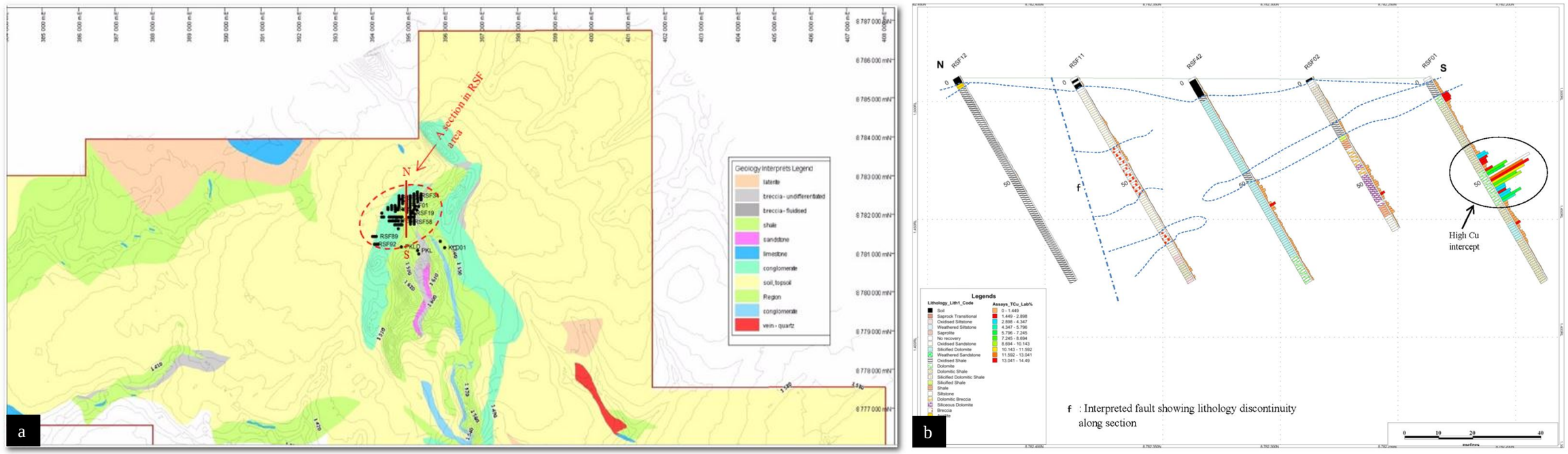


Figure 15: (a) Example of a North-South drill section located at RSF area; (b) Successful interpreted North-South drill section over maximum geochemistry anomalies with respect to reverse circulation holes only. Note that this section was drilled, logged and interpreted by the author of the present work.

### 2.2.2. Diamond drilling

After the potential bodies were detected through destructive drilling, core diamond drilling was used to probe the contents of the known ore deposits and simultaneously to increase the geological knowledge by undertaking lithological, structural (bedding, foliation, fault and fold data), geotechnical, mineralogical and alteration studies.

Core diamond drilling is very expensive and therefore drilling sections were designed with precautions. It was executed following a rectangular drilling pattern to facilitate good statistical coverage for accurate mineral resource estimate.

A logging exercise of diamond drill cores was undertaken on site and core sawing in Lubumbashi from where half core was sampled, bagged, labeled and transported door-to-door by SDV Sprl courier service from Lubumbashi to the accredited Genalysis Laboratory Services.

In PR851 area this drilling method was executed successively by Kluane Drilling of Whitehorse, Yukon, Canada and Ox Drilling of Ndola, Zambia.

## CHAPTER 3: GEOLOGICAL SETTING AND REGIONAL GEOLOGY

### 3.1. Geotectonics

The Lufilian Arc of South-Central Africa (Figure 16) , also called as Katangan Belt, is defined as the curvilinear belt of Neoproterozoic Katangan sediments which was deformed during the Pan African orogeny in the Democratic Republic of Congo and Zambia, and the Westward extension of similar rock sequences into Botswana, Angola and Namibia (Lobo-Guerrero, 2006). Kampunzu et al. (1999) defined the Lufilian Arc as a zone of low to high grade metasedimentary (and subsidiary igneous) rocks of Neoproterozoic age hosting highgrade Cu-Co-U and Pb-Zn mineralization. The Katangan sequences were deposited over a lengthy period of Neoproterozoic time from around 880 Ma (Lower Roan) to less than 590 Ma (Upper Kundelungu) which coincides with the Cryogenian Period, or so-called 'Snowball Earth'.

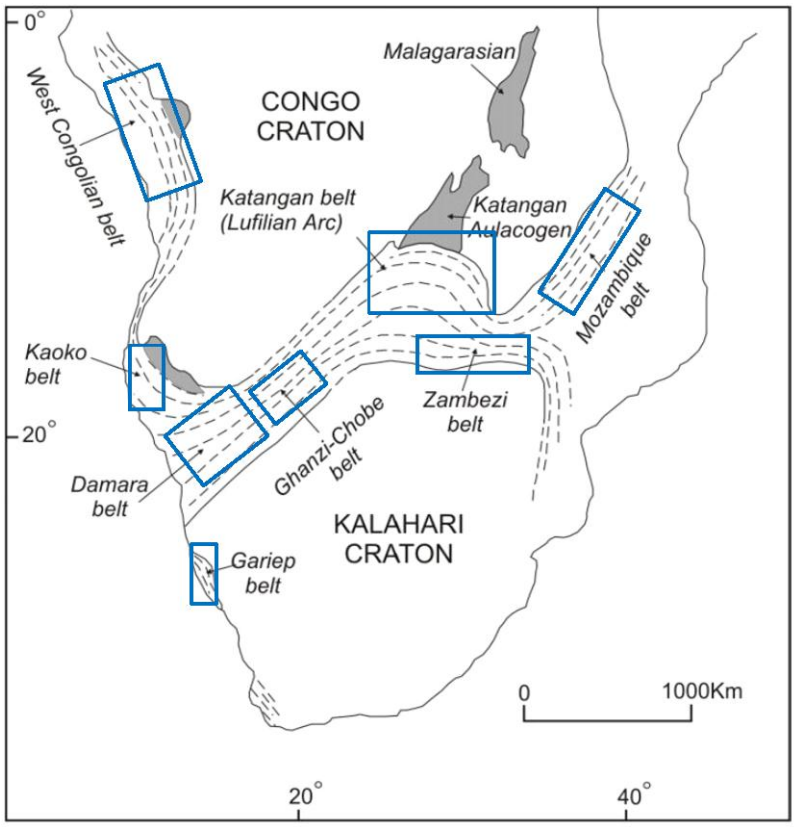


Figure 16: Lufilian Arc of the Central African among other Neoproterozoic Belts in subequatorial Africa (modified after Kampunzu et al., 2000).

During the Lufilian orogeny of Panafrican age, the Katangan Supergroup rocks were folded and thrusted. This main orogeny has been considered as the cause event that led to the assembly of the East – West Gondwana during the Neoproterozoic and early Paleozoic times (Wilson et al., 1997). The Lufilian orogeny produced the arcuate structure of the Katangan Belt that also led to it being called as the Lufilian Arc (Figure 17).

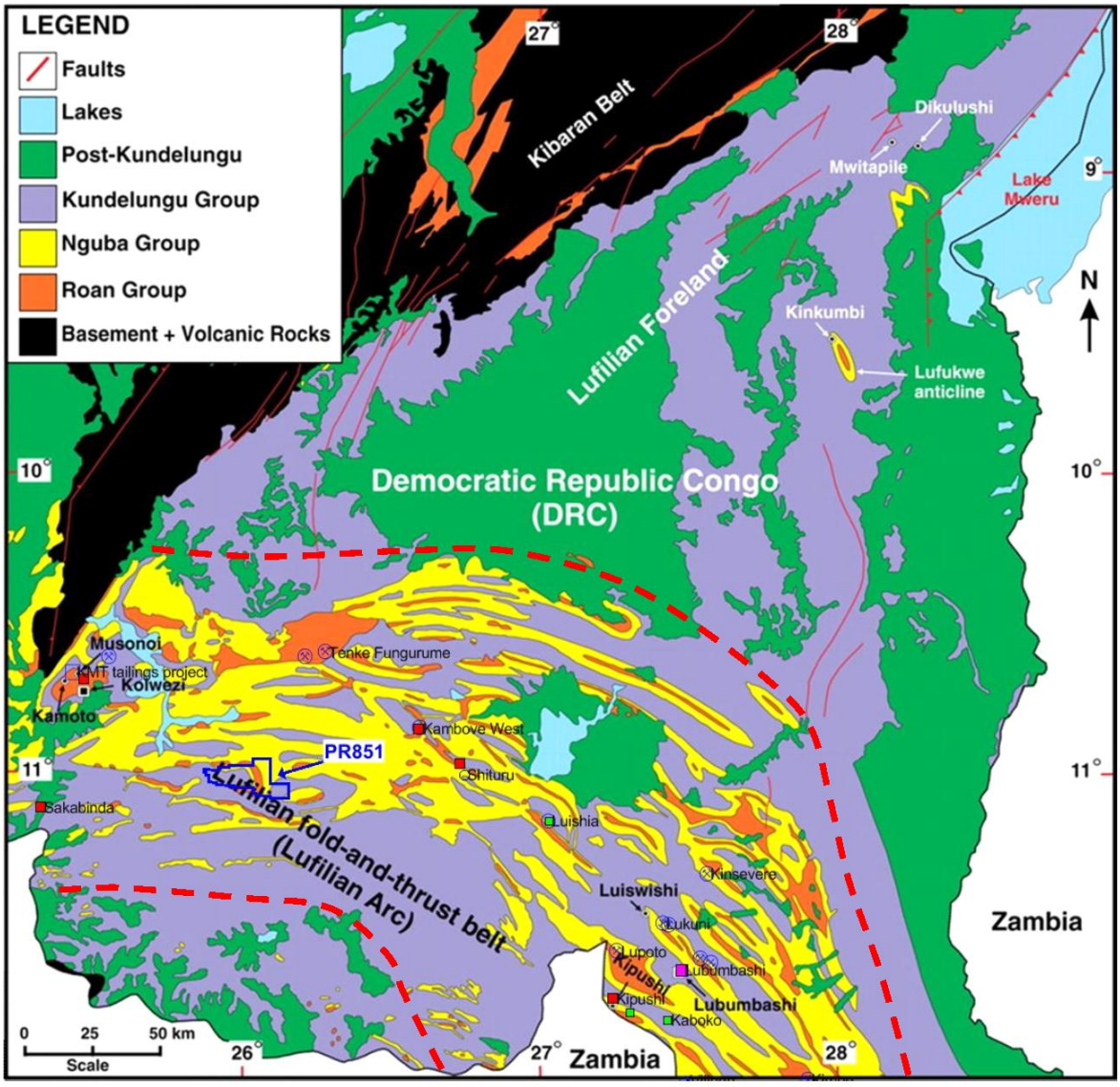


Figure 17: The Lufilian Arc of the Central African Copperbelt in D.R.of Congo including the study area PR851 lease polygon in blue among other surrounding Cu-Co localities. Note the arcuate form of the belt in red dashed line (modified from Lepersonne, 1974).

The Lufilian Arc deforms the Neoproterozoic Katangan sedimentary series in southeast of Democratic Republic of Congo and Zambia in a fold- and thrust belt with large tectonic breccias and abundant brittle deformation structures (Francois, 1987, 1993, 2006; Kampunzu and Cailteux, 1999; Jackson et al., 2003; Wendorff, 2011). Unlike the other Pan-African belts, it is a bent orogeny and hosts the world class Cu-Co mineral deposits. The latter are either stratiform deposits or associated to faults systems (Robert, 1956; Oosterbosch, 1962; Cailteux et al., 2005b; El Desouky et al., 2010).

The Lufilian Arc, its Kundelungu foreland and adjacent Kibaran belt are presently undergoing continental extension and are involved in the poorly defined SW branch of the East African Rift System (Sebagenzi and Kaputo, 2002; Kipata, 2007). The present-day stress field is extensional as determined from the inversion of earthquake focal mechanisms (Delvaux and Barth, 2010). Between the early tectonic stages of the Lufilian orogeny and recent to still active rift-related crustal extension, little is known for this~550 Ma long tectonic evolution which occurred mainly in brittle regime. If the general tectonic evolution of the Lufilian Arc is relatively well documented by regional studies and mining exploration, the brittle faulting evolution has never been analyzed in detail although it is known that it contributed significantly to successive stages of mineral remobization and enrichments led to form the mineral deposits.

De Swardt and Drysdall (1964); Daly et al. (1984) identified three structural zones in the Lufilian Arc (Figure 18), namely (i) the Outer Lufilian corresponding to the Fold-and-Thrust belt mostly located in Katanga, (ii) the Middle Lufilian which is characterized by the Domes region situated in the northern part of Zambia and slightly exposed in the Democratic Republic of Congo along the Congo-Zambia border and (iii) the Inner Lufilian which encompasses a southern synclinorium of Katangan cover entirely located in Zambia. The Kundelungu plateau represents the foreland of the Lufilian arc, squeezed between the Kibaran margin and the Bangweulu block. Grantham et al. (2003) and Dewaele et al. (2008) suggested that the development of the Lufilian arc is linked to the amalgamation of the Gondwana Supercontinent in south-central and eastern Africa during the Pan-African orogeny. Porada and Behorst (2000); Frimmel et al. (2011) argued that it formed, together with the Zambezi belt, during collision between the Congo and Kalahari cratons around 650-600 and 530 Ma, peaking at ~ 550 Ma and ending at ~ 530 Ma.

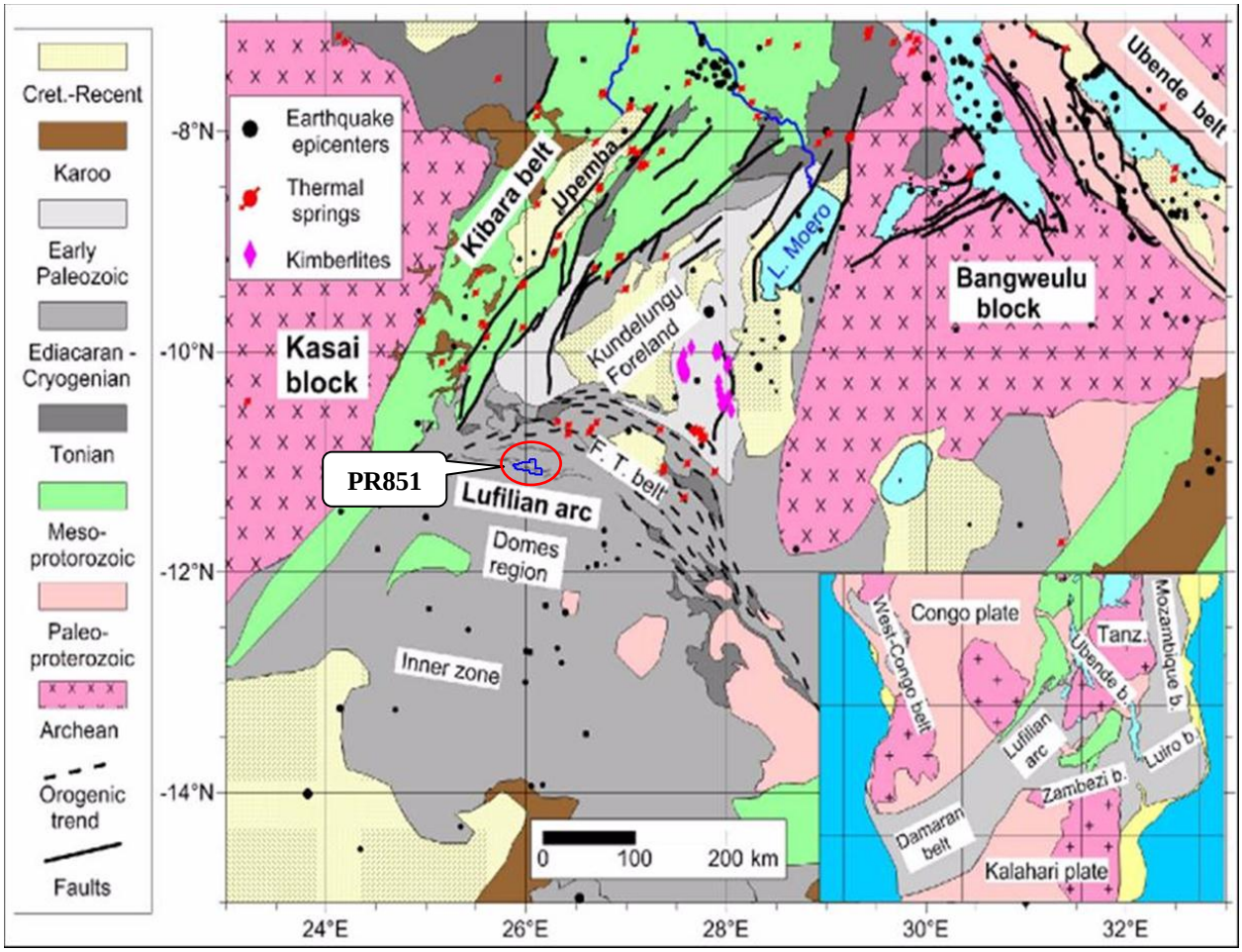


Figure 18: Geological and tectonic framework map of the Lufilian arc, Kundelungu foreland and Kibaran belt and surrounding regions with structural subdivisions of the Lufilian arc (after Kampunzu and Cailteux, 1999 in Kipata et al., 2013

Note PR851 lease blue polygon circled in red. Location of Eocene-Oligocene Kimberlite pipes in the Kundelungu plateau (from Batumike et al., 2008 in Kipata et al., 2013) thermal springs (after Robert, 1956 in Kipata et al., 2013) and seismic epicentres (USGS, IRIS and South African catalogs). Source: Kipata et al. (2013).

## 3.2. Regional geology

### 3.2.1. Lithostratigraphy

The sediments in the Lufilian Arc and its forelands were deposited during the Neoproterozoic in a Paleo- to Mesoproterozoic basement. Sediments started to be deposited in an intra-cratonic rift (Porada et al., 2000 and Unrug, 1988) but Jackson et al. (2003) believed in sedimentation within an epicontinental marine embayment. These sediments were affected and deformed during the Lufilian orogeny (Cahen et al., 1954; Kampunzu and Cailteux, 1999; Porada et al., 2000). The exposed region of the Lufilian Fold-and-Thrust belt and its foreland are bordered by the Archean-Paleoproterozoic Bangweulu block to the Southeast, the Paleoproterozoic Ubende belt to the East and the Mesoproterozoic Kibaran belt to the West (Figure 18). The Katangan Supergroup overlies the kibaran basement with a basal unconformity to the North and North-West (Cahen, 1954; Kokonyangi et al., 2006).

The Katangan Supergroup is believed to have been deposited in an extensional rift context and consists of a 7 to 10km thick sequence (Kampunzu and Cailteux, 1999; Cahen, 1954). The subdivision of the Katangan Supergroup has been progressively a debate over time. Previously it was subdivided from bottom upwards into three Groups, namely (i) the Roan Group, (ii) the Lower Kundelungu Group and (iii) the Upper Kundelungu Group (Cailteux et al., 1994). Actually based on the presence of two well exposed diamectites of regional significance (Cailteux et al., 2005a), the Katangan Supergroup is divided from the bottom to the top into Roan Group, Nguba Group (formerly known as Lower Kundelungu Group) and Kundelungu Group (previously identified as Upper Kundelungu Group, (Figure 19). The two diamectites, the Grand-Conglomerat at the base of Nguba Group and the Petit-Conglomerat at the base of Kundelungu Group have been largely considered as regional markers.

| SIMPLIFIED STRATIGRAPHY OF THE LUFILIAN ARC | | | | | | |
|---|---|---|---|---|---|---|
| Age (Ma) | Supergroup | Group | Formation | Local Name | Description | Thickness (m) |
| ~ 320 | Karoo | | | | | |
| 650 | KATANGA | KUNDELUNGU | | | Sediments, at base limestones, calcschists grading into shales, sandstones at base Petit Conglomerat | 30 - 50 |
| 750 | | NGUBA | | | Sediments, sandstones and shales, at base Grand Conglomerat | 200 - 500 |
| 850 | | ROAN | Mwashya (R4-1and 2) | MWASHYA | Shales, siltstone, sandstone to dolomites, limestones, oolithic, jasper and frequently siliceous beds and cherts | 50 -100 |
| | | | Dipeta (R3-2) | DIPETA | Shales and sandy schists with intercalated dolomites and limestones | 1000? |
| | | | Dipeta (R3-1) | RGS | Roches Greseuse Superieur, dolomitic shales and sandy schists, towards top beds of silicified dolomites | 100 -200 |
| | | | Mines (R2-3) | CMN | **Calcaire a Minerais Noirs**, light coloured dolomites with thin beds of white sandstone argilitic dolomites alternating with schists, sometimes graphitic and two collenia (stromatolite) horizons locally, at base dolomitic sandstones | 130 |
| | | | Mines (R2-2) | SDS | **Schistes Dolomitic Superieur**, upper dolomitic shales, subdivided as follows:-<br>SD 3b finely laminated black, graphitic shales, highly micaceous, sandy dolomites<br>SD 3a micaceous, sandy shales, dolomitic, grey-green, well bedded<br>SD 2d shale, dolomitic and graphitic<br>SD 2c shale, dolomitic and sandy, grey-green<br>SD 2b dolomite, massive, light coloured, collenia (stromatolitic) dolomite<br>SD 2a dolomitic, graphitic black shale, micaceous<br>SD 1b BOMZ (Black Ore Main Zone) blue-grey, crystalline dolomite | 50 -80 |
| | | | Mines (R2-1) | SDB | SD 1a **Schistes De Base**, shale dolomitic, well bedded, micaceous, light grey nodule horizons at base | 10 -15 |
| | | | | RSC | **Roches Silicieuses Cellulaire**, massive, crystalline light coloured dolomite, black crystals present (heterogenite ?), locally developped collenia horizons, occasionally shales at bottom and top, extreme cellular weathering | 12 -25 |
| | | | | RSF | **Roches Silicieuses Feuilletees**, siliceous, dolomitic shales, micaceous, light-grey weathering whitish, extremely finely laminated | 5 |
| | | | | D STRAT | **Dolomie Stratifiee**, argilitic dolomite, well bedded to laminated, light-grey in colour light-brown, yellow weathering, chert horizons, nodule layer towards top | 3 |
| | | | | RAT grises | **Roches Argilleuses Talceuse**, argilitic sandstones, massive and dolomitic, light-grey talc present in varying quantities | 2 -5 |
| | | | R.A.T. (R1) | RAT 2 | **Roches Argilleuses Talceuse**, argilitic siltstones, dolomitic, banded to well bedded containing beds of dolomitic sandstone and occasionally beds of collenia (stromatilitic) | 190 |
| | | | | RAT 1 | **Roches Argilleuses Talceuse**, upper portion silty argillite, red and bedded. Lower portion unknown | 40 |
| | | | | POUDINGUE | Unknown formation, transgression conglomerate and arkoses in other localities | ? |
| 1000 | 883±10 Ma Nchanga granite | | | | | |
| | Paleo- & Mesoproterozoic | | | | | |

Figure 19: Simplified stratigraphy of the Lufilian Arc (modified from Cailteux et al., 2005a, 2005b, 2007; Batumike et al., 2007 from Kipata et al., 2013 and Africo, 2013).

### *3.2.1.1. Roan Group*

This Group is mainly composed of carbonate and siliciclastic rocks and is divided into four Sub-groups from bottom upwards (i) Roches Argilo-Talqueuses (R.A.T. or R1), (ii) Mines (or R2), (iii) Dipeta (R3) and (iv) Mwashya (R4).

- The R1 Sub-group, called the Roches Argilo-Talqueuses (R.A.T.) Sub-group consists essentially of massive or irregularly stratified detrital formations with hematite present as authigenic plates and red pigment, attesting to the primary oxidizing conditions (Cailteux, 1994). The base of the Roches Argilo-Talqueuses (R.A.T.) Sub-group in the southern part of Katangan Province in the Democratic Republic of Congo has been subject to controversy. Most authors (Francois, 1973b, 1974; Intiomale, 1982) did not find any equivalent of the basal Roches Argilo-Talqueuses as described in Zambia in the Katanga Province. Nevertheless, a polymictite conglomerate, composed in most cases of clasts from the Kibaran Supergroup, occurring in the western Katangan belt has been interpreted to be the basal part of the Katangan Supergroup (Buffard, 1988). A more detailed subdivision of the Roches Argilo-Talqueuses Sub-group (Francois, 1973b and Intiomale, 1982) comprises three formations in ascending order: R1.1 composed of conglomerate, siltstones and shales; R1.2 made up of siltstones, dolomitic shales and dolomites and finally R1.3 which consists of dolomitic sandy shales, shales and siltstones.

  The sedimentary transition to the Mines Subgroup is continuous at some certain localities whereas a tectonic breccia developed at the contact in other places. This tectonic breccia which formed during the detachment of the Mines Subgroup, aided by fluidization of evaporitic material, probably present near the top of the R.A.T. Sub-group (Cailteux and Kampunzu, 1995 cited by Batumike, 2004 unpubl.).

- The R2 Sub-group, also called the Mines Sub-group is a carbonate package unit that hosts the richest important stratiform Cu-Co-U mineralization. Cailteux (1994) subdivided the Mines Sub-group (R2) into three formations (from bottom to top): The Kamoto formation (R2.1) made up of chloritic to dolomitic siltstones, dolostones and laminated or massive siliceous rocks; the Dolomitic Shales formation (R2.2) formed of impure and/or stromatolitic dolostones, arkoses or feldspathic sandstones, shales and dolomites; and the Kambove formation (R2.3) is composed of organic matter-rich dolostones with chloritic and dolomitic siltstones.

- The R3 Sub-group, also called the Dipeta Subgroup consists of sandstones, siltstones, dolomitic shales, arkoses and psammites. Cailteux (1994) subdivided this Sub-group into R3.1, R3.2, R3.3 and R3.4. Dolostones and siltstones (known as 'Roches Greseuses – Siliceuses'); stromatolitic beds characterize the R3.1, R3.2 and R3.4 respectively whereas the upper zone of the R3.3 is formed by limestones and oolites. The Dipeta Sub-group (R3) is affected by tectonic discontinuities and associated breccias within the Katangan belt (Batumike, 2004 unpubl.). Cailteux (1994) and Hitzman et al. (2012) stated that after the deposition of the Mines Sub-group, a regression occurred during the Dipeta (R3) Sub-group sedimentation period which deposited siliciclastic rocks including oxidized hematitic & dolomitic siltstones and sandstones pretty similar to R.A.T. facies.
- The R4 Sub-group known as the Mwashya Sub-group is subdivided into two formations according to Francois (1973b): the Lower Mwashya (R4.1) and the Upper Mwashya (R4.2). From Cailteux (1994) the R4.1 is marked by the presence of dolostones. But nodular dolomitic and carbonaceous shales, silicified dolostones, jaspers, siltstones, feldpathic sandstones, oolitic and hematitic-magnetitic beds occur at the top of the formation whereas the R4.2 is characterized by fine and sandy beds at the base. In areas, a very typical conglomerate called 'Conglomerat de Mwashya' demarcates the Lower from the Upper Formations (Van den Brande, 1932b cited by Batumike, 2004 Unpubl.). The Mwashya Sub-group was deposited between 760 and 735 Ma (Master et al., 2005).

The continuous stratigraphic sequence for the Roan group, as proposed by François (1974) and Cailteux (1994) has been largely contested by some authors. Porada and Berhorst (2000) agreed that the Roches Argilo-Talqueuses was deposited on the pre-Katangan basement, but they believe that the overlying Mines (R2), Dipeta (R3) and Mwashya (R4) Subgroups form a platform facies association, which became a Copperbelt-type tectonostratigraphical succession through the development of foreland propagating thrust faults.

Considering Wendorff (2000, 2005) views, he does not interpret the brecciated contacts as being of a tectonic origin. He proposed that they should be called conglomerates derived from erosion of advancing thrust sheets during the Lufilian orogeny. The R.A.T. and the Dipeta Groups are olistostromes, deposited at the border of the developing Lufilian Orogen (Wendorff, 2005).

Nevertheless in contrast to the disagreement about the stratigraphy of the Roan most of all authors agree that sedimentation of the Nguba Group started with the deposition of a diamictite -

the Grand Conglomérat, which likely formed part of the Sturtian glacial deposits (Kampunzu et al., 2005). François (1974) observed that the 'Grand Conglomérat' thickens towards the north and is at least observed as far north as Pweto, which is a town to the north of Dikulushi (Cahen, 1954).

#### *3.2.1.2. Nguba Group*

It begins with the diamictite formation, the 'Grand Conglomerat', representing a regional stratigraphic marker for this particular group within the entire region of the Katangan Belt. The 'Grand Conglomerat' also indicates the limit with the underlying Roan Group. Two Subgroups, (i) the Likasi (Ng1) and (ii) the Monwezi (Ng2) characterize the Nguba Group in the Katangan Belt of the Central African Copperbelt. Cailteux (1994) distinguished further subdivisions within each of the two Subgroups. The Grand Conglomerat, at the base of the Likasi Sub-group, is a 100 to 950m thick diamictite within the Katangan Belt (Francois, 1973b) with angular to rounded clasts ranging from mm to 50cm in diameter poorly sorted in a muddy matrix which becomes more carbonaceous towards the southern part of the Katangan Belt.

The Likasi Subgroup contains a combination of shale and dolomite in the south and a lateral facies change towards pure shale in the north of the basin (François, 1974). In the middle of the Likasi Subgroup the Kakontwe limestone formation is only observed towards the south in the Lufilian belt. This Kakontwe limestone formation could be a cap carbonate, supporting the interpretation of the 'Grand Conglomérat' as a glacial tillite (Porada and Berhorst, 2000).

Stratigraphically situated on top of the Likasi Sub-group, the Monwezi Sub-group was deposited to the end of the Nguba and is made up of more detrital lithologies with relatively thin arkose layers in the north and thick, slightly carbonatised pelites and fine sands in the south (François, 1974). An overlying diamectite, the 'Petit Conglomerat' seals the upper boundary of the Nguba Group indicating the transition to the overlying Kundelungu Group. The 'Petit Conglomerat' forms part of the lower Sub-group of the Kundelungu Group, the Kalulwe Sub-group. It has been suggested that the 'Petit Conglomerat' layer could have been deposited during the Marinoan-Varanger ice age (http://edit.africamuseum.be/geco_website/?page=katanga-geology).

### *3.2.1.3. Kundelungu Group*

The Kundelungu Group starts with the diamictite called 'Petit Conglomerat' which constitutes a regional lithostratigraphic marker which also shows the upper boundary of the underlying Nguba Group. This Kundelungu Group forms the upper part of the Katangan Supergroup and is being subdivided into three Sub-groups (i) the Kalule (Ku1), (ii) the Kiubo (Ku2) and the Plateaux (Ku3). With reference to Cailteux (1994) each Sub-group of the Kundelungu Group is divided into different formations based on lithology changes.

The Kalule Subgroup is similar to the Likasi Subgroup, since it also contains a thin cap carbonate (the 'Calcaire Rose') overlying the 'Petit Conglomérat'. The Kalule Subgroup becomes more detrital towards its top, with the deposition of dolomitic siltstones, sandy shales and pink oolitic limestone. The 'calcaire rose' is, unlike the Kakontwe limestone from the Likasi Subgroup, continuous from the south to the north, with a layer thickness of around 5m (François, 1974). The Kiubo Subgroup overlies the Kalule Subgroup and consists of sandstones and shales (Cailteux et al., 2005), arkoses, siltstones, and sandy shales (Batumike, 2004 unpubl.). The top of the Kundelungu group is formed by the Plateau Subgroup that consists of shales, arkoses (http://edit.africamuseum.be/geco_website/?page=katanga-geology); feldspathic sandstones, siltstones and shales containing dolomite or limestone beds which rocks are reddish and generally subhorizontal and cropping out only in the extreme northern side of the Katangan Belt (Batumike, 2004 unpubl.).

## 3.2.2. Structure

Structural analysis from some open casts and underground mines in the Katanga fragment of the Central African Copperbelt led by Cailteux et al. (1999) established and confirmed three major successive deformation phases:

The first phase (D1) called *"Kolwezian phase"* which developed folds and thrust sheets with a northward transport direction. This phase occurred in the Lufilian Arc between ca. 800 and 710 Ma with a peak in the range of 790-750 Ma (Kampunzu and Cailteux, 1999). Batumike (2004, unpubl.) stated that the related D1 folds are characterized by NW-SE trend and predominantly northeastward vergence observed between Ndola and Likasi areas; NE-SW trend and predominantly northwestward vergence between the southwestern end of the belt and Kolwezi area and a well-marked E-W trend in the central and northernmost part of the Lufilian Arc, including as well as southward facing folds. These orientations indicate a shortening direction

that is consistent with the pattern of folding marking a NE-SW compressive event in the eastern part of the Lufilian Arc observed in the present day;

The second phase (D2) called *"Monwezi phase"* including several large left-lateral strike-slip faults which have been activated successively. It is during this deformation period of time that the eastern bloc of the belt rotated clockwise showing the actual day North-West/ South-East trend of D1 structures in this portion of the Lufilian Arc generating its convex geometry. This deformation (D2) occurred between ca.690 and 540 Ma, and is correlated with the ca. 650 Ma orogenesis in the Damara belt (Miller, 1983; Kampunzu and Cailteux, 1999). This lengthly period of deformation is attributed to the migration of strike-slip faults developed sequentially from south to north and probably also to low convergence velocity during the collision between the Congo and Kalahari cratons (Kampunzu and Cailteux, 1999);

The third deformation (D3), a late event is called the "Chilatembo phase", is marked by structures transverse to the trends of the lufilian arc. It is mainly characterized by North-East/ South-West trending syncline (e.g. chilatembo syncline) representing transverse structure in regional scale. Large, open and upright folds trending NNE-SSW up to ENE-WSW, and N-S, E-W trending faults characterize this phase in some mine areas in the Democratic Republic of Congo such as Etoile, Luiswishi and Luisha (Batumike, 2004 unpubl.). This is younger than 540 Ma and probably early Paleozoic (Kampunzu and Cailteux, 1999).

On the tectonic point of view, a more complete classification was proposed by Unrug (1988), who distinguished five tectonic domains in the Katangan belt of the Lufilian Arc which are known as:

a. The 'External Fold-Thrust Belt' or Domain I, marked by the pilling up of nappes (Kolwezi, Mamfwe areas …). The Mines Sub-group deposits are constricted between two thrust horizons. The roof thrusts are most generally folded. A tectonic breccia demarcates the Mwashya and Roan Groups (The allochthonous Mine Sub-group), (Porada and Berhost, 2000);
b. The 'Domes area' or Domain II, which is represented by several pre-Katanagn basement inliers;
c. The 'Synclonorial Belt' or Domain III, poorly exposed but define large fold structures at a low metamorphic grade;

d. The 'Katanga high' or Domain IV, poorly known but would correspond to the opposite active continental margin of an "Angola plate" (Porada, 1989), and

e. The 'Katangan Aulacogen', also called 'Golfe du Katanga' or Domain KA (Figure 19a) or Domain V, which acted as the foreland during the northward thrusting in the external zone of the Lufilian Belt (Figures 20 and 21).

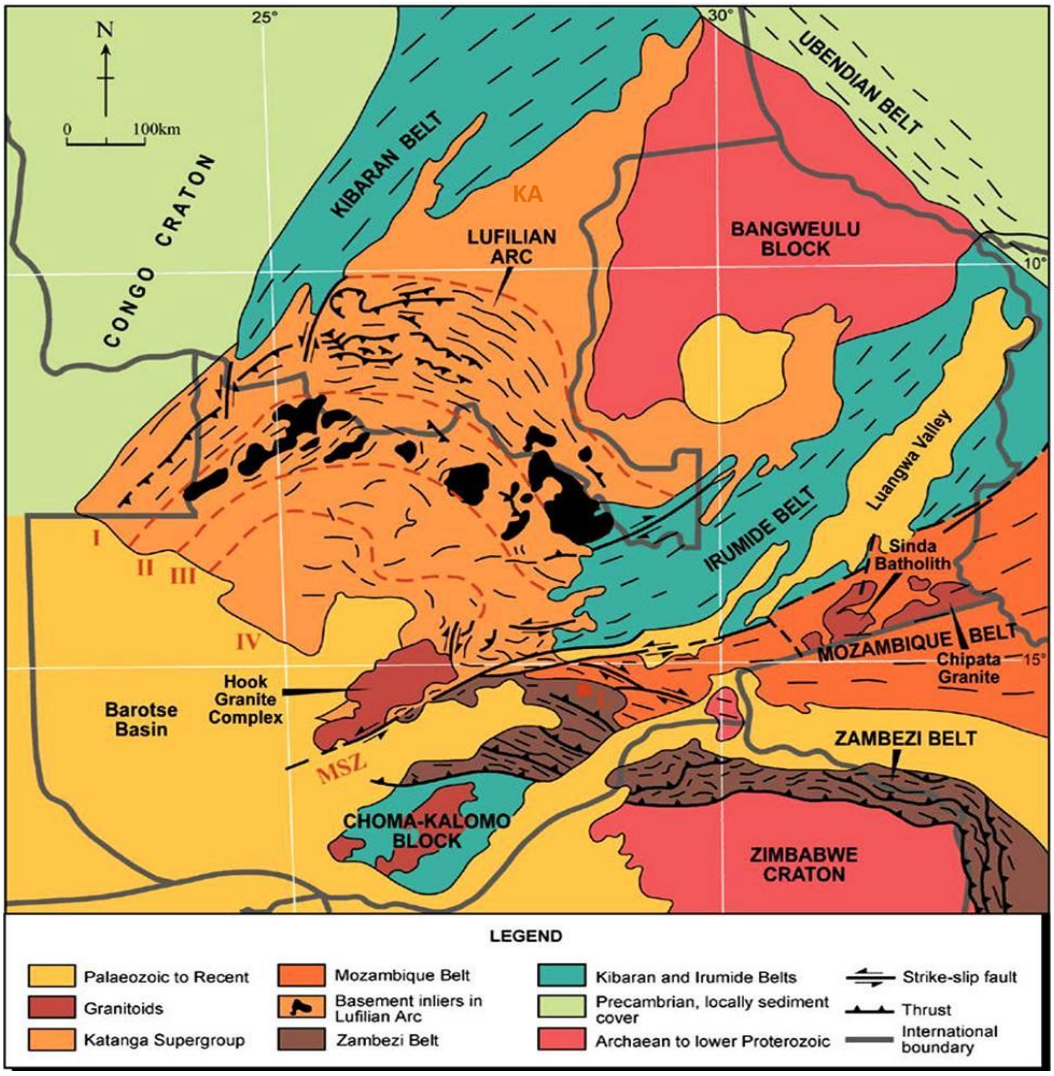


Figure 20: Structural subdivision of the Lufilian Arc (After Porada, 1989).

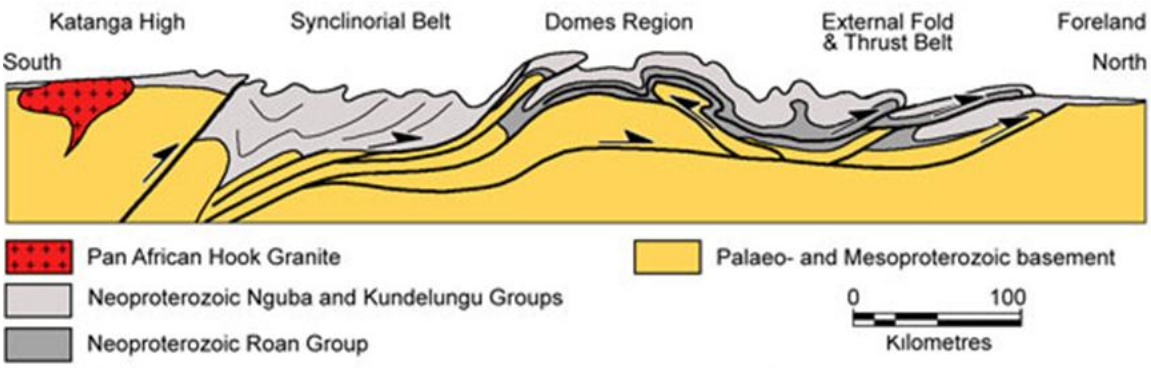


Figure 21: Illustration of a North-South section through tectonic domains of the Lufilian Arc from Democratic Republic of Congo to Zambia (After Bernau, 2007; Selley et al., 2005 and Porada, 1989).

### 3.2.3. Magmatism

The basement of the world class Cu-Co deposits of the Katangan Belt is regarded as a magmatic arc copper enriched in itself and therefore it does have implications for ore-forming models in the region. The chemical characteristics and new U-Pb SHRIMP zircon age data from the basement of the Katangan Sequence in the Central African Copperbelt confirm the existence of a Palaeoproterozoic calc-alkaline volcanic arc (Rainaud et al., 1999). Despite having a strike length of 880km, the Central African Copperbelt in the Lufilian Arc of the Katangan Belt in the Democratic Republic of Congo and in Zambia, has its basement mainly exposed in the Zambian Copperbelt and within the immediate surrounding areas of Katanga. But some exposures of this basement have been observed and is mainly dominated by the granitoids whereas the other half of it consists of Muva complex and Lufubu schists. On one hand, in the Zambian Copperbelt; Rainaud et al. (1999) argued that the Lufubu schists are calc-alkaline metavolcanics with composition ranging from trachyandesite to rhyodacite and rhyolite, the granitoids intruded in the schists range in composition from biotite granites to quartz monzonites, granodiorites and tonalites (Mendelsohn, ed., 1961), the provenance for the Muva sediments clearly shows both the local Palaeoproterozoic basement and Archaean crust as well (Rainaud et al., 1999). On the other hand, the Pre-Neoproterozoic basement rocks migmatites, reworked Archean to Mesoproterozoic metagranites, metavolcanic and metasedimentary units from Katangan Belt in the Democratic Republic of Congo, occur within the two northeast-trending belts located at the northwestern (Kibaran) and southeastern (Irumide) peripheries of the Lufilian Fold (Hanson, 2003; Johnson et al., 2005). Selley et al. (2005) discussed that the extension associated with early rifting led to the development of isolated fault-controlled basins and subsequent linkage of these basins along

master faults at the time of Copperbelt Orebody Member deposition. A later period of extension occurred during late Mwashya to early Kundelungu time (~765–735 Ma) and is associated with limited mafic magmatism. Also the lack of volcanism in the lowermost, synrift rock units of the Katangan Supergroup favors initial basin evolution during a time of relatively subdued crustal heat flow and attenuation. In brief, Rainaud et al. (1999) concluded that the Katangan Sequence hosting the world-class Cu-Co mineralization of the well-known Central African Copperbelt, overlays a basement which comprises a Palaeoproterozoic calc-alkaline magmatic arc, tonalite-granodiorite gneisses at Mkushi and more granitoids in Mufulira and Chambishi areas which indicate the plutonic phases of a major intermediate to acid volcanic region emplaced between 2050 – 1950 Ma ago.

### 3.2.4. Metamorphism

During the Lufilian Orogeny the Katangan Sequences underwent regional metamorphism associated with major deformation phases. This regional metamorphism of lower greenschist facies is characterized by the development of phyllosilicates, feldspars, carbonates and quartz (Chabu, 1990). Drysdall et al. (1972) demonstrated that there is an increasing degree of regional metamorphism. From prehnite-pumpellyite facies in the northern boundary of the Katangan Sequence of the Lufilian Belt in the Democratic Republic of Congo (Lefebvre and Patterson, 1982), up to medium-pressure amphibolite facies metamorphism in the southern part of the copperbelt, near the domes area within the northern part of Zambia (Ramsay and Ridgeway, 1986). High pressure eclogites and whiteschists occur south of the Domes area (Vrana et al., 1975). Kampunzu et al. (1999) established that a major southward dipping thrust contact demarcates the high pressure Katangan metamorphic assemblages in the south to southwest of the Domes area and other medium-pressure to low-pressure metamorphic complexes located in the north of the Domes area. The presence of silicates such as chlorite, clay minerals, talc, micas favor for a regional metamorphism of lower greenschist facies within PR851 area.

### 3.2.5. Mineralization

The Central African Copperbelt is the world's class largest sediment-hosted stratiform copper districts on Earth. It has high grade sedimentary copper provinces, located at different stratigraphic levels in the Katangan belt (Hitzman et al., 2012) (Figure 22) and contains close to 200 Mt of copper produced or in reserves and the world's largest reserves of cobalt (Table 4) (Lydall and Auchterlonie, 2011; Cox et al., 2007). A total resource of 6 Mt of cobalt is an equivalent to more than 50% of the total world production (Cailteux et al., 2005). The most important copper and cobalt minerals of orebodies in the Central African Copperbelt occur in form of chalcopyrite and/or bornite for Cu and carrolite for Co.

The Central African Copperbelt also contains very important deposits of other metals such as nickel, zinc, lead and uranium. These deposits within the Central African Copperbelt present differences but they are all a result of an evolving basinal system and all can be related to processes observed in other sedimentary copper districts (Hitzman et al., 2005). In the Democratic Republic of Congo, the Congolese Copperbelt is estimated to have over 85 Mt of combined and reserves of Cu (Hitzman et al., 2005) contained in three large deposits (Tenke-Fungurume, Kolwezi and Kamoa) and in a number of smaller deposits. In contrast to Cu reserves in the Democratic Republic of Congo, the Zambian Copperbelt contains six large deposits (Konkola-Musoshi, Nchanga-Chingola, Nkana-Mindola, Mufulira, Luanshya-Baluba and Chambishi), with combined production and reserves/resources totaling approximately 100 Mt Cu (Hitzman et al., 2005). Beside three other large deposits (Sentinel, Lumwana and Kansanshi) are known in the North-Western Province of Zambia with a combined production and reserves/resources of nearly 9 Mt of Cu (Hitzman et al., 2005).

The origin of Cu-Co ore deposits like any other mineralization in the Central African Copperbelt has been under ongoing debate through the time (Sweeney and Binda, 1994).

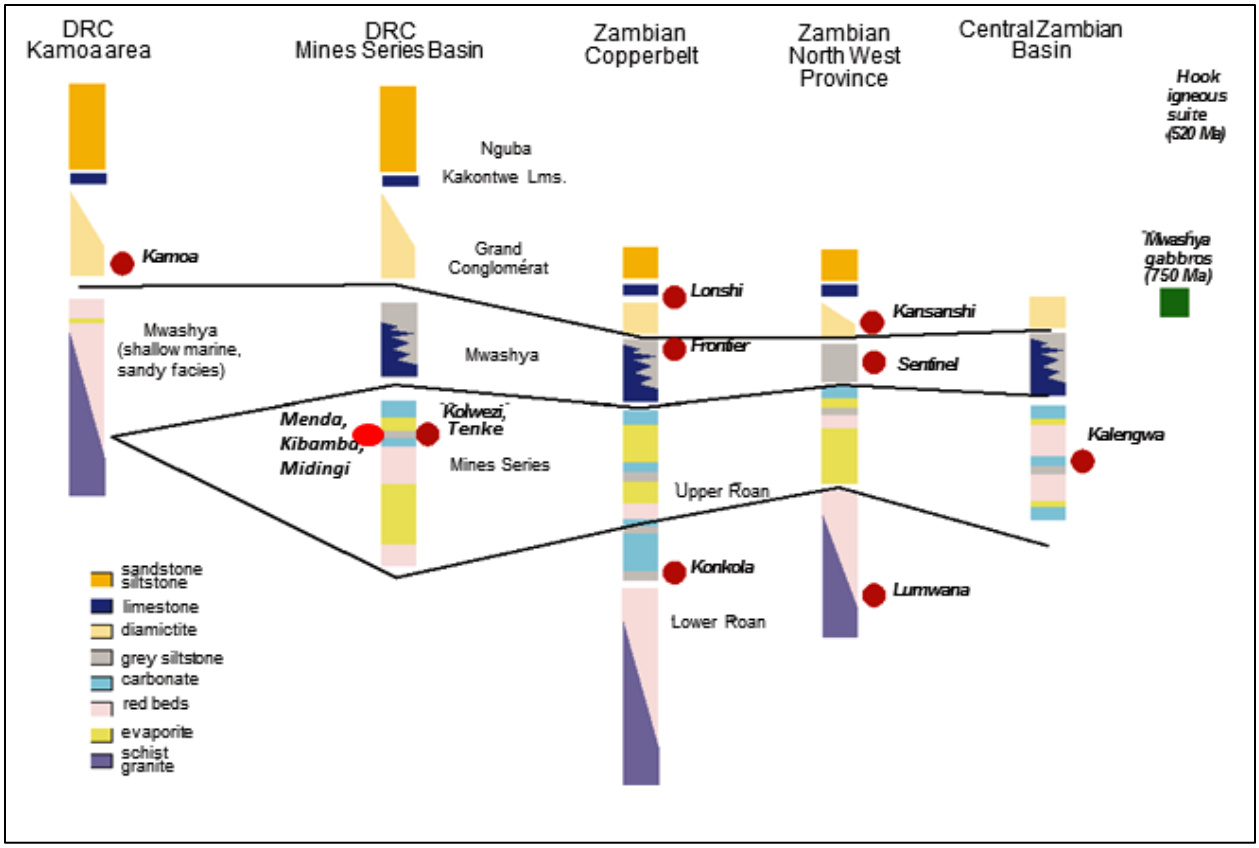


Figure 22: Illustration of highly generalized stratigraphic correlation between the Congolese Copperbelt, Zambian Copperbelt and North-Western Province in Zambia of selected Cu-Co deposits. Note that Menda and Midingi deposits border with PR851 area whereas Kibamba Cu-Co deposit is inside PR851 area (modified after Hitzman et al., 2012).

Table 4: Cu-Co contained, production and reserves in the Central African Copperbelt (Hitzman et al., 2005)

| Deposit | Latitude/ Longitude | Contained Cu (Mt) | Production and reserves (Mt, ore)[1] | % Cu | Grade other metals | Dominant sulfide mineralogy |
|---|---|---|---|---|---|---|
| Zambian Copperbelt | | | | | | |
| Chambishi (main and west) | 28.047 / -12.659 | 3.1 | 123.9 | 2.55 | 0.12% Co | Chalcopyrite, bornite |
| Chibuluma (East and West) | 28.106 / -12.824 | 1.6 | 36.4 | 4.26 | 0.19% Co | Chalcopyrite |
| Fishtie (Kashime) | 29.409 / -13.356 | 0.5 | 41 | 1.25 | | Chalcocite |
| Frontier | 28.473 / -12.732 | 2.1 | 182.1 | 1.16 | | Chalcopyrite |
| Konkola-Musoshi | 27.797 / -12.347 | 26.8 | 894 | 3 | | Chalcopyrite, bornite |
| Luanshya-Baluba group | 28.330 / -13.093 | 10.1 | 406.5 | 2.66 | Baluba: 0.15% Co | Chalcopyrite, bornite |
| Lonshi | 28.941 / -13.178 | 1.5 | 42 | 3.6 | | Chalcocite |
| Mufulira | 28.241 / -12.528 | 10.5 | 332.1 | 3.15 | | Chalcopyrite, bornite |
| Nchanga-Chingola group | 27.843 / -12.507 | 23.4 | 1082.5 | 2.16 | Nchanga Upper orebody: 0.48% Co | Chalcopyrite, bornite |
| Nkana-Mindola group | 28.195 / 12.834 | 15.3 | 612.7 | 2.5 | 0.13% Co | Chalcopyrite, bornite |
| Samba | 27.833 / 12.717 | 0.3 | 50 | 0.5 | | Chalcopyrite |
| Congolese Copperbelt | | | | | | |
| Kakanda group | 26.399 / -10.730 | 1.3 | 41.3 | 3.13 | 0.14% Co | Chalcopyrite, bornite, carrolite |
| Kambove-Kamoya group | 26.602 / -10.884 | 2.5 | 44.5 | 5.7 | 0.2% Co | Chalcopyrite, bornite, carrolite |
| Kamoa | 25.256 / -10.751 | 21.8 | 810 | 2.69 | | Chalcopyrite, bornite, chalcocite |
| Kinsevere group | 26.602 / -10.884 | 1.6 | 41 | 3.84 | 0.25% Co | Chalcopyrite |
| Kipushi | 27.237 / -11.760 | 4.4 | 68.9 | 6.3 | 11% Zn, 1% Pb, 160 g/t Ag | Chalcopyrite, bornite, sphalerite |
| Kisanfu | 25.950 / -10.780 | 1.3 | 55 | 2.32 | 1.08% Co | Chalcopyrite, bornite, carrolite |
| Kolwezi district | 25.412 / -10.718 | 32.5 | 726 | 4.48 | 0.33% Co | Chalcopyrite, bornite, chalcocite, carrolite |
| Luishia-Kasongwe group | 27.009 / -11.173 | 1.8 | 62.9 | 2.82 | 0.09% Co | Chalcopyrite, bornite, carrolite |
| Luiswishi | 27.438 / -11.517 | 0.5 | 12.4 | 4.32 | 0.95% Co | Chalcopyrite, bornite, carrolite |
| Tenke-Fungurume district | 26.237 / -10.606 | 19.1 | 547 | 3.5 | 0.27% Co | Chalcopyrite, bornite, chalcocite, carrolite |
| Kwatebala deposit (Tenke-Fungurume district) - included in above | 26.160 / -10.380 | 3.5 | 105 | 3.31 | 0.29% Co | Chalcopyrite, bornite, chalcocite, carrolite |
| North West Province | | | | | | |
| Kansanshi | 26.428 / -12.093 | 3.3 | 261.4 | 1.25 | 0.17g/t Au | Chalcopyrite |
| Lumwana group | 25.814 / -12.235 | 7 | 1073.9 | 0.65 | | Chalcopyrite |
| Sentinel | 25.312 / -12.259 | 5.3 | 1047 | 0.51 | | Chalcopyrite |

1 Additional production and resources figures for many of the deposits are included in Hitzman, M. W., et al., 2005
2 Approximate dimensions not given for deposits hosted in blocks of Mines Subgroup rocks in the DRC (allochthonous) as geometries of the blocks Commonly highly complex

### *3.2.5.1.Genetic model for Cu-Co mineralization in the Central African Copperbelt*

In the Cu-Co ore forming processes of the stratiform-type of mineralization in the Central African Copperbelt, structures (faults & folds) and host-rocks are the most important control factors to be established. The structural relationships between the sulphide mineralization and the host-rock stratigraphy are vital in order to interpret the origin, the timing and the source of ore formation (Tillberg, 2012).

Cailteux et al. (2005) established that the stratiform Cu-Co mineralization is deposited in the lower part of the Roan Group. The Democratic Republic of Congo-type ores are hosted in dolomites and dolomitic shales whereas in Zambia an argillite shale sequence and a siliciclastic rock unit composed of arenites close to the underlying pre-katagan basement hosts 70 and 30% respectively of the ores (Selley et al., 2005).

It is believed that the ores were deposited in several stages during a prolonged time interval including diagenetic, synorogenic, post-orogenic precipitation and synorogenic remobilization as well. Because of the structural, chemical and mineralogical differences, it reflects the variance in ore forming and remobilization processes (Tillberg, 2012).

- Syn-and diagenetic mineralization:

Firstly Cailteux et al. (2005) believed that the earliest mineralization in the Central African Copperbelt is syngenetic to early diagenetic sulphides, which have being dominated by framboidal pyrite with occasional Cu-sulphides in disseminated form in the host-rocks. From El Desouky et al. (2009) the Cu-Co mineralization occurring as fine-grained disseminations, fine bands or in nodules is postdating the early diagenetic pyrite generation. The diagenetic Cu-Co mineralization phase was formed by a moderately saline, relatively low-temperature fluid at ~115-220˚C. Later Cailteux et al. (2005) supported the idea stating that the Cu-Co sulphides with chalcopyrite and carrollite inclusive were introduced in a second phase, later than the early diagenetic pyrite-dominated sulphides.

- Synorogenic mineralization and sulphide remobilization:

It appears that syngenetically and diagenetically deposited sulphides are the dominating genesis of ores in the Katangan Belt (Cailteux et al., 2005) and that the early sulphides have been remobilized by synorogenic processes and supergene enrichment into more massive deposits. On the other hand, Muchez et al. (2010) supported that remobilization of the diagenetic and early synorogenic sulphides in the Zambian Copperbelt produced irregular crosscutting ore veins during increasing compression. And so, massive unfolded ore veins were formed during peak deformation as fluids extensively were

transported along faults. It is then possible that the fluid circulation increased when faults were re-activated during the highest compressional phase, leading to addition in the sulphur and metal which explains the reason why the peak deformational deposits are massive (Muchez et al., 2010). The same authors support the idea that there should be another different fluid responsible for the enrichment of the fault- and fold hinge-associated vein-type deposits explaining the increased amount of cobalt in the massive veins.

- Late- to post- orogenic Cu-Zn-Pb deposits:

In the Central African Copperbelt, vein-type Cu-Zn-Pb (i.e. Kipushi type in the Democratic Republic of Congo) are not associated with the extensive larger diagenetic and synorogenic stratiform Cu-Co ores. These vein-type deposits are mostly hosted in the sediments overlying the Roan Group containing most of the stratiform Cu-Co mineralization. From investigations on the timing and general characteristics of two distinct late-stage mineralizations, Haest and Muchez (2011) established that Cu-dominated Cu-Zn veins dated to ~530-500 Ma, which is in the retrograde stage of the Lufilian orogeny. Schneider, Melcher and Brauns (2007) argued that Zn-dominated Zn-Cu-Pb deposits formed at ~450 Ma are post-orogenic. These vein-type deposits are being interpreted as Mississippi Valley-type deposits described as epigenetic stratabound ores hosted within a calm shallow marine sequence (Tillberg, 2012).

In brief, based on recent studies on the Central African Copperbelt, Tillberg (2012) suggested that the sediment-hosted stratiform Cu-Co mineralization formed by extended multistage deposition initialized early in the rift-stage and increasing in strength during the folding and thrusting of the basin; the different mineralization stages consist of syngenetic and early diagenetic framboidal pyrite, later diagenetic Cu-Co sulphides, synorogenic massive and irregular vein-type Cu-Co sulphides, and late- and postorogenic Cu-Zn-Pb veins.

After all, there are complex processes that are still not completely well understood in the origin of the Central African Copperbelt ores although many extensive studies have been undertaken for years (Hitzman et al., 2005). These authors argued that the stratiform Cu-Co deposits require sources of sulphur and metal, a source and driving heat of leaching and transporting fluids and the chemical process to precipitate the sulphides.

# CHAPTER 4: LOCAL GEOLOGY IN PR851 AREA

## 4.1. Stratigraphy

Not many outcrop exposures have been encountered in the area due to the very thick regolith profile cover found in this part of the tropical environment.

The stratigraphy of the PR851 area has derived to some limited extent from regional surface mapping conducted within the entire prospect area, complimented by outcrops description from a single surface trench in the Subo area and more importantly to greater well logged geology outcomes from both reverse circulation and diamond drilling done inside the lease. Nevertheless PR851 area revealed lithologies of the Roan Group from Roche Argilo-Talqueuses (R1) through the full sequence of the Mines (R2), Dipeta (R3) up to Mwashya (R4) Sub-groups (Figures 23 and 24). Also the overlying diamectite, the Grand Conglomerat of the Nguba Group, on top of the Roan Group is present.

The lithostratigraphic succession in PR851 area is as follows, from the bottom upwards:

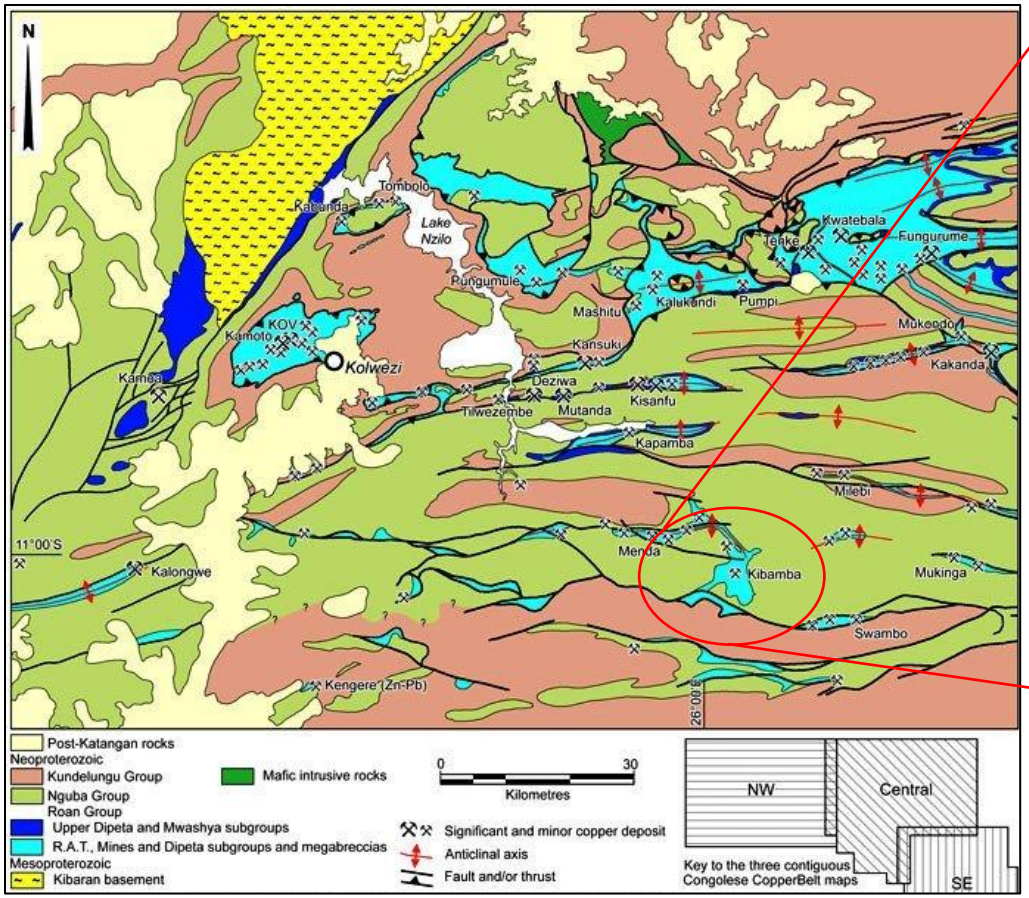


Figure 24: Geology map of the north-western Congolese Copperbelt showing regional stratigraphy of PR851 area circled in red. Modified after Francois, 1974; Kampunzu et al. (1990) and Kipata et al. (2013).

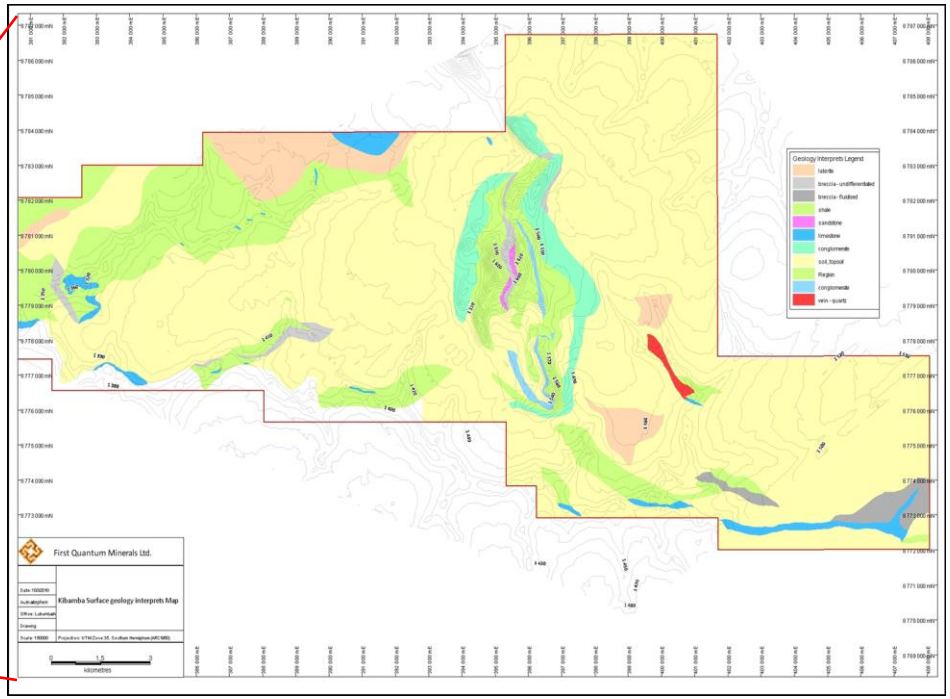


Figure 23: Interpreted surface geology map of PR851 area (After CoMiSa Sprl, 2010 unpubl.)

### 4.1.1. Roan Group

#### *4.1.1.1. Roches Argilo-Talqueuses (R.A.T.)*

To the southern part of the prospect area, a large (maybe 500m wide) slab of the Roches Argilo-Talqueuses (Figures 25a and 25b) is evident presenting a dolomitic to talcose and argillaceous silt to sandstone facies. This unit is lilac to red in colour, characteristically hematitic and may show a brecciated textute or bedded. In contrast with the Roches Greseuses Siliceuses (R.G.S) which has nearly a similar colour, the Roches Argilo-Talqueuses (R.A.T.) has high content of specular hematite and locally consists of a mixture of rocks of different nature, from conglomerate clasts in places at the bottom to siltstone, shales, dolomitic shales, dolomite, and dolomitic sandy shales upwards. Acosta et al. (2014, unpubl.) defined the Roches Argilo-Talqueuses as red and hematitic monolithic siltstone unit which may have formed by in-situ dissolution of evaporates and subsequent collapse and infill. Francois (1973b) observed that the Roches argilo-Talqueuses (R.A.T.) is the lowest unit of the Roan Group showing color variations from lilac to red, most of the time largely structureless.

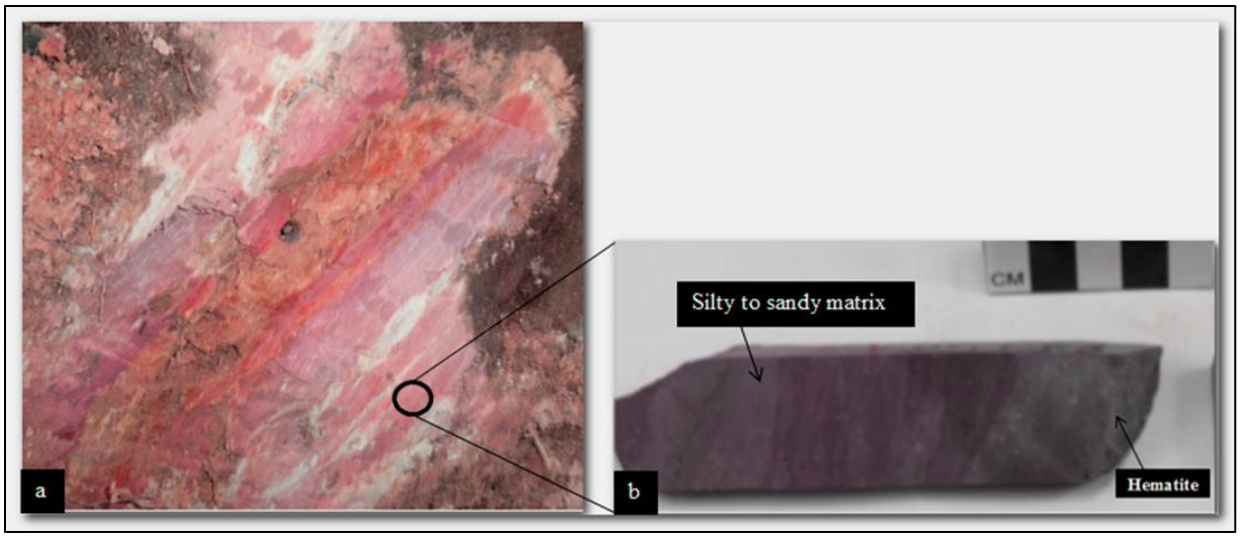


Figure 25: (a) Outcrop showing lilac to red Roches Argilo-Talqueuses (R.A.T.); (b) R.A.T. rock sample showing high hematite content in a silty to sandy matrix.

#### *4.1.1.2 Dolomie Stratifiée (DSTRAT) – Lower Roan*

The DSTRAT (Figure 26) is a stratified dolomite, 2 to 3m thick, showing similarities with the overlying Roches Siliceuses Feuilletees (RSF) although it is comprised of thick well-bedded argillaceous dolomites. The lower part of the DSTRAT is characterized by an argillaceous banded horizon whereas a nodular chert-rich horizon can be observed on the upper portion near the top boundary. Light-grey to light brown in colour, moderately weathered, this unit is also part of the Lower Ore Zone in the Katangan stratigraphy and has been observed at PR851 area.


Figure 26: Outcrop showing a stratified dolomite locally called DSTRAT.

#### *4.1.1.3. Roches Siliceuses Feuilletées (RSF) – Lower Roan*

In PR851 area, the RSF (Figure 27) presents a distinctive laminated and silicified facies. This rock unit is obviously made up of very thin and more or less silicified bedded dolomitic shales. It consists of ondulated laminae or lenses, black in colour indicating a high content of carbon and remains very significant as it hosts Cu-Co mineralization of the Lower Ore Zone which is developed close to the contact with the overlying Roches Siliceuses Cellulaires (R.S.C.). The apparent thickness of the RSF in the study area averages 5m.

Figure 27: Drill core sample of weathered black RSF carbon rich in borehole RSFD01 at 60m depth. Note that the black mineral is heterogenite.

#### *4.1.1.4. Roches Siliceuses Cellulaires (RSC) – Lower Roan*

The RSC (Figures 28a and 28b) is a silicified crystalline light coloured dolomite to black in colour, extremely cellular weathered, massive to stromatolitic, characterized by cavities / vuggs. Generally poorly mineralized but sometimes secondary enrichment in the hypogene zone is excellent in places. The hydrothermally altered stromatolites are sporadically rich in black heterogenite (Cobalt oxide). In the field the RSC highly resistant to erosion than the adjacent stratigraphy forms as a result outcrops and low ridges that are prominent in the otherwise flat terrain. It expresses specular up-reliefs at the crests of hills from 50 up to 100m above the surrounding land. The unit ranges in thickness between 10 to 25m.

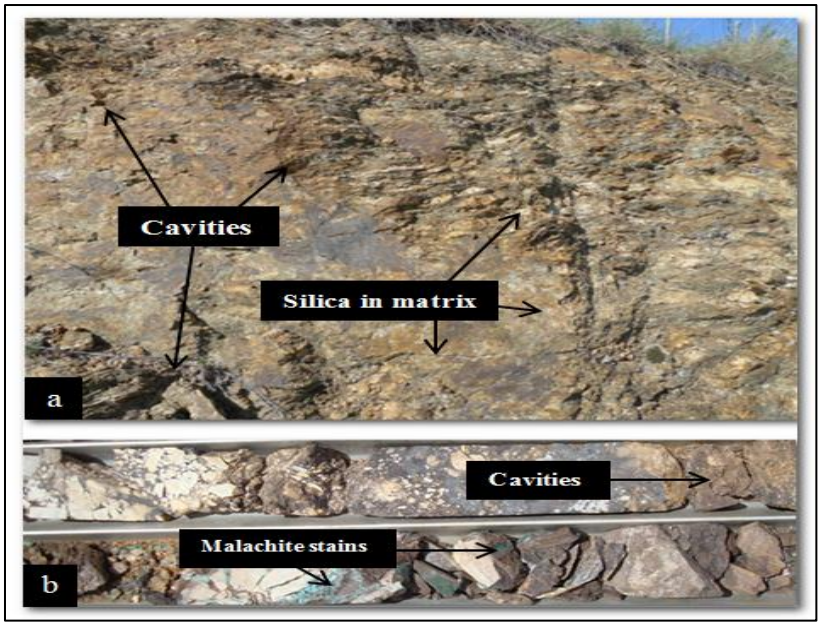


Figure 28: (a) Outcropping massive and stromatolitic RSC unit showing vuggs. (b) Drill core sample of RSC from borehole RSFD01 at 57m depth. Note presence of malachite mineralization in the hole.

#### *4.1.1.5. Calcaire à Minerais Noirs (CMN) – Upper Roan*

CMN units (Figure 29) have been mapped respectively to the South-East, East, towards the North-West and in the center of prospect area. The CMN unit is wrongly called 'limestone'. Actually, it is calcareous, light coloured dolomitic shale including algal layers, thin beds of white dolomitic sandstones and sometimes argillic dolomites surrounded by breccias in places.

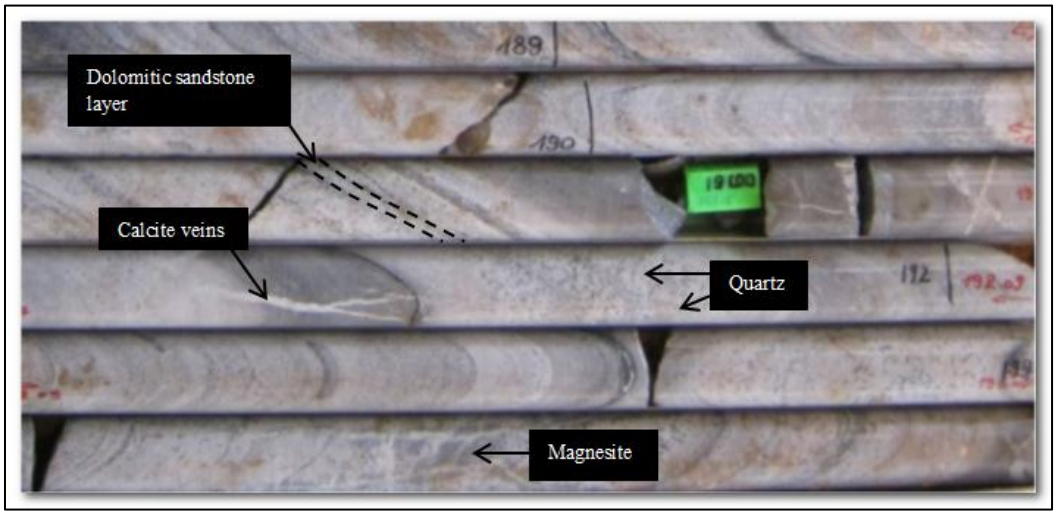


Figure 29: Drill cores showing CMN units from near Kibamba hill in PR851 area.

#### *4.1.1.6. Mwashya Shales*

This unit which is black to light and dark grey in colour consists of finely bedded carbonaceous shale known as 'Black Shale' (Figure 30). Sometimes it contains feldspar, pervasive muscovite and/or biotite. Also a typical alternance of thinly silicified dolomite, light-dark grey shales, sandstone, with jasper, cherts and siliceous beds characterizes this unit. In places oolitic horizons are present and it appears to be lack of bedding and looks like carbonaceous mudstone or argillite. Pyrite and very less amount of chalcopyrite have been observed in form of dissemination into the rock matrix, along bedding or to some extent associated to calcite/quartz veinlets. Pyrite amount in this rock-unit averages 1 to 2%. Above all the lithologies observed, this is the most reduced formation of the full Katangan sequence. It usually represents a regional lithostratigraphic marker of the Mwashya Sub-group in the entire Katangan stratigraphy (Cailteux, 2007) and has been observed continuously underlying the 'Grand Conglomerat' of the Nguba Group (Francois, 1973; CoMiSa Sprl, 2008 unpubl.; Hitzman et al., 2005; Mendelson, 1961).

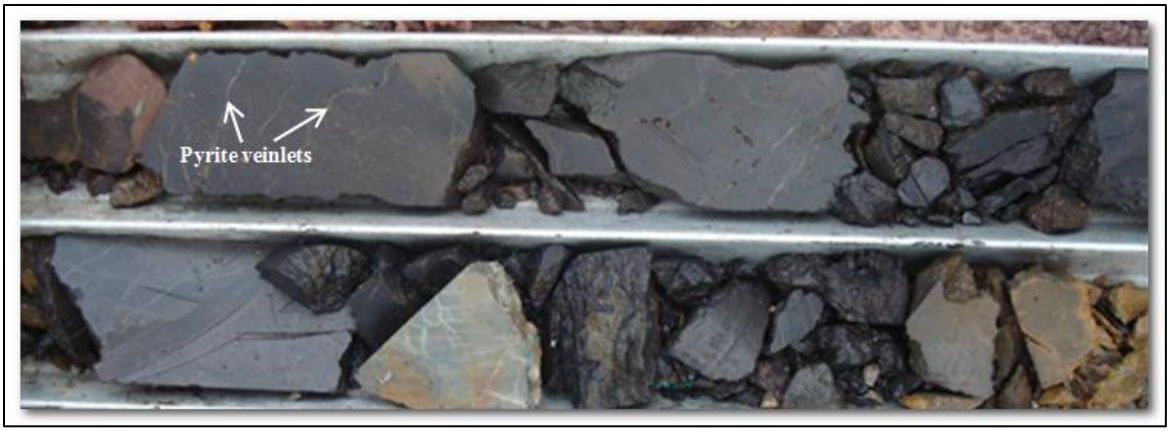


Figure 30: Drill core showing carbonaceous Mwashya Shale crosscutted by pyrite veinlets from boherole SUD3 (130-131m depth) at Subo target area.

### 4.1.2. Nguba Group

#### *4.1.2.1. The Grand Conglomérat*

In the study area, the Grand Conglomérat (Figure 31) is observed on outcrops in up-relief due to its resistance to erosion caused by the presence of hard and siliceous pebbles. It is represented by a dolomitic, shaly, silty and sometimes sandy matrix supported clasts. Clasts are sub-angular to rounded varying from 5 to 20cm in size from the observed outcrops and consist of sandstone, siltstone, dolomitic shale, dolomite indicating their origin from the underlying rocks of the Mwashya Sub-group. In places less sulphide minerals like pyrite and chalcopyrite occur in form of disseminations or blebs inside the rock matrix and sometimes associated to crosscut quartz/calcite veins. In the present case study the Grand Conglomérat varies between 100-500m thick. This diamectite unit is lying directly on the base of the Nguba Group and constitutes the most known regional marker overlying the Mwashya Group. It has been observed that when the Grand Conglomerat lies directly on the Mwashya graphitic shale it has a carbonaceous matrix and becomes silty to sandy when overlying the arkosic sandstone of the Upper Mwashya. Master and Wendorff (2011) attribute the facies change to the ongoing tectonic, variation of sedimentation condition with regression-transgression, variation of climate and ice dynamic. Intiomale (1982) argued that the Grand Conglomérat is characterized by clasts that are angular to well-rounded randomly dispersed within a carbonaceous matrix and contains shale and sandstone beds. Buffard, R. (1988) discussed that the development of shale beds towards the south of the Katangan Sequence indicates that the ice movement was southwards.

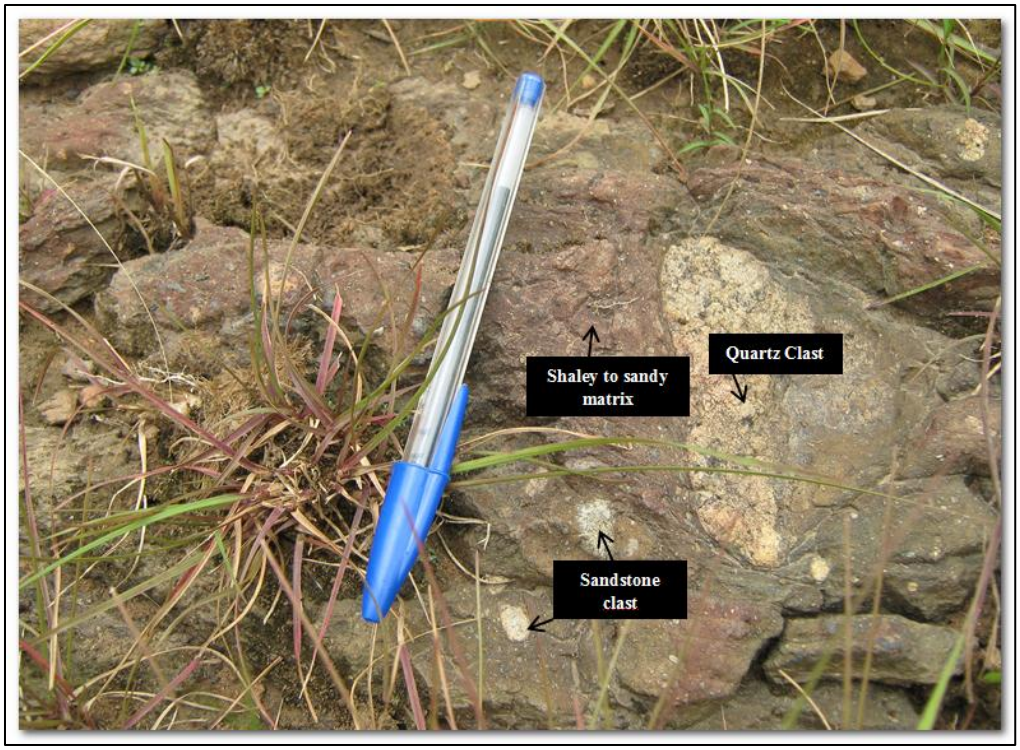


Figure 31: Outcrop showing clasts of different nature within a shaly to sandy matrix of the Grand Conglomerat

### 4.1.3. Axial Breccia

The axial breccia unit (Figure 32) is more tectonic rather than a lithostratigraphic unit in the study area although it is located above the CMN rock sequence and separates the Upper Mines and Dipeta Sub-group.

Fragments in the breccia are generally angular but occasionally rounded, ranging from millimetres to several centimetres in size. The variable colours (Red, grey, tan, brown, white) of clasts within a white carbonate matrix have derived from all rock types of the Roan Mines Sub-group. Acosta et al. (2014, unpubl.) argued that the breccia may have formed during halokinesis of salt in and below the Roches Argilo-Talqueuses.

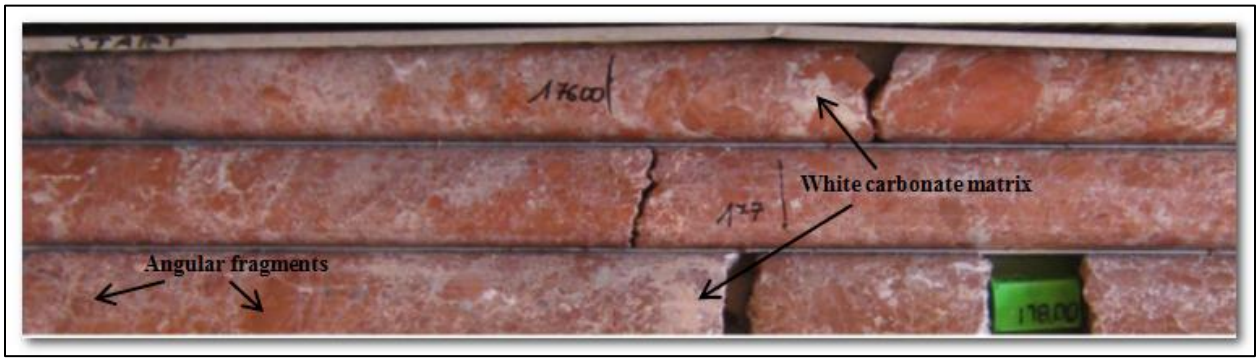


Figure 32: Drill core showing angular fragments in a white carbonate matrix of an axial breccia

## 4.2. Structure

In order to establish a relationship between structural features and mineralization deposits combined with lithostratigraphy within the study area, aerial photographs and landsat images remain powerful exploration tools. Ridges formed by rocks resistant to erosion are easily identified from the satellite images. For example, the Roches Siliceuses Cellulaires (RSC) of the Mines Subgroup being highly silicified and resistant to erosion appears like high topography / ridges with under-and overlain Mine Subgroup sequence on both sideways. Furthermore, these ridges are mainly located along the margins of thrust fragments and to the associated faults. From Hobbs et al. (1976) understanding of lineaments as linear topographic features of regional extent that reflects crustal structure, it appears a clear relationship between Cu-Co mineralization and the ridges.

The present study area is characterized by fragments of Mines Subgroup in form of a folded anticline (Figure 23) in the middle of two slabs of Mwashya and RAT Subgroups respectively identified as tectonic breccias.

The mapped folded fragments from drilling form tight upright and steeply dipping anticlinal structures with variable vergence on a regional scale. The folding is probably associated with early ductile event locally visible as discrete zones of foliation development and stretching of primary features (Jigsaw Geoscience PTY LTD, 2009 unpubl.). Subsequently this could have been followed by brecciation of the Katangan sequence and the emplacement of carbonate-pyrite-chalcopyrite veins and as a result of brittle structures.

Towards the northern part of PR851 area, fragments of the Mines Subgroup are terminated by faults on the lateral extension (CoMiSa Sprl, 2008 Unpubl.) which could have acted as pathways for fluids responsible for hypogene alteration process and remobilization of Cu-Co mineralization.

Recently with the identification of nickel mineralization in the ground adjacent to the prospect area northwards, Acosta et al. (2014, unpubl.) documented that this part of the Congolese Copperbelt has been highly affected by salt tectonics (Figure 33).

For a better understanding of the structural architecture of PR851 area, aerial photographs in such an area of fewer outcrops are required and there after more surface mapping will be needed to verify the interpreted features with the geology on the ground.

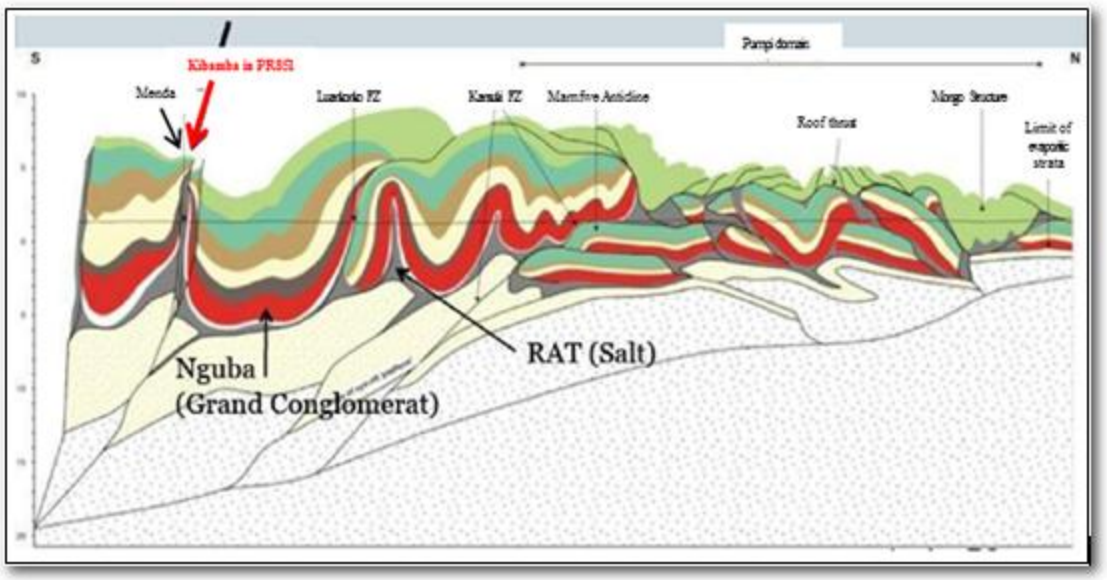


Figure 33: High influence of salt tectonics on PR851 area of the Congolese Copperbelt (Modified after Acosta et al., 2014, unpubl.)

### 4.3. Magmatism and metamorphism

Almost no significant magmatism has been encountered inside the prospect area although widespread volcanics within the lower Mwashya Subgroup and evidences of magmatism (like small sills and dykes of dolerite) intersected in drill holes intruding Mwashya formations remain common.

The degree of metamorphism within the prospect area is of low grade characterized by the presence of chlorite and talc minerals suggesting the evidence of the lower green schist facies which have been also observed elsewhere in the thrust-and-folded Katangan Belt. This is consistent with the observed low strain rocks mainly found in the prospect area illustrated by not considerably flattened spherical nodules within the dolomitic shale as well as wide-space and non-penetrative crenulation. This confirms Kampunzu et al. (1999) observations on the presence of microlithic to porphyritic basic rocks and volcanics associated to the lower part of the Mwashya Subgroup throughout the entire Central African Copperbelt.

During the Lufilian orogeny the Katangan Belt underwent a regional metamorphism of lower green-schist facies marked by the development of phyllosilicates, feldspars, carbonates and quartz (Chabu, 1990). Kampuzu et al. (2000) established the geothermal gradient for this regional metamorphism between 30-45˚C.

## 4.4. Mineralization

Mineralization in PR851 area is associated with large fragments of the Mines Subgroup foating in the Roches-Argilo-Talqueuses (RAT) although the entire regional context is yet to be well understood. At Subo locality inside PR851 area, drill holes and trenches at surface located exclusively copper mineralization (Malachite and chrysocolla, Figures 34a and 34b) relatively restricted in distribution. Meantime, no obvious primary sulphide mineralization associated with Subo locality has been observed so far. However core drilling in this area reflected the evidence of minor pyrite disseminated in the lower Mwashya shale as well as a primary hematite down-hole. It is possible that this primary hematite reflects an iron-enrichment event below the mineralized zone even if this has not been visible due to the overprint of the deep weathering.

Elsewhere in the center-up-north of PR851 area where the Roches Siliceuses Feuilletees (RSF) of the Mines Subgroup occurs, primary mineralization is located in carbonate-chalcopyrite-pyrite breccia and tensional veins but it appears to lack continuity between sections. Also albite alteration has been found in close association with mineralization. Furthermore the higher grade Cu-Co mineralization in the weathered zone is located as a sub-horizontal to gently inclined cover and is considered to crosscut the differing lithologies of the Mines Subgroup. Cobalt mineralization appears in form of dark black and soft material called heterogenite whereas copper mineralization is seen as chalcopyrite, bornite and locally as malachite and chrysocolla.

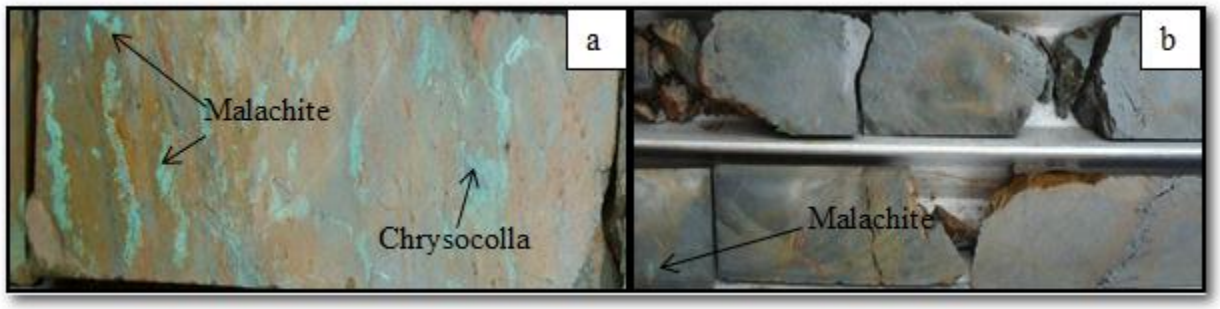


Figure 34: (a) Copper mineralization (malachite and chrysocolla) from drillhole SUD2 at 153m; (b) Infill copper mineralization (malachite) in fractures from drillhole SUD1 at 76m (modified after Jigsaw Geoscience PTY LTD, 2009 unpubl.).

## CHAPTER 5: SOIL ASSAYS DATA PROCESSING AND INTERPRETATION

### 5.1. Database

Soil sampling data were stored following an existing data management system in place within the company. Data were collected on paper log sheets, scanned and captured by hand into soft excel spreadsheets. Niton/XRF results were downloaded into csv files and later converted into excel and stored in that manner. Laboratory assay results were attached next to their relevant soil sample ID's before being loaded and stored in an access database onto the server in CoMiSa Sprl Lubumbashi office. Ideally it could be more convenient to load and manage data in specialized programs such as datashed, acquire and/or sable for easy checking of duplicate data and later data validation. For instance a good geochemical database should follow specific data management steps as illustrated on the following chart (Figure 35).

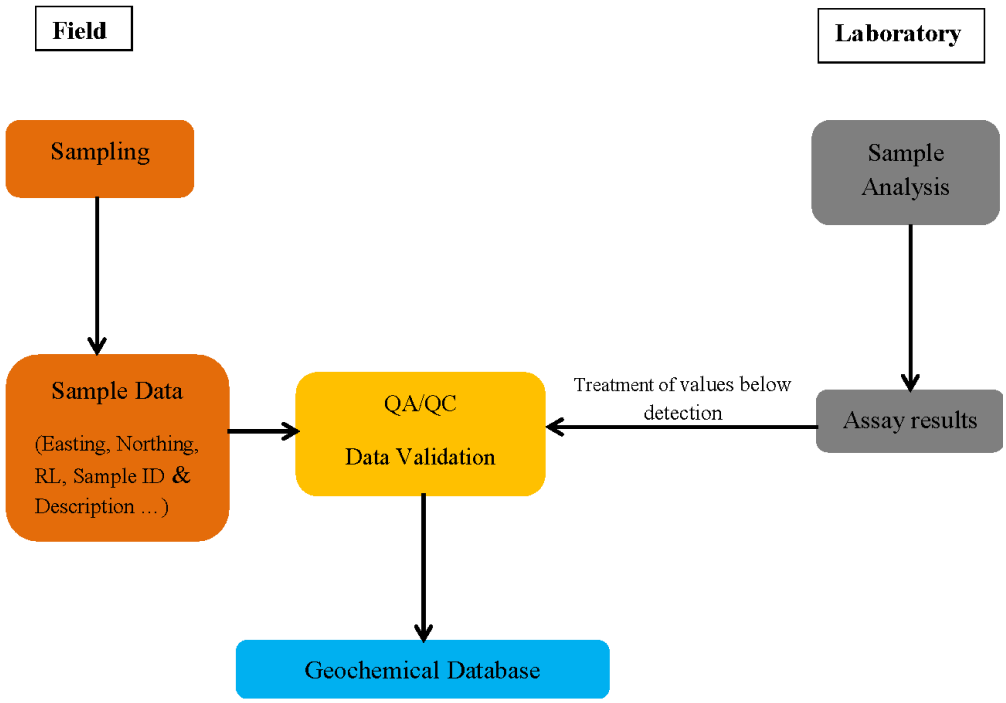


Figure 35: Proposed data management chart for a geochemical database designed by the author of the present thesis.

Soil sampling data were planned then processed using MapInfo and Surpac softwares for statistical applications and interpretation. In this specific case study, Mapinfo version 12.5 combined with Discover 2014 software programs have been used for basic statistics, data interpolation (gridding and contouring), map geo-referencing, data plotting, point classification for target generation and prioritization. An illustration of PR851 area soil sampling database, not in exhaustive form, is illustrated in Table 5.

Table 5: Illustration of PR851 area soil sampling database (Refer to Figure 7 for codes explanation)

| | | Actual location | | Local Grid | | | | | | | | | | | | Lab Assays | | |
|---|---|---|---|---|---|---|---|---|---|---|---|---|---|---|---|---|---|---|
| Sample ID | QA/QC | UTM_Easting | UTM_Northing | Grid name | Line # | Local East | Local North | Sampling depth(cm) | Regolith type | Colour | Colour tone | Land cover | Moisture | Sampled by | Sampling date | Cu_ppm | Co_ppm | Comments |
| E0802 | | 394043 | 8776568 | Grid 1 | L1 | E 9,000 | N10,000 | 35.00 | ISO | BNYE | M | FOR | DY | P.Katombe | Oct-04 | 69 | 8 | |
| E0803 | | 394044 | 8776672 | Grid 1 | L1 | E 9,100 | N10,000 | 35.00 | ISO | BNYE | M | FOR | DY | P.Katombe | Oct-04 | 63 | 10 | |
| E0804 | | 394044 | 8776768 | Grid 1 | L1 | E 9,200 | N10,000 | 30.00 | ISO | BROR | M | FOR | DY | P.Katombe | Oct-04 | 67 | 13 | |
| E0805 | | 394045 | 8776862 | Grid 1 | L1 | E 9,300 | N10,000 | 35.00 | LAT | BROR | L | FOR | MT | P.Katombe | Oct-04 | 65 | 10 | |
| E0806 | | 394047 | 8776956 | Grid 1 | L1 | E 9,400 | N10,000 | 25.00 | LAT | BKGY | D | FOR | WT | P.Katombe | Oct-04 | 71 | 10 | Near dambo |
| E0807 | | 394044 | 8777060 | Grid 1 | L1 | E 9,500 | N10,000 | 30.00 | ISO | BNBK | M | FOR | MT | P.Katombe | Oct-04 | 66 | 6 | |
| E0808 | | 394039 | 8777154 | Grid 1 | L1 | E 9,600 | N10,000 | 30.00 | ISO | BNOR | M | FOR | DY | P.Katombe | Oct-04 | 63 | 4 | |
| E0809 | | 394035 | 8777258 | Grid 1 | L1 | E 9,700 | N10,000 | 25.00 | ISO | BNTN | L | FOR | DY | P.Katombe | Oct-04 | 63 | 4 | |
| E0810 | | 394038 | 8777356 | Grid 1 | L1 | E 9,800 | N10,000 | 35.00 | ISO | BNRD | D | FOR | DY | P.Katombe | Oct-04 | 59 | 3 | |
| E0811 | CRM | | | Grid 1 | L1 | | | | | | | | | | | | | |

## 5.2.Anomaly threshold and interpretation

### 5.2.1. Basic statistics

After an optimum soil sampling data collection based on an orientation survey as indicated previously in this study, combined with assays data from laboratories; our data are of appropriate quality and representative. Thereafter, a rigorous evaluation of quantitative data by using statistical methods is the focus in this paragraph. Emphasis will be placed on interpretation emerging through examination of data by relatively simple basic statistical techniques.

Basic statistics (Table 6) for both copper and cobalt are concerned initially with measures of central tendency (mean, median, and mode) and dispersion (range, variance, standard deviation, percentiles and coefficient of variation) of unbiased samples, as parameters that are useful and important in describing attributes of the probability density function of soil sampling data set from PR851 area. The basic statistic parameters hereunder are tabulated with respect to two datasets of soil samples respectively. Firstly a dataset of 3536 soil samples from 800X100m and 200X100m grids which were initially implemented over localized fragments of Roan Group lithology sequence due to the very limited budget at that time to run the sampling program on the entire PR851 area; and secondly a data population of the first 3536 samples combined with an addition of 1493 soil samples collected from 400X400m grid conducted to cover the rest of PR851 area. Sampling following the 400X400m grid was undertaken after a successful follow up from the initial sampling program which led to the evaluation of the Kibamba Cu-Co discovery within PR851 area.The next following chapter six will highlight the resource report of the Kibamba Cu-Co deposit.

Table 6: Basic statistics for both copper and cobalt with respect to the soil sample population from initial reconnaissance and detailed grids.

| Basic statistic parameters | Dataset from initial sampling program (Based on 800X100m and 200X100m grids) | | Dataset from all grids ( 800X100m, 200X100m and 400X400m) | |
|---|---|---|---|---|
| | Fields | | Fields | |
| | Cu_ppm | Co_ppm | Cu_ppm | Co_ppm |
| Count | 3536.00 | 3536.00 | 5029.00 | 5029.00 |
| Minimum | 0.00 | 0.00 | 0.00 | 0.00 |
| Maximum | 7119.75 | 282.00 | 7119.75 | 282.00 |
| Sum_Total | 337079.57 | 19104.00 | 2801983.60 | 84697.00 |
| Mean | 95.33 | 5.40 | 557.17 | 16.84 |
| Median | 62.00 | 4.00 | 104.76 | 7.00 |
| Mode | 0.00 | 0.00 | 0.00 | 0.00 |
| Range | 7120.00 | 282.00 | 7120.00 | 282.00 |
| Variance | 26443.84 | 93.92 | 674919.80 | 479.79 |
| Standard Deviation | 162.62 | 9.69 | 821.54 | 21.90 |
| Skewness | 24.53 | 11.50 | 1.51 | 1.70 |
| Kurtosis | 996.24 | 249.99 | 1.33 | 5.42 |
| Percentile50 | 62.00 | 4.00 | 104.76 | 7.00 |
| Percentile75 | 119.23 | 8.00 | 846.00 | 25.00 |
| Percentile90 | 214.55 | 13.00 | 2042.20 | 55.00 |
| Percentile95 | 291.56 | 17.00 | 2325.60 | 62.00 |
| Percentile98 | 365.00 | 23.00 | 2695.44 | 72.00 |
| Coefficient of Variation | 1.71 | 1.79 | 1.47 | 1.30 |
| Count_Equal_Zero | 379.00 | 1639.00 | 379.00 | 1639.00 |

From the above values of standard deviation and mean in Table 6; the coefficient of variation, defined as the ratio of the standard deviation to the arithmetic mean, has been therefore calculated.

As far as statistical interpretations are concerned in the present work only soil samples collected from the initial sampling program following 800X100m and 200X100m grids respectively will be considered. Note that 1632 samples over the entire dataset have no assay results for Co and therefore only soil samples with both Cu-Co assay results will be considered further down in schematic scatter plots showing Cu-Co distributions (Figures 36 and 37) and correlation between the two Cu-Co pairs of variables (Figure 38).

From Table 5, on a total of 3536 soil samples copper values varies from 0 to 7119.75ppm

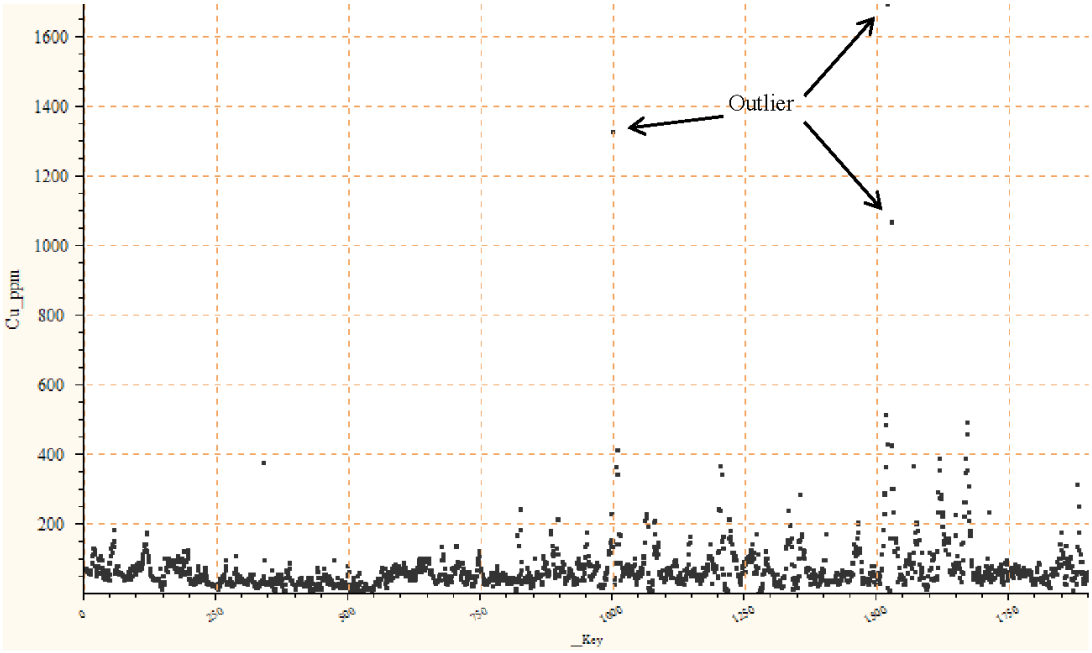


Figure 36: Schematic scatter plot diagram illustrating Cu distribution for 1904 soil samples from the initial 800X100m grid within PR851area.

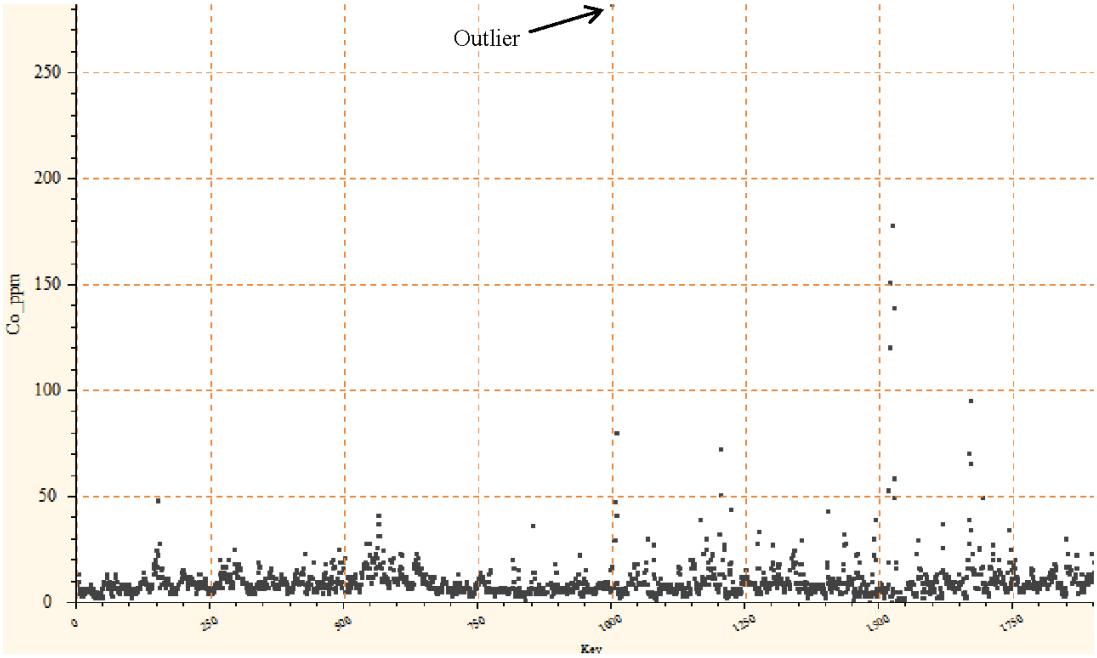


Figure 37: Schematic scatter plot diagram illustrating Co distribution for 1904 soil samples from the initial 800X100m grid within PR851 area.

Statistical analysis will help to understand and visualize the nature of data distribution from diagrams and also to determine the anomaly thresholds as well.

As shown in Figure 38, a measure of similarity between paired Cu-Co assays data has been estimated by mean of a correlation. So the R-mode statistical treatment dealing with correlation between pairs of variables (Cu and Co in our case) has been used. Therefore with considerations to soil samples with Cu and Co lab results only, the correlation coefficient (R) has been calculated to 0.6549 (Figure 38). This shows that the two paired Cu-Co data are increasing sympathetically illustrating a strong positive correlation and can be understood that both Cu and Co are originally from the same mineral source and probably from the same mineral assemblage or paragenesis. Deborah (2011) demonstrated that in statistics, the correlation coefficient (R) is always between +1 and -1 and a value closest to +0.70 illustrates a strong positive linear relationship. From basic statistics copper and cobalt in PR851 area showed a linear correlation which is consistent with numerous Cu-Co stratiform-stratabound deposits examined in the surrounding areas within the Lufilian Arc.

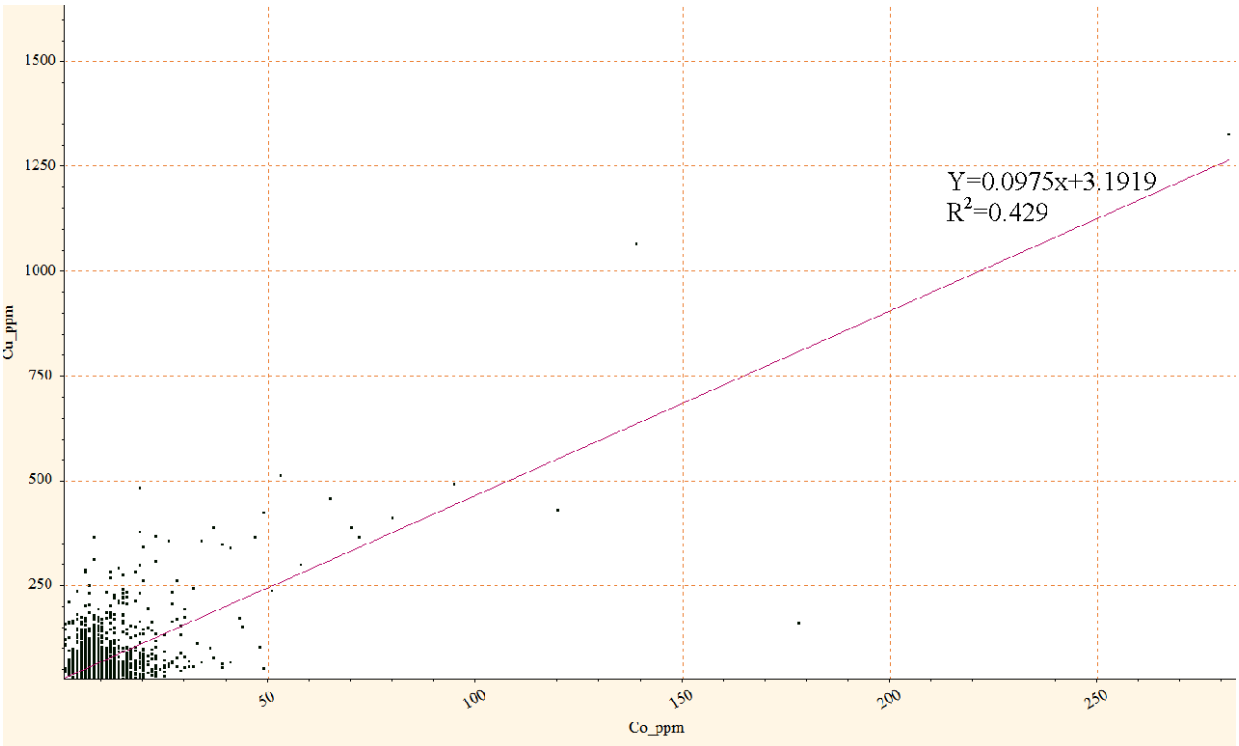


Figure 38: Schematic scatter plot diagram illustrating Cu-Co strong positive correlation.

### 5.2.2. Literature comparison

Anomaly threshold definition for geochemical dataset by literature comparison remains subjective. Levinson (1974) defined average abundance of selected minor and trace elements in various natural media. He stated that Cu in soil varies between 2-100ppm whereas Co in the same media goes up to 1.4ppm. Therefore these indicated values for copper and cobalt elements represent background values above which copper as well as cobalt become anomalous in soil. However, it is very important when defining anomaly threshold by literature comparison for a given area to take in account personal experience as an exploration geologist and geological knowledge of that area. For example, regional background value of copper in the Congolese Copperbelt is relatively high and set at 200ppm above which copper becomes anomalous. CoMiSa Sprl which conducted soil survey from 2003 to 2008 over PR851 area, with more than 10 years' experience in mineral exploration on the southeastern part of the Central African Copperbelt from Greenfield to brownfield and a record of more than 93,479 soil samples collected over 33 exploration licence areas in D.R of Congo making a total of 10,000km$^2$ covered surface, used 200ppm as a subjective threshold to implement initial test drilling. So with its experience of Lonshi, Frontier copper mines and Kibamba Cu-Co deposit CoMiSa Sprl discoveries following geochemical anomalies, the company could define test drilling on soil anomaly equal or above 200ppm.

### 5.2.3. Standard deviation

The standard deviation is a parameter which measures how concentrated the data are around the mean. In fact, a small standard deviation means that values in a given dataset remain close to the mean of that data set on average, whereas a large standard deviation means that values in the dataset are far away from the mean on average. In our case, calculated standards deviations for Cu and Co are 162.62 and 9.69 respectively. And from recorded Cu and Co laboratory analytical results, standard deviations shows large values which are not necessarily a bad thing and have just reflected a large amount of variation in the data set which is being studied. As shown in Figures 36 and 37, one and three outlier(s) for Co and Cu simultaneously affected the standard deviation values. Basically similar to the mean, outlier does affect standard deviation value. After all, the mathematics behind the standard deviation includes the mean. Therefore, by removing outliers from our dataset, standard deviation will decrease and the rest of Cu-Co assay

values will be more concentrated around the mean. Standards deviations become 55.17 for copper and 9.44065 for cobalt.

From Table 6, the 2 and 3 orders standard deviations can be calculated in order to estimate the 1st and 2nd anomaly thresholds. Calculated values for 2 and 3 orders standard deviations for both Cu and Co are shown in Table 7.

Table 7: Two and three order standards deviations for Cu and Co from PR851 area soil samples dataset

| | Cu | Co |
|---|---|---|
| Standard deviation | 162.62 | 9.69 |
| 2 order standard deviation | 325.24 | 19.38 |
| 3 order standard deviation | 487.86 | 29.07 |

As a result, any value above 325.24 for Cu and 19.38 for Co is considered to be the 2nd anomaly threshold and values above 487.86 for Cu and 29.07 for Co will be the 1st anomaly threshold. These two types of anomaly thresholds help in anomalies prioritization for a further follow up. Nevertheless, anomaly threshold definition by literature comparison and standard deviations needs to be complemented with other methods such as histogram and log probability which methods remain most useful in determining realistic anomaly threshold in the way that anomalies can be seen and detected from charts where peaks occur. So from a large amount of data to a single graph that shows peaks in data, it is easy to have a visual representation of the statistical significance of peaks.

However, as far as our work is concerned, anomaly thresholds defined by literature comparison and standard deviation will be complimented by points classification ( graduated symbols and colours, spatial analysis, gridding and contouring maps) which are presented further down to highlight zones of high anomalies to be followed up later with reverse circulation and diamond drillings.

### 5.2.4. Spatial analysis

Thematic maps for copper generated by classification of Cu assays using Point ranges - sequential Red HSV in Mapinfo version 12.5 (Figure 39) together with gridded and contoured of Cu laboratory assay results (Figures 40 and 41) has been applied to determine and localize in geographic space within PR851 area numerous zones of high Cu-Co anomaly values. Therefore, spatial analysis coupled with literature comparison and standard deviations methods helped in target prioritization following zones of maximum geochemical anomalies.

From observations on Figures 40 and 41, it appears that peaks in Cu anomalies coincide in both gridded and contours maps.

In PR851 area, a number of targets was categorized by order of first, second, third and forth priority. In this present study, only targets 1 and 2 quoted as first and second priority have been investigated due to budget availability and limited time.

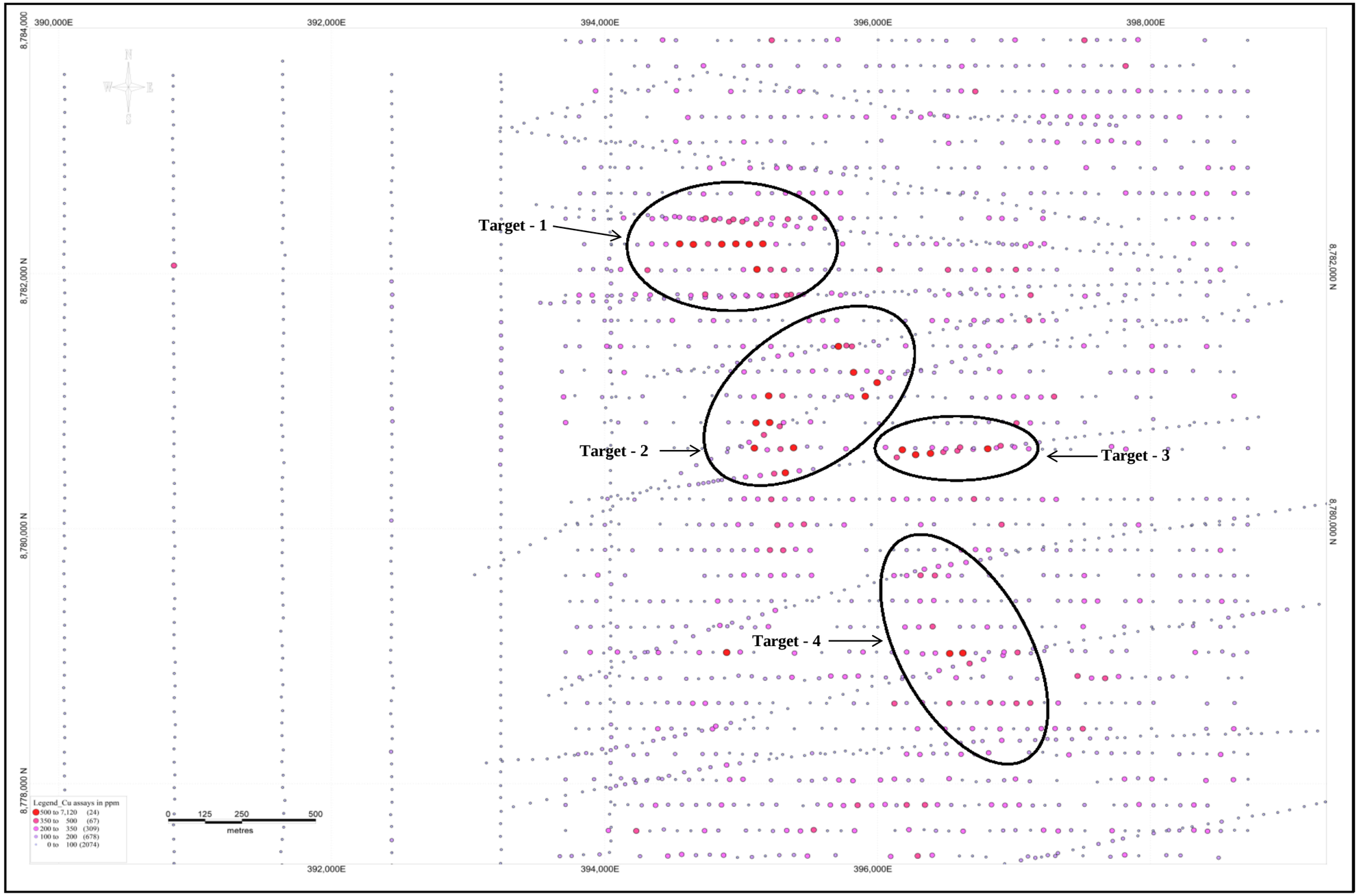


Figure 39: Illustration of classified Cu_ppm assays from the central part of PR851 area where Kibamba Cu-Co deposit was identified. Note Targets-1, -2, -3 and -4 delineated by the author of the present thesis for a later follow up.

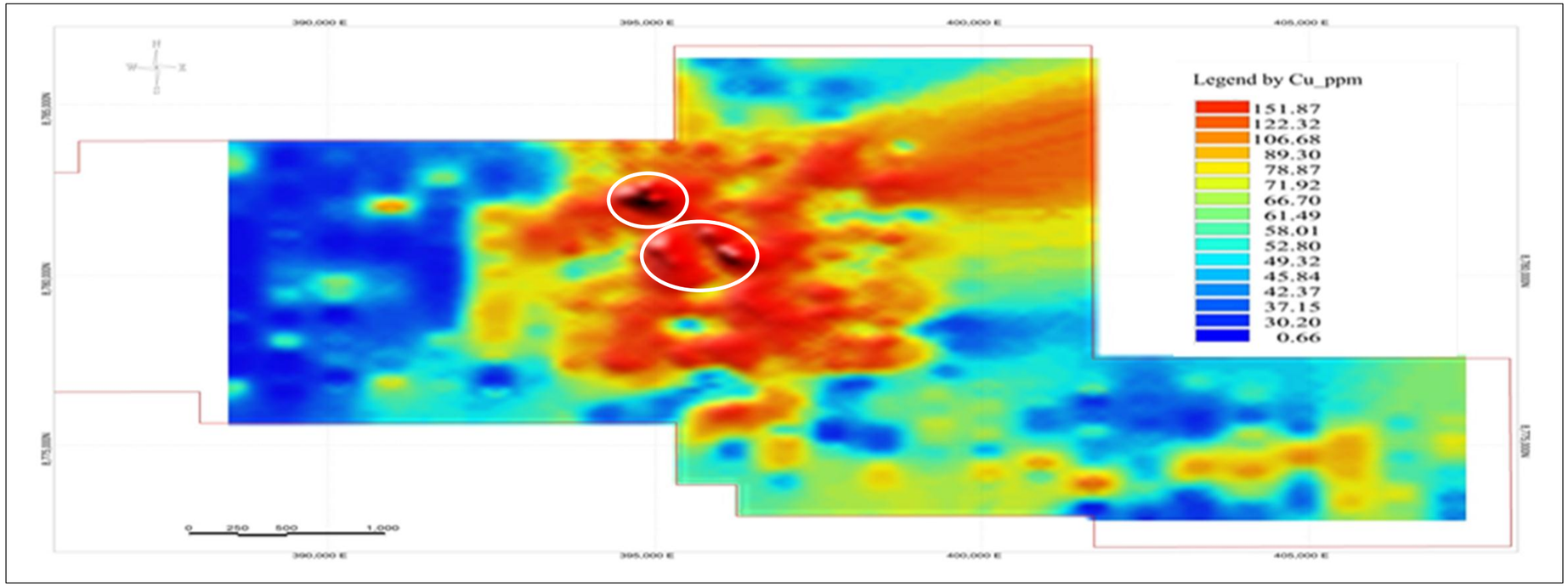


Figure 40: Illustration of a gridded map of Cu_ppm assays from central part of PR851 area showing zones of high anomalies. Note peaks in Cu_ppm anomalies circled in white defined by the author of the present thesis.

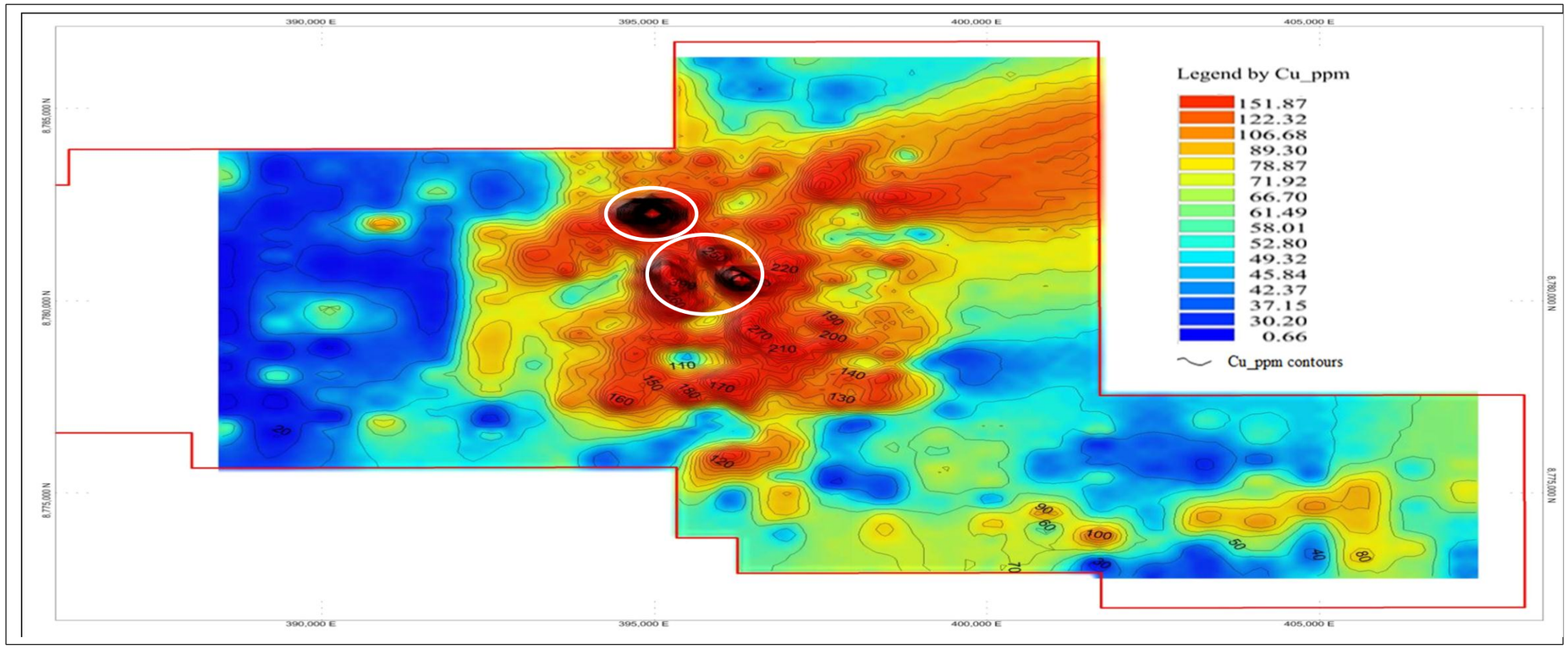


Figure 41: Illustration of a contours map of Cu_ppm assays from central part of PR851 area showing zones of high anomalies. Note peaks in Cu_ppm anomalies circled in white defined by the author of the present thesis.

## CHAPTER 6: KIBAMBA Cu-Co DEPOSIT

### 6.1. Provision of data

The prospect area was investigated by soil geochemical, airborne magnetics and radiometrics surveys, geological mapping techniques and consequently explored by a combined reverse circulation and core diamond drilling. Targets in the area were generated with considerations to all available different datasets although soil assay results were prioritized in places where other exploration methods were not implemented. However among numerous targets identified in the area only few of them (Target 1 and target 2, Figure 39) have been following up and likely a good ore resource known as Kibamba Cu-Co deposit has been successfully identified. The following paragraphs will outline provision of data from the investigated targets which led to the copper and cobalt resource estimates.

#### 6.1.1. Targets -1 and -2

Locally called RSF-target, target-1 was drilled at 100m line spacing over a selected zone of maximum geochemical anomalies to the north limb of the Kibamba anticline where drilling identified and allowed delineation of copper and cobalt resource. Meanwhile the south limb of the same Kibamba anticline had very limited drilling and therefore was not taken into account in the resource estimation done successicely by Digital Mining Services from Harare - Zimbabwe and CoMiSa Sprl geologists.

A total of 11,000m of reverse circulation drilling and slightly over 5,000m of diamond cores have been collected, and more than half of these samples were assayed for total copper and total cobalt. All samples which tested >0.25% TCu or >0.1% TCo have been assayed for acid soluble copper and acide soluble cobalt. Tables 8 and 9 summarize different drilling programs; sample assays numbers and drill holes results from RSF- and Subo - targets respectively accountable for the resource estimation of Cu-Co orebodies. It should be observed that nearly twice as much reverse circulation drilling has been undertaken when comparing to diamond drilling (Table 8). Drillhole data (collars, surveys, geology, assays, orezone_Cu strings, orezone_Co strings and styles - tables required by Surpac for the graphical colour coding) was verified and later imported from an Excel preadsheet format into Surpac database.

Target-2 also known as Subo-target was accounted for three reverse circulation and two diamond boreholes making a total of 300m and 443.70m respectively drilled 50m along northeast-southwest oriented lines, 100m apart and perpendicularly to the strike.

Table 8: Summary of both reverse circulation and diamond drilling (Source: Hanssen, M. G., 2008 unpubl.)

| Hole Type | Year Drilled | No. of holes | Total drilling | Assays Received |
|---|---|---|---|---|
| Diamond Holes | 2005 | 9 | 1,999 | 1,733 |
| Reverse Circulation | 2005 | 28 | 2,696 | 2,660 |
| Diamond Holes | 2006 | 6 | 1,478 | 1,308 |
| Reverse Circulation | 2006 | 42 | 4,196 | 4,113 |
| Diamond Holes | 2007 | 5 | 1,670 | - |
| Reverse Circulation | 2007 | 10 | 1,243 | - |
| Reverse Circulation | 2008 | 19 | 3,016 | - |
| *Total Diamond Holes* | | *20* | *5,148* | *3,041* |
| *Total Reverse Circulation* | | *99* | *11,151* | *6,773* |
| Grand Total | | 119 | 16,299 | 9,814 |

Table 9: Drill holes results taken into account in the resource estimates of Cu-Co orebodies in PR851 area. (Source: http://www.first-quantum.com/Media-Centre/Press-Releases/Press-Release-Details/2006/First-Quantum-Minerals-Announces-New-Discovery-at-RSF- Prospect-Democratic-Republic-of-Congo/default.aspx).

| **Drill Intersections greater than 0.3%TCu** | | | | | | | | |
|---|---|---|---|---|---|---|---|---|
| Hole | Hole Depth (metres) | From (metres) | To (metres) | Interval (metres) | Total Copper (%) | Acid Soluble Copper (%) | Total Cobalt (%) | Acid Soluble Cobalt (%) |
| RSF01 | 100 | 2 | 82 | 80 | 2.20 | 1.98 | 0.25 | 0.13 |
| RSF02 | 74 | 38 | 68 | 30 | 0.73 | 0.62 | 0.04 | 0.03 |
| RSF03 | 89 | 9 | 84 | 75 | 1.12 | 1.05 | 0.03 | 0.02 |
| RSF04 | 91 | 0 | 72 | 72 | 1.20 | 1.10 | 0.07 | 0.05 |
| RSF05 | 100 | 8 | 36 | 28 | 0.75 | 0.70 | 0.12 | 0.10 |
| RSF05 | 100 | 55 | 78 | 23 | 0.78 | 0.71 | 0.03 | 0.02 |
| RSF05 | 100 | 93 | 100 | 7 | 0.60 | 0.40 | 0.11 | 0.05 |
| RSF06 | 98 | 41 | 63 | 22 | 0.93 | 0.68 | 0.24 | 0.17 |
| RSF06 | 98 | 72 | 87 | 15 | 0.55 | 0.37 | 0.07 | 0.02 |
| RSF07 | 100 | No significant intersections | | | | | | |
| RSF08 | 100 | No significant intersections | | | | | | |
| RSF09 | 100 | No significant intersections | | | | | | |
| RSF11 | 100 | 21 | 42 | 21 | 0.40 | 0.28 | 0.16 | 0.15 |
| RSF12 | 100 | No significant intersections | | | | | | |
| RSF13 | 100 | 25 | 100 | 75 | 0.44 | 0.27 | 0.05 | 0.03 |
| RSF14 | 100 | 39 | 74 | 35 | 0.61 | 0.32 | 0.08 | 0.06 |
| RSF15 | 100 | 12 | 66 | 54 | 0.90 | 0.67 | 0.14 | 0.10 |
| RSF16 | 100 | 18 | 100 | 82 | 1.88 | 1.65 | 0.12 | 0.05 |
| RFS17 | 100 | 23 | 64 | 41 | 0.89 | 0.49 | 0.18 | 0.10 |
| RFS18 | 100 | No significant intersections | | | | | | |
| RSF19 | 100 | No significant intersections | | | | | | |
| RSF20 | 96 | 27 | 58 | 31 | 0.41 | 0.35 | 0.07 | 0.07 |
| RSF21 | 100 | No significant intersections | | | | | | |
| RSF22 | 100 | No significant intersections | | | | | | |
| RSF23 | 100 | No significant intersections | | | | | | |
| RSF24 | 100 | 23 | 52 | 29 | 0.41 | 0.11 | 0.03 | 0.02 |
| PTRSF | 82 | 18 | 31 | 13 | 0.41 | 0.09 | 0.31 | 0.15 |
| SU01 | 100 | 78 | 95 | 17 | 0.67 | 0.31 | 0.08 | 0.04 |
| SU02 | 100 | 26 | 100 | 74 | 0.68 | 0.47 | 0.02 | 0.01 |
| SU03 | 100 | 28 | 46 | 18 | 0.49 | 0.11 | 0.05 | 0.02 |

The following Figure 42 shows drillhole layout in relation to the orebody and geochemistry within RSF-Target.

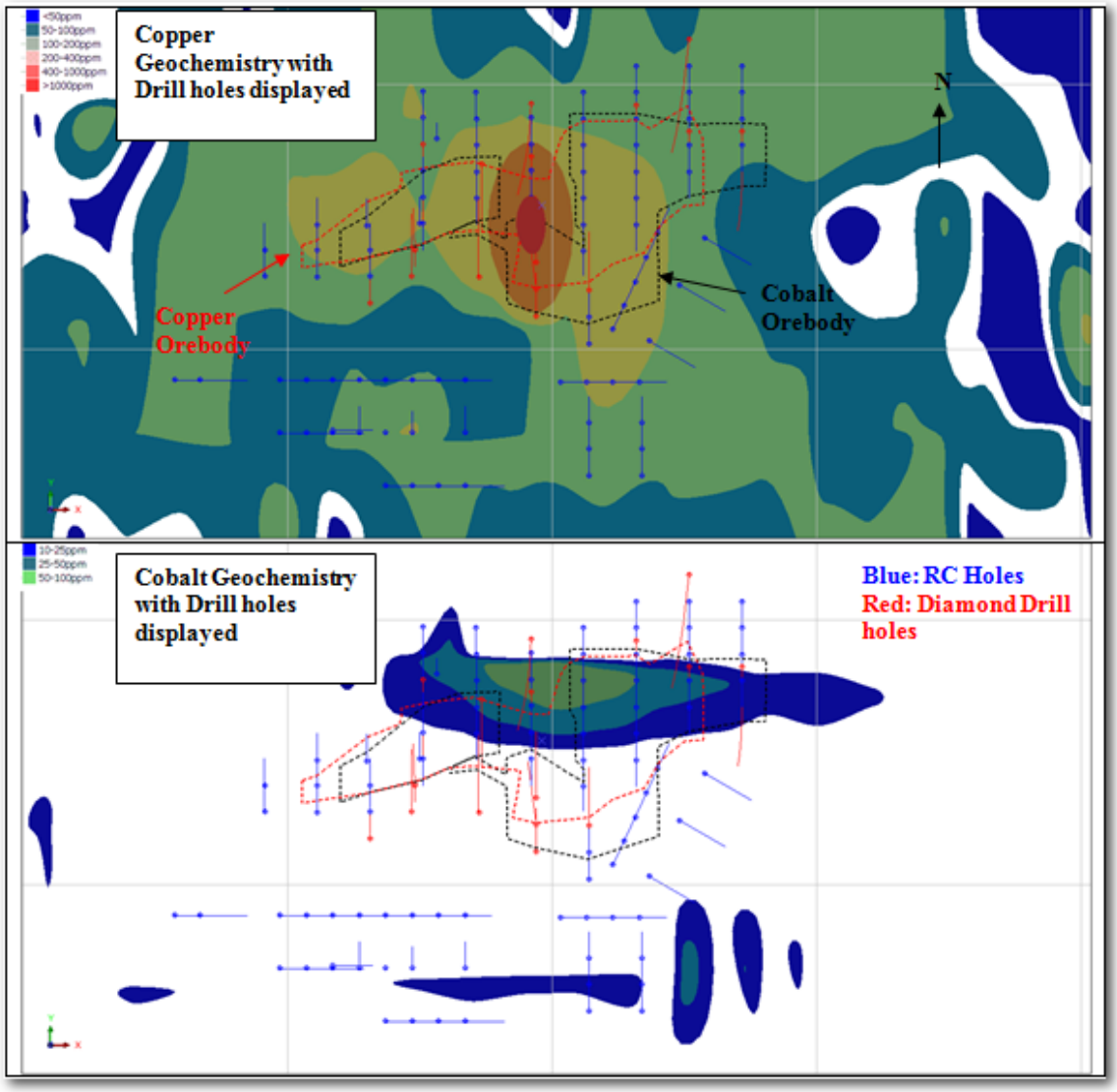


Figure 42: Drillhole Layout in relation to the Cu-Co orebody and soil geochemistry in plan view (Hanssen, 2008 Unpubl.)

### 6.1.2. Target-1 Geology model

Drill section lines displayed in Figure 43 have been used to interpret the target-1 geology and orebody. The section lines are running north-south considered to be perpendicular to the strike and 100m apart from each other.

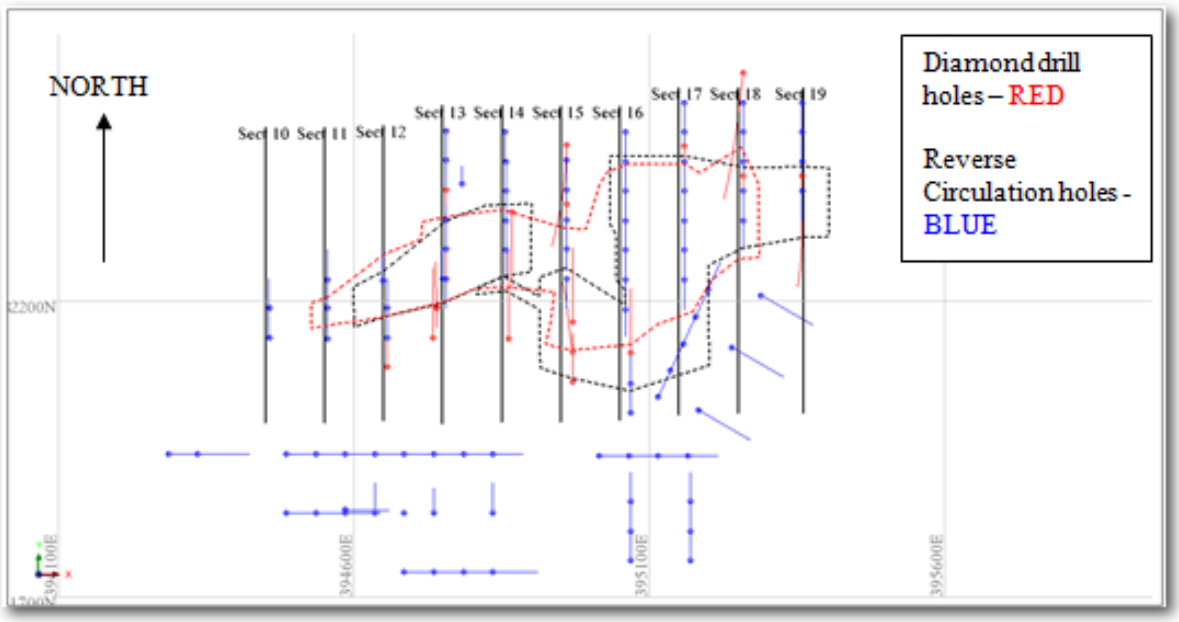


Figure 43: Illustration of section lines for geology and orebody interpretation. Note dotted red line shows Cu orebody boundary and dotted black line Co boundary (Source: Hanssen, 2008 unpubl. in CoMiSa Sprl, 2008 Unpubl.)

The Roches Argilo-Talqueuses (R.A.T. breccia) in PR851 area located to the south of target-1 and the Mwashya units towards the north characterized the main stratigraphic units (Figure 44). The Mines Subgroup units hosting Cu-Co mineralization are situated between the Mwashya and the Roches Argilo-Talqueuses (Figure 44). Here in target-1, the Grand Conglomerat is in contact with the Mines Subgroup due to a thrust structure between the mineralized Mines and Mwashya Subgroup units. The Dipeta shales are observed overlying the Mines Subgroup to the far East. By using interpreted sections the Mwashya, R.A.T. and Dipeta units have been drawn and linked to form 3D models as illustrated In Figure 44.

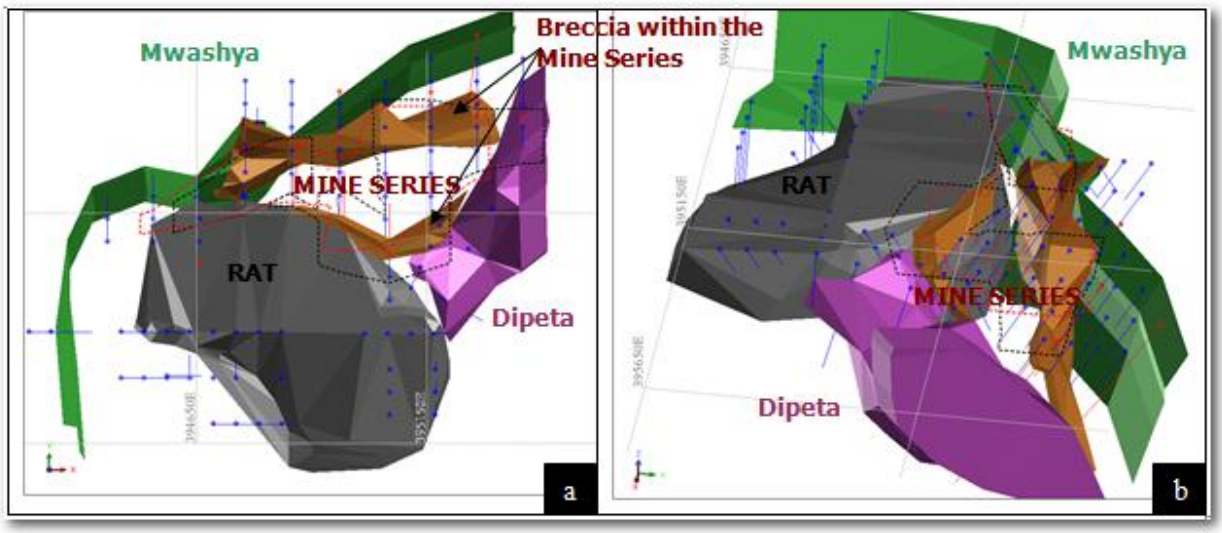


Figure 44: Target-1 geological units models: (a) Plan view (b) view from the southeast (Modified after Hanssen, 2008 Unpubl. in CoMiSa Sprl, 2008 Unpubl.)

### 6.1.3. Target-1 Orebody model

Copper mineralization appears to be closely related to the breccia cross-cutting the Mines Subgroup sequences and wholly located in the Mines Subgroup rock packages (Figure 45a). Generally copper mineralization is found towards the south of this major breccia. But the fact that the northern breccia zone plunges down towards the east (as seen on Section 16 of Figure 43) and copper mineralization is located on the northern side of the breccia, this is suggested to be a 'Calcaire a Minerais Noirs' (CMN) mineralization and associated with the primary lithologies. Sometimes, copper mineralization is considered to be a result of supergene enrichment and seems to be cross-cutting numerous lithologies of the Mines Subgroup. The highly folded Mines Subgroup units were not well defined due to the 100m line spacing drilling. Nevertheless there is a distinctive thickening of the orebody on the eastern side of section line 15 (Figure 43) which is also reflected in the cobalt orebody as a break into mineralization. Geophysical survey (first vertical derivative, contoured on a very low level) mapped this break which suggests evidence of cross faulting (Figure 46).

At the other hand, cobalt mineralization is also a supergene feature closely in association with the lithologies and cross-cutting the entire Sequence of the Mines Subgroup. The cobalt zone in target-1 is divided into two zones (Figure 45b) with a gap in the mineralization around section 15 as seen on Figure 43.

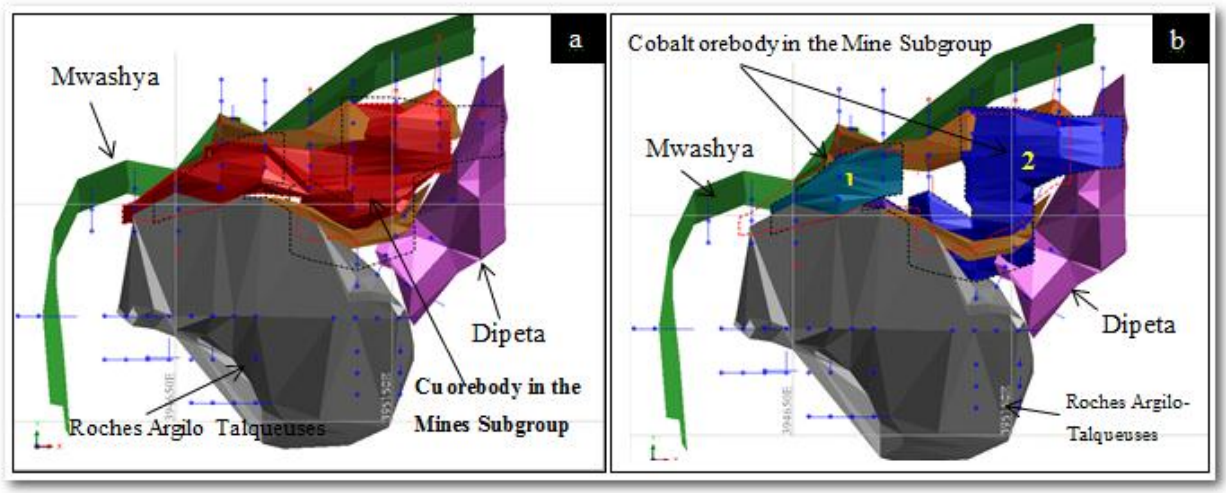


Figure 45: (a) Illustration of copper orebody; (b) Illustration of cobalt orebody. Note the gap between cobalt orebodies 1 and 2 (Modified after Hanssen, 2008 Unpubl. in CoMiSa Sprl, 2008 Unpubl.)

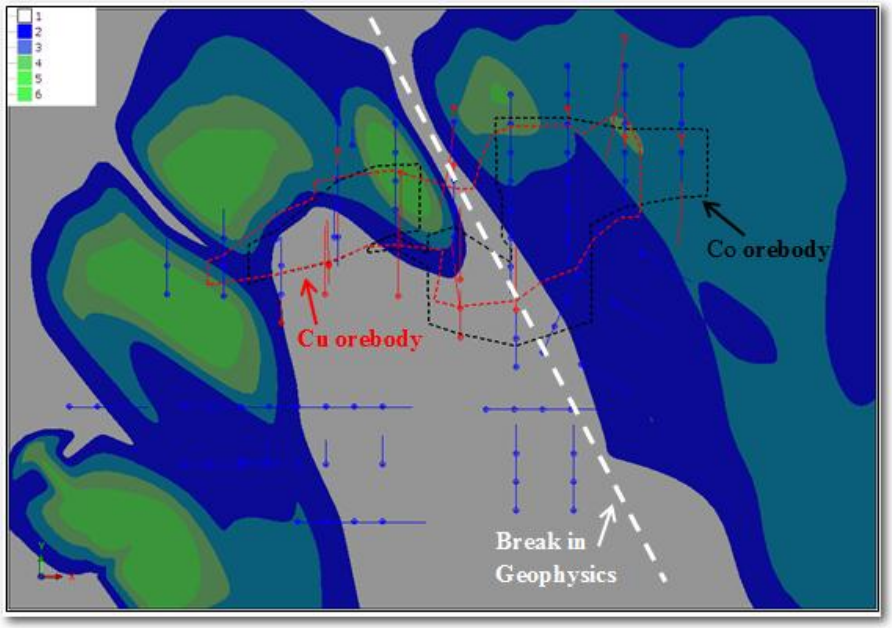


Figure 46: Interpreted geophysical map (First Vertical Derivative contoured at 1 and Cu-Co orebodies positions) shows a break suggesting a fault (Modified after CoMiSa Sprl, 2008 Unpubl.)

The block model was created to encompass the Kibamba orebody in PR851 area. Block sizes equates to half the line spacing. Preferably it has been better to get a hole passing through 80% of the blocks. A fairly standard bench height of 5m has been used. And for a better volume estimation of the modeled orebody, the blocks have been sub-blocked to half the size. Therefore the block model was constructed with cubic blocks of 50x50x5m with block sizes equate to half the line spacing. Furthermore, the blocks were sub-blocked down to 25x25x2.5m (Note that partial blocking has not been used). The following Table 10 gives the block model summary:

Table 10: Block model summary (Including block size)

| | Y | X | Z |
|---|---|---|---|
| Minimum Coordinates | 8781650 | 394400 | 1200 |
| Maximum Coordinates | 8782650 | 395600 | 1600 |
| Block Size | 50 | 50 | 5 |
| Sub Block Size | 25 | 25 | 2.5 |
| | Bearing | Dip | Plunge |
| Rotation | 0 | 0 | 0 |

### 6.2. Resource estimates (Grade and tonnes)

Kibamba Cu-Co deposit (RSF and Subo targets) was estimated using an Inverse Distance Squared ($ID^2$) method by Digital Mining Services of Harare with the input of CoMiSa Sprl geologists. Copper as well as cobalt mineralization are not coincident. So based on the same section lines used to define the geology the orebody outlines have been drawn on the lower cut off grades as follows (Table 11):

Table 11: Cu-Co cut off grades

| | |
|---|---|
| Copper oreboby | 0.5% TCu |
| Cobalt orebody | 0.1% TCo |

From the solid model (Figures 45a and 45b) described above, copper and cobalt volumes are calculated to (Table 12):

Table 12: Calculated volumes of solid models (CoMiSa Sprl, 2008 Unpubl.)

| Orebody | Volume (m3) |
|---|---|
| Copper orebody | 3,521,720 |
| Cobalt orebody | 3,346,712 |
| Where Cu and Co intersect | 1,277,461 |

Afterwards the oxide and sulphide ores were classified as indicated, inferred and then reported separately. The following criteria were used in the classification of the resource:

- Indicated: Each block should contain not less than 12 estimating samples, which have been estimated by using 2 different drill holes considering that a block cannot be estimated by a single drill hole. The average distance of estimating samples should not be more than 100m;
- Inferred: All blocks that do not meet the criteria above, however fall within the modeled orebody as defined in section 6.1.3 of the present work.
- Measured resource was subject to 50m drill spacing intervals for a greater continuity in the resource which should allow a valid variogram to be formed of the mineral continuity. Therefore measured resource is not reported in the present work due to lack of closer drill spacing. However in the present case study only results from the resource estimates (indicated and inferred) of RSF target are reported in Tables 13 and 14 although preliminary resource estimates from Subo target were not made available for the present work since it was firstly stated for company's internal decisions only.

The following specific gravity has been considered in the resource estimates: 1.5 (for oxide material and 2.2 (for sulphide material).

Table 13: Kibamba total drilled copper resource (CoMiSa Sprl, 2008 Unpubl.)

| Category | Oxide | | | Sulphide | | | Total | | |
|---|---|---|---|---|---|---|---|---|---|
| | Tonnes | % TCu | Contained Cu | Tonnes | % TCu | Contained Cu | Tonnes | % TCu | Contained Cu |
| **INDICATED RESOURCE - Total Copper** | | | | | | | | | |
| Cut to 0.25 | 4,851,563 | 1.19 | 57,581 | 570,625 | 1.31 | 7,502 | 5,422,188 | 1.20 | 65,083 |
| 0.5 | 4,814,063 | 1.19 | 57,413 | 570,625 | 1.31 | 7,502 | 5,384,688 | 1.21 | 64,915 |
| 1 | 2,700,000 | 1.50 | 40,500 | 515,625 | 1.36 | 7,013 | 3,215,625 | 1.48 | 47,513 |
| | | % AsCu | | | % AsCu | | | % AsCu | |
| **INDICATED RESOURCE - Acid Soluble Copper** | | | | | | | | | |
| Cut to 0.25 | 2,943,751 | 0.88 | 26,011 | | | - | 2,943,751 | 0.88 | 26,011 |
| 0.5 | 2,423,438 | 0.99 | 23,930 | | | - | 2,423,438 | 0.99 | 23,930 |
| 1 | 731,250 | 1.56 | 11,408 | | | - | 731,250 | 1.56 | 11,408 |
| | | % TCu | | | % TCu | | | % TCu | |
| **INFERRED RESOURCE - Total Copper** | | | | | | | | | |
| Cut to 0.25 | 14,063 | 0.85 | 120 | 68,750 | 1.63 | 1,121 | 82,813 | 1.50 | 1,240 |
| 0.5 | 14,063 | 0.85 | 120 | 68,750 | 1.63 | 1,121 | 82,813 | 1.50 | 1,240 |
| 1 | | | | 68,750 | 1.63 | 1,121 | 68,750 | 1.63 | 1,121 |
| | | % TCu | | | % TCu | | | % TCu | |
| **TOTAL RESOURCE - Total Copper** | | | | | | | | | |
| Cut to 0.25 | 4,865,626 | 1.19 | 57,701 | 639,375 | 1.31 | 8,623 | 5,505,001 | 1.20 | 66,323 |
| 0.5 | 4,828,126 | 1.19 | 57,532 | 639,375 | 1.31 | 8,623 | 5,467,501 | 1.21 | 66,155 |
| 1 | 2,700,000 | 1.50 | 40,500 | 584,375 | 1.36 | 8,133 | 3,284,375 | 1.48 | 48,633 |

Table 14: Kibamba total drilled cobalt resource after (CoMiSa Sprl, 2008 Unpubl.)

| Category | Oxide | | | Sulphide | | | Total | | |
|---|---|---|---|---|---|---|---|---|---|
| | Tonnes | % TCo | Contained Co | Tonnes | % TCo | Contained Co | Tonnes | % TCo | Contained Co |
| **INDICATED RESOURCE - Total Cobalt** | | | | | | | | | |
| Cut to 0.1 | 4,917,188 | 0.19 | 9,502 | 130,625 | 0.26 | 340 | 5,047,813 | 0.19 | 9,842 |
| 0.25 | 829,688 | 0.36 | 2,962 | 55,000 | 0.33 | 182 | 884,688 | 0.36 | 3,143 |
| 0.5 | 70,313 | 0.54 | 380 | | | - | 70,313 | 0.54 | 380 |
| | | % AsCo | | | % AsCo | | | % AsCo | |
| **INDICATED RESOURCE - Acid Soluble Cobalt** | | | | | | | | | |
| Cut to 0.1 | 1,739,063 | 0.20 | 3,505 | | | - | 1,739,063 | 0.20 | 3,505 |
| 0.25 | 351,563 | 0.41 | 1,424 | | | - | 351,563 | 0.41 | 1,424 |
| 0.5 | 51,563 | 0.90 | 464 | | | - | 51,563 | 0.90 | 464 |
| | | % TCo | | | % TCo | | | % TCo | |
| **INFERRED RESOURCE - Total Cobalt** | | | | | | | | | |
| Cut to 0.1 | 34,375 | 0.25 | 85 | | | | 34,375 | 0.25 | 85 |
| 0.25 | 27,500 | 0.26 | 72 | | | | 27,500 | 0.26 | 72 |
| 0.5 | | | | | | | | | |
| | | % TCo | | | % TCo | | | % TCo | |
| **TOTAL RESOURCE - Total Cobalt** | | | | | | | | | |
| Cut to 0.1 | 4,951,563 | 1.19 | 9,586 | 130,625 | 1.31 | 340 | 5,082,188 | 0.20 | 9,926 |
| 0.25 | 857,188 | 1.19 | 3,033 | 55,000 | 1.31 | 182 | 912,188 | 0.35 | 3,215 |
| 0.5 | 70,313 | 1.50 | 380 | - | 1.36 | - | 70,313 | 0.54 | 380 |

## CHAPTER 7: DISCUSSIONS

### 7.1. Cu-Co mineralization vs. stratigraphy

The Central African Copperbelt is one of the most important stratiform-stratabound Cu-Co bearing and producing regions of the world. Cu-Co mineralization is hosted in Neoproterozoic sediments of the Katangan basin. The formation of Cu-Co stratiform and stratabound types of deposits stands on a number of conditions (Cliff, D. T. et al., 2010) which are basically:

- The metal source rocks,
- Brines,
- Fluid flow and pathways,
- Organic matters,
- Confining beds and containment structures.

Spatial association of sediment-hosted stratiform- stratabound Cu-Co deposits with continental red beds indicates that these kinds of rocks are mandatory for the formation of this type of deposits. Continental red beds are known as first-cycle, immature sediments that have been deposited under oxidizing conditions and their red coloration might have coming from the early diagenetic development of hematite. Copper in red beds may be adsorbed on goethite and hematite (Cliff et al., 2010). Generally the metals source rocks in the Central African Katangan basin and particularly in PR851 area are still so far unclear. Nevertheless, the Roches Argilo-Talqueuses of the Katangan Sequence underlying the Mines Subgroup are believed to be the potential source of copper and hence looked at as red beds.

Evaporites from the Mines Subgroup and pyritic layers have been considered to be source of sulfur to some extent. Other alternative sources of copper in the Katangan basin are basaltic and/or mafic volcanic rocks and which may be far away from the site of ore deposition. Hitzman et al. (2005) demonstrated that brines capable of dissolving and transporting copper in solution could pore fluids developed within the basin (evolved seawater brines, residual bittern brines, brines from evaporate dissolution, aqueous fluids derived from dehydration reactions during diagenesis) or meteoric waters whose high salinities are generated through dissolution of evaporites.

The Katangan basin underwent sub-basin scale fluid flow which caused partial to total evaporite dissolution, brine formation, and upwards cross-stratal brine migration. Brine migration could

have been caused by compaction driven fluid flow (Swenson, et al., 2004) or topographically driven fluid flows (Brown, 2005).

PR851 area basement rocks source of metals considered for the Katangan basin have never been mapped. However the Roches Argilo-Talqueuses considered being potential source of copper has been identified (Figure 25). Cu-Co resources in the study area have been preliminarily defined associated to rocks of the Mines Subgroup. Obviously discoveries of Cu-Co resources located at different stratigraphic levels of the Katangan Sequence should favor the idea that mineral exploration in the study area should target also the entire Katangan Sequence rather than focus on the Mines series only. The Mwashya shale (Figure 47a) associated to iron formation (Figure 47b) known as markers of Lower Mwashya has been localized and discussed as a favorable reductant to precipitate Cu-Co mineralization.

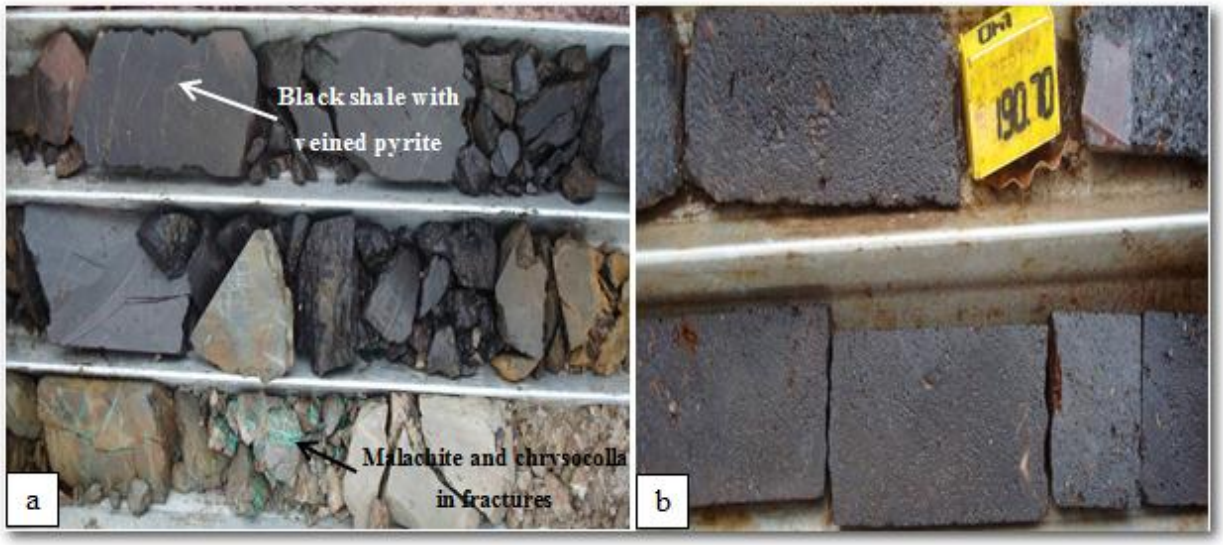


Figure 47: (a) Mwashya shale with supergene copper mineralization in fractures at Subo - target; (b) Iron rich formation marker of Lower Mwashya (Modified after Jigsaw Geoscience PTY LTD (2009, unpubl.)

### 7.2. Cu-Co supergene ore vs. weathering

In PR851 area, oxidized copper and iron minerals include, but not limited to malachite, chrysocolla, azurite and hematite. In the tropical climate which characterizes PR851 area, copper released by weathering reactions is precipitated as sulfide minerals, chalcopyrite and chalcocite, where fluids from weathering encounter a reducing environment (i.e. Black shale) at or below the water table, making thereafter a zone of supergene enrichment. Broadly supergene processes have been observed in the prospect area relatively near the ground surface like at Subo-target. Observations done suggested that meteoric waters circulation oxidized the hypogene sulphide ore minerals and redistributed the metallic ore elements and supergene enrichment occurred at the base of the oxidized side of the mineralized body. Copper as well as cobalt metals that have been leached from the oxidized ore were carried downward by percolating groundwater reacting thereafter with hypogene sulphides at the supergene / hypogene boundary. As a result, secondary sulphides with Cu-Co metals contents higher than those of the primary ore were produced. Therefore Cu-Co mineralization observed in the prospect area (i.e. malachite and chrysocolla seen on Figure 47a) is interpreted to be a result of supergene enrichment. However here at Subo-target no obvious primary sulphide mineralization associated was detected so far.

### 7.3. Cu-Co anomalies in soil vs. landform

Extended from flat-lying topography to rolling hills the study area in particular is also dominated by swamps locally called ‘dambos’. It is very important to bear in mind that zones of flat terrain are mainly dominated by a thick red soil overburden resulting from weathering of dolomite whereas silicified units such as the Roches Siliceuses Cellulaires (R.S.C.) of the Mines Subgroup show ridges in the region.

Precautions were taken to interpret Cu-Co anomalies in soil with regards to the landform within the prospect area. A good geochemical background with integration of different geological datasets of an area is compulsory in the interpretation of transported vs *in-situ* anomalies. Nevertheless it has been observed that Cu-Co anomalies at the bottom of hills are most of the times transported anomalies with a causative body sometimes far away uphill. In-situ anomalies can also reflect a shallow hidden sulfide body and these anomalies were most of the time found in plane area sitting on top of the mineralized body.

The landform also plays a very important role in the formation of regolith other than geochemical dispersion only. Hence taking into account geochemical anomalies in relation to

regolith types remains obvious in the way that it helps to discriminate false transported from true *in- situ* anomalies.

One other possibility applied to analyze Cu-Co anomalies versus topography in soil in PR851 area was by plotting the two variables. It appears that when displaying soil anomalies over a DTM elevation profile, all high Cu-Co anomalies observed on crest of relatively higher altitude were believed to be *in-situ* anomalies whereas those occurring along river beds and swamps were considered to be transported anomalies. However precautions should be carefully taken since anomalies in dambo proved to be in-situ and sitting on top of a causative body have been found.

In PR851 area like one of the copper and cobalt ore-systems in the Congolese Copperbelt, some hills have no trees on them and sometimes grassless. These hills are dominated by rocks of the Mines Subgroup and Cu-Co anomalies in soil could have been too much toxic for most plants except for the so-called 'Copper flower'or Becium Homblei (Figure 48) and other few grasses. Geobotany uses copper flowers as excellent indicators of copper anomalies during exploration of copper in the present case particularly and in the Central African Copperbelt in general. Reedman, J., 1979 argued that Copper-flowers require a soil copper content of 50-1600ppm Cu to thrive, which conditions remain very poisonous to most of plants. This plant is very common in the study area of the Congolese Copperbelt rather than in the Zambian Copperbelt due to the fact that Cu-Co deposits are outcropping and sit at shallow depth in Democratic Republic of Congo whereas in Zambia most of the deposits are found at great depth resulting in a lower copper content of the surface soils.

Figure 48: Illustration of one variety of Copper-flower from the Congolese Copperbelt also seen in PR851 area.

### 7.4. Target generation

Prior to any further follow up with drilling techniques to test Cu-Co anomalies in the PR851 area, a definition of orders of anomalism was prioritized. Soil assays were processed using Discover software combined to MapInfo program for basic statistics and interpretation. It is worth to mention that background value of copper for instance in the study area is very high and therefore it remains uncertain and not precise to set up in mind the definition of anomaly threshold based on the literature comparison only with no consideration of other methods, due to the fact that this cannot be reproducible either in other different geological environment or among exploration geologists. Therefore, spatial analysis and standard deviations methods coupled with literature comparison helped in target prioritization following zones of maximum geochemical anomalies. Although Cu-Co anomalies can be detected in soil profile within the prospect area through soil geochemical anomalies, the use of other exploration tools remain useful in a way that different datasets from different methods can compliment each others. Geophysical surveys for instance (gravity, magnetic and electromagnetic surveys) can be deployed to map the basement topography, bedrock geology and to some extent basin margins.

Sulfide minerals of copper deposits are conductive and may be detected by resistivity and induced polarization surveys providing that the area does not contain carbonaceous shale (Black shale) or high pyrite content.

Remote sensing of colors using Landsat Imagery or remote sensing of ferric oxides using Lansat, ASTER, or AVIRIS imagery can be used to map bleaching of red beds as discussed also by Beitler et al. (2003). By using of specialized softwares such as MapInfo & Discover and/or Arc GIS which are capable of putting together data of different nature it has become easier to select very potential target areas accurately and with more confidence.

## CHAPTER 8: CONCLUSIONS AND RECOMMENDATIONS

Soil geochemical exploration conducted in PR851 area has been very useful in this prospect with well-developed soil profiles. The B soil horizon has been sampled during the soil surveys and this is usually at an average depth of about 35cm in plane areas of the prospect license. Copper is highly mobile, easily detected in secondary dispersion and most of the time developped wider soil geochemical anomalies on surface that the true width of the undercover reef. The present work has considered soil geochemical exploration like one of the applied exploration techniques in the discovery of stratiform-stratabound Kibamba Cu-Co deposit within PR851 area followed up by reverse circulation and diamond drilling. Soil samples collected following local grids and being the most important media in geochemical prospecting have been used at the reconnaissance and detailed stages respectively and later taken to Genalysis laboratories for Cu-Co wet geochemical analyses only rather than multielements assays due to budget constraints. After QAQC test, data management and validation, assay results interpretation was the next step forwards which helped in anomaly threshold definition and later targets prioritization.

After zones of anomalies have been carefully idenfied in the prospect area, a follow up by reverse circulation and diamond drilling was conducted. Most of the interpreted drilling sections over zones of maximum geochemical anomalies showed a good relationship between the surface geochemical anomalies and mineralization which explained that most of the soil geochemical anomalies were in-situ formed.

Logging exercise of rock chips and drill cores respectively has revealed that the stratiform and stratabound Cu-Co mineralization in PR851 area is located in the Mines Subgroup rocks packages foating in Roches Argilo-Talqueuses of the Roan Group.

The preliminary resources presented in this work confirmed that PR851 prospect area has Cu-Co potential for mining. Even then recommendations for more confidence in measured resource need to be defined if drill spacing can be decreased to 50m intervals to allow a greater continuity in the Cu-Co resource. Also, it is worth to mention that individual units of the Mines Subgroup in the area were not yet accuratelly correlated in modeling due to lack of closer drilling.

Soil geochemistry in PR851 area was firstly centred over known Mines Subgroup rock packages of the Roan Group. Although Cu-Co anomalies in the study area were detected within the Mines Subgroup units which are in line with the known deposits of the Congolese Copperbelt but those anomalies occurring at other stratigraphic levels of the Katangan Sequence shouldn’t be ignore

since the entire sequence has demonstrated to be prospective. This opens up possibilities of potential for further discoveries in both Mines Subgroup fragments and at adjacent stratigraphic levels of the Katangan Belt Sequence present in the PR851 area.

Due to very limited budget PR851 area was partially and not deeply investigated. There is a need to further carry out more research work in order to try and understand for instance the source of hypogene mineralization in the area and follow up on other targets yet to be properly defined and investigated.

Subject to budget availability, multi-element analysis of soil samples from PR851 area should be a very good option which will allow detection of more elements, their respective anomalies and also copper pathfinders and scavengers. Emphasis should be put on nickel analysis with respect to the recent nickel mineralization discovered in Menda, a ground adjacent to PR851 area towards the north-west.

It is also recommended that surface mapping of the dolomitic shales hosted in breccias be undertaken to see if a similar Cu-Co high grade supergene concentration can be determined therein.

Finally soil geochemical exploration tool has proven to be very effective for shallow deep Cu-Co bodies and particularly in PR851 area.

**REFERENCES**


Acosta, C. J., Ball, S., Berger, M., Lowe, J., Hitzman, M. W., Lauderdale, J. and Twigg, H., 2014 (unpubl.): Geol 515-Menda Central. Department of Geology and Geological Engineering, Colorado School of Mines, Golden, Co.80401 USA and ENRC management (PTY)LTD., 54 Melville Road, Illovo, Johannesburg, RSA. CSM-ENRC 28/2/2014, p.1-29.

Africo, 2013: Kalukundi Copper – Cobalt Project, Democratic Republic of Congo. NI 43-101 Technical Report on Updated Mineral Resource Estimate. Project No.: 172100, May 2013-Page 7-5, p.238.

Armstrong, R., Master, S. and Robb, L., 2005: Geochronology of the Nchanga granite and constraints on the maximum age of the Katangan Supergroup, Zambian Copperbelt. *Journal of African Earth Sciences,* 42(1), 32-40.

Batumike, J. M., 2004 (unpubl.): Geochemistry and Petrography of the Nguba and Kundelungu Groups, Neoproterozoic Katangan Supergroup, Southeast Democratic Republic of the Congo: Tectonic setting, Paleoweathering condition and sediment provenance, Department of Geoscience, Shimane University, Japan. p.1-119.

Batumike, M. J., Kampunzu, A. B. and Cailteux, J. L., 2007: Lithostratigraphy, basin development, base metal deposits, and regional correlations of the Neoproterozoic Nguba and Kundelungu rock successions, Central African Copperbelt. Gondwana Research, 11(3), 432-447.

Beitler, Brenda, Chan, J.A., and Parry, W.T., 2003: Bleaching of Jurassic Navajo Sandstone on Colorado Plateau Laramide highs - Evidence of exhumed hydrocarbon super-giants: Geology, v. 31, p. 1041–1044.

Bernau, R., 2007: The Geology and Geochemistry of the Lumwana basement hosted Copper-Cobalt (Uranium) Deposits, North Western Zambia. University of Southampton, PhD thesis, p.1-198.

Boyle, R.W., Brown, A.C., Jefferson, C.W., Jowett, E.C., and Kirkham, R.V., eds., 1989: Sediment-hosted stratiform copper deposits: Geological Association of Canada Special Paper 36, 710p.

Broughton, D and Rogers, T., 2010: Discovery of the Kamoa copper deposit, Central Africa Copperbelt, D.R. of Congo. Society of Economic Geologists, Special Publication, 15, v.1, p. 287-298.

Brown, A.C., 2005: Refinements for footwall red bed diagenesis in the sediment-hosted stratiform copper deposits model: Economic Geology, v. 100, no. 4, p. 765–771.

Buffard, R., 1988: Un Rift Intracontinental du Precambrien Superieur: Le Shaba meridional (Zaire). Doctorate Thesis, University of Maine, France, 316p.

Cadastre Minier, 2010: Permis de Recherche, CAMI-31/07/2010 (*http://www.congomines.org/map)*

Cahen, L., 1954: La geologie du Congo belge. Vaillant H. Carmanne, Liege, 577p.

Cailteux, J. L., 1994: Lithostratigraphy of the Neoproterozoic Shaba-type (Zaire) Roan Supergroup and metallogenesis of associated stratiform mineralization. In: Kampunzu, A. B., Lubala, R. T. (Eds.): Neoproterozoic Belts of Zambia, Zaire and Namibia. Journal of African Earth Sciences, 19, 279-301.

Cailteux, J., Binda, P. L., Katekesha, W. M., Kampunzu, A. B., Intiomale, M. M., Kapenda, D., Kaunda, C., Ngongo, K., Tshiauka, T. and Wendorff, M., 1994: Lithostratigraphical correlation of the Neoproterozoic Roan Supergroup from Shaba (Zaire) and Zambia, in the Central African Copper – Cobalt Metallogenic Province. In: Kampunzu, A. B., and Lubala, R. T. (Eds.): Neoproterozoic Belts of Zambia, Zaire and Namibia. Journal of African Earth Sciences 19 (4), 265 – 278.

Cailteux, J. L. H., 2003: Proterozoic sediment-hosted base metal deposits of Western Gondwana, Abstract volume of the conference and field guidebook, 3rd IGCP-450 meeting and field workshop, Lubumbashi, D.R. of Congo, 223pp.

Cailteux, J. L. H., Kampunzu, A. B., Lerouge, C., Kaputo, A. K., and Milesi, J. P., 2005: Genesis of sediment-hosted stratiform copper & cobalt deposits, central African Copperbelt. *Journal ofAfrican Earth Sciences, 42*(1-5), 134-158.

Cailteux, J., Kampunzu, A. and Batumike, M., 2005a: Lithostratigraphic position and petrographic characteristics of RAT (Roches Argilo-Talqueuses) Subgroup, Neoproterozoic Katangan Belt (Congo). Journal of African Earth Sciences, 42 (1), 82-94

Cailteux, J.L.H., Kampunzu, A.B., Lerouge, C., Kaputo, A.K. and Milesi, J. P., 2005b: Genesis of sediment-hosted stratiform copper-cobalt deposits central African Copperbelt. Journal of African Earth Sciences, 42, 134-158.

Cailteux, J.L.H. and Misi, A., 2007: Neoproterozoic sediment-hosted base metal deposits of Western Gondwana. Gondwana Research, 11(3), 344-345.

Chabu, M., 1990: Metamorphism of the Kipushi carbonate hosted Zn-Pb-Cu deposit (Shaba, Zaire). *Regional Metamorphism of Ore Deposits,* pp.27-47.

Cliff D. Taylor, J. Douglas Causey, Paul D. Denning, Jane M. Hammarstrom, Timothy S. Hayes, John D. Horton, Michael J. Kirschbaum, Heather L. Parks, Anna B. Wilson, Niki E. Wintzer, and Michael L. Zientek, 2010: Descriptive Models, Grade-Tonnage Relations, and Databases for the Assessment of Sediment-Hosted Copper Deposits-With Emphasis on Deposits in the Central African Copperbelt, Democratic Republic of the Congo and Zambia. *Scientific Investigations Report 2010-5090-J. U.S. Department of the Interior, U.S. Geological Survey.*

CoMiSa Sprl, 2005 (unpubl.): Internal soil sampling spreadsheets.

CoMiSa Sprl, 2008 (unpubl.): Internal technical reports.

CoMiSa Sprl, 2010 (unpubl.): Interpreted surface geology map of PR851 area

Cornet, J., Franz Eduard, S. and Henri Jean Francois, B., 1908: Geology Congo (Democratic Republic) Katanga; Mines and mineral resources Congo, Annales du Musee du Congo. Geologie, geographie physique, mineralogy et paleontology. Ser. Ii. Katanga. t.1, Bruxelles

Cox, D.P., Lindsey, D.A., Singer, D.P., Moring, B.C., and Diggles, M.F., 2007: Sediment-hosted copper deposits of the world: Deposit models and database: U.S. Geological Survey Open File Report 03-107, 53 pp.

Dale, 2013 (unpubl.): Geochemical exploration techniques, MSc Rhodes Exploration Course, Unpublished.

Daly, M.C., Chakraborty, S.K., Kasolo, P., Musiwa, M., Mumba, P., Naidu, B., Namateba, C., Ngambi, O. & Coward, M.P., 1984: The Lufilian arc and Irumide belt of Zambia: results of a traverse across their intersection. Journal of African Earth Science, 4, 311-318.

De Swardt, A.M.J. & Drysdall, A.R., 1964: Precambrian geology and structure in central Northern Rhodesia. Geological Survey of Northern Rhodesia Memoir 2, 82.

Deborah J. Rumsey, 2011: Statistics for Dummies, 2nd Edition. *ISBN: 978-0-470-91108-2,* p.384.

Delvaux, D. & Barth, A., 2010: African stress pattern from formal inversion of focal mechanism data. Tectonophysics, 482, 105-128.

Dewaele, B., Johnon, S.P. & Pisarevsky, S.A., 2008. Paleoproterozoic to Neoproterozoic growth and evolution of the eastern Congo Craton: Its role in the Rodinia puzzle. *Precambrian Research, 160,* p.127-141.

Drysdal, A. R., Johnson, R. L., Moore, T. A., Thieme, J. C., 1972: Outline of the geology of the Zambia.

El Desouky, H., Muchez, Ph., Boyce, A.J., Schneider, J., Cailteux, J., Dewaele, S. & von Quadt, A, 2010: Genesis of sediment-hosted stratiform copper–cobalt mineralization at Luiswishi and Kamoto, Katanga Copperbelt (Democratic Republic of Congo). Mineralium Deposita, 45(8), 735-763.

Elk, K. and Gelderman, R. H., 1988: Soil sample preparation. p. 2-4. In W.C. Dahnke (ed.) Recommended chemical soil test procedures for the North Central Region. North Dakota Agric. Exp. Stn. Bull. 499.

First Quantum Minerals LTD, 2014 (unpubl.): KPR-JV Soil sampling and pH testing procedure. *Regional exploration*, p.1-11.

Fleischer, V., 1984: Discovery, geology and genesis of copper-cobalt mineralization at Chambishi South-East prospect, Zambia. Precambrian Research, 25 (1), 119-133.

Francois, A., 1973b: L'extremite occidentale de l'Arc Cuprifere Shabien. Etude Geologique. Bureau d'Etudes Geologiques, Gecamines-Exploitation, Likasi, Zaire, 65p.

Francois, A., 1974: Stratigraphies, tectonique et mineralisations dans l'Arc Cuprifere du Shaba (Rep. du Zaire). In: Bartholome (Ed), Gisements Stratiformes et Provinces Cupriferes. Centenaire Societe Geologique de Belgique, Liege, pp.79-101.

Francois, A., 1987: Synthese geologique sur l'Arc Cuprifere du Shaba (Republique du Zaire), Centenaire Societe Belge de Geologie, pp.15-65.

Francois, A., 1993: The tectonic structure of the Katanguien in the area of Kolwezi (Shaba, Zaire): Annales de la Societe Geologique de Belgique, p.87-104.

Francois, A., 1995: Problemes relatifs au Katanguien du Shaba; In: Wendorff, M. and Tack, L. (Eds.), Late Proterozoic Belts in Central Africa. Musee Royal de l'Afrique Centrale, Tervuren, Belgique. Annales des Sciences Geologiques, v. 101, pp. 1-20.

Francois, A., 2006: La partie centrale de l'arc cuprifère du Katanga: étude géologique. Tervuren African Geoscience Collection, 109, 61p.

Frimmel, H.E., Basei, M.S. & Gaucher, C., 2011. Neoproterozoic geodynamic evolution of SW-Gondwana: a southern African perspective. International Journal of Earth Sciences, 100(2-3), 323- 354.

GECO Project, 2009: Stratigraphy overview of the Lufilian Belt

Grantham, G.H., Maboko, M. & Eglington, B.M., 2003. A Review of the Evolution of the Mozambique Belt and Implications for the Amalgamation and Dispersal of Rodinia and Gondwana. Geological Society of London, Special Publications, 206, 401-425.

Gustafson, L.B. and Williams, N., 1981: Sediments-hosted stratiform deposits of copper, lead and zinc: Economic Geology 75th Anniversary Volume, p.139-178.

Haest, M., and Muchez, P., 2011: Stratiform and vein-type deposits in the Pan-African Orogen in central and southern Africa: evidence for multiphase mineralization. *Geologica Belgica*, *14*(1-2), 23-44.

Hanson, R. E., 2003: Proterozoic geochronology and tectonic evolution of Southern Africa: Geological Society of London Special Publication, v. 206, p. 427-463.

Hanssen, M. G., 2008 (unpubl.): Kibamba Copper Prospect Licence 851, Katanga, DRC. *Resource Report, CoMiSa Sprl, September 2008,* p.1-22.

Hitzman, M. W., Kirkham, R., Broughton, D., Thorson, J. and Selley, D., 2005: The sediment-hosted stratiform copper ore system: Economic Geology 100th Anniversary Volume, p.609-642.

Hitzman, M. W., Selley, D., Broughton, D., Bull, S., Croaker, M., Koziy, L., Large, R., McGoldrick, P., MacKay, W. & Pollington, N. and Scott, R., 2005: A new review of the Zambian Copperbelt. *Econ. Geol. 100th Anniv.Volume*

Hitzman, M. W., Broughton, D., Selley, D., Woodhead, J., Wood, D. and Bull, S., 2012: The Central African Copperbelt: Diverse Stratigraphic, Structural, and Temporal Settings in the World's Largest Sedimentary Copper District. Society of Economic Geologists, Inc. Special Publication 16, pp.487-514.

Hobbs, B. E., Means, W. D., Williams, P. F., 1976: An outline of structural Geology. *Wiley, New York,* 571pp.

http://edit.africamuseum.be/geco_website/?page=katanga-geology

http://www.first-quantum.com/Media-Centre/Press-Releases/Press-Release-Details/2006/First-Quantum-Minerals-Announces-New-Discovery-at-RSF- Prospect-Democratic-Republic-of-Congo/default.aspx

Intiomale, M. M. and Oosterbosch, R., 1974: Geologie et geochimie du gisement de Kipushi, Zaire. Centenaire Societe Geologique de Belgique, Gisements stratiformes et Provinces cupriferes, pp. 123-164.

Intiomale, M. M., 1982: Le gisement Zn-Pb-Cu de Kipushi (Shaba, Zaire). Etude Geologique et Metallogenique. Doctoral Thesis, Universite Catholique de Louvain, Belgium, 170p.

Intionmale, M. M., 1983: Etude comparative des gisemsnts de Kipushi, Lombe, Kengere, Brokenhill et Tsumed (unpublished)

Jackson, M.P.A., Warin, O.N., Woad, G.M. and Hudec, M.R., 2003: Neoproterozoic allochthonous salt tectonics during the Lufilian orogeny in the Katangan Copperbelt, central Africa. Bull. Geol. Soc. Am., 115(3), 314-330.

Jigsaw Geoscience PTY LTD, 2009(unpubl.): Prospect Summary and Evaluation. RSF Fact sheet. *FQM Internal Report, p.1-4.*

Jigsaw Geoscience PTY LTD, 2009(unpubl.): Prospect Summary and Evaluation. Subo Fact sheet. *FQM Internal Report*, p.1-4.

Johnson, S. P., Rivers, T., and De Waele, B., 2005: A review of the Mesoproterozoic to early Palaeozoic magmatic and tectonothermal history of South-Central Africa: Implications for Rodinia and Gondwana: Journal of the Geological Society of London, v. 162, p. 433-450.

Kampunzu, A. B., Wendorff, M., Kruger, F. J. and Intionale, M. M., 1998: Pb isotopic ages of sediment-hosted Pb-Zn mineralization in the Neoproterozoic Copperbelt of Zambia and Democratic Republic of Congo (ex-Zaire): Re-evaluation and implications. Chroniques de Recherche Miniere 530, 55-61.

Kampunzu, A. B. and Cailteux, J., 1999: Tectonic Evolution of the Lufilian Arc (Central Africa Copper Belt) During Neoproterozoic Pan African Orogenesis, Gondwana Research, 2(3), p. 401-421.

Kampunzu, A. B., Tembo, F., Matheis, G., Kapenda, D. and Huntsman-Mapila, P., 2000: Geochemestry and tectonic setting of mafic igneous units in the Neoproterozoic Katangan Basin, Central Africa: Implimentation for Rhodinia Break up. Gondwana Research 3, 2, 125-153.

Kampunzu, A. B., Cailteux, J. L. H., Moine, B. and Loris, H. N. B. T., 2005: Geochemical characterisation, provenance, source and depositional environment of 'Roches Argilo-Talqueuses' (R.A.T.) and Mines Subgroups sedimentary rocks in the neoproterozoic Katangan Belt (Congo): Lithostratigraphic implications. Journal of African Earth Sciences, 42(1–5), 119-133.

Katombe, P., 2005 (Unpubl.): Soil sampling in PR851 area (CoMiSa Sprl Internal map).

Kipata, M.L., 2007: Inventaire et analyse au moyen d'un SIG de la tectonique active dans le SE de l'Afrique: Sud-est de la RDC et Nord de la Zambie. MSc. thesis, Faculteit Wetenschappen, K.U.Leuven, Belgium, 106pp.

Kipata, M. L., Delvaux, D., Sebagenzi, M. N., Cailteux, J. L. and Sintubin, M., 2013: Brittle tectonic and stress field evolution in the Pan-African Lufilian Arc and its foreland (Katanga, DRC): From orogenic compression to extensional collapse, transpressional inversion and transition to rifting. Geologica Belgica (2013) 16/1-2: 001-017.

Kokonyangi, J.W., Kampunzu, A.B., Armstrong, R., Yoshida, M., Okudaira, M., Arima, M. and Ngulube, D.A., 2006: The Mesoproterozoic Kibaride belt (Katanga, SE D.R. Congo). Journal of African Earth Sciences, 46(1-2), 1-35.

Laznicka, P., 2010: Giant metallic deposits: Future sources of industrial metals

Lefebvre, J. J. and Paterson, L. E., 1982: Hydrothermal assemblages of aluminian-serpentine, florencite and kyanite in the Zairian Copperbelt. Soc. Geol. Belgique. Annales 105, 51-79

Lepersonne, J., 1974: Carte Geologique du Zaire. Departement des Mines, Republique du Zaire: Tervuren, Belgium, Musee Royal de l'Afrique Centrale.

Levinson, A. A., 1974: Introduction to exploration geochemistry.

Lobo-Guerrero S. A., 2006: Geochemistry, Geochronology and Metallogeny of Pre-Katangan and Post-Katangan Granitoids of the Greater Lufilian Arc, Zambia and Namibia

Lydall, M.I. and Auchterlonie, A., 2011, The Democratic Republic of Congo and Zambia: Growing global 'hotspot' for copper-cobalt mineral investment and exploitation: 6th S. Afr. Base Metals Conf 2011, South African Institute of Mining and Metallurgy, p. 25–37.

Marjoribanks, R. W., 2010: Geological methods in mineral exploration and mining, Springer.

Master, S., Rainaud, C., Armstrong, R., Phillips, D., and Robb, L., 2005: Provenance ages of the Neoproterozoic Katanga supergroup-Central African Copperbelt, with implications for basin evolution. Journal of African Earth Sciences, 42(1), 41-60.

Master, S. and Wendorff, M., 2011: Neoproterozoic glaciogenic diamictites of the Katanga Supergroup, Central Africa. Geological Society, London, Memoirs, 36(1), 173-184.

Mendelson, F., 1961: The geology of the Northern Rhodesian Copperbelt: London, MacDonald, 523p.

Meuris, C., 2001: Synopsis – Scramble for Katanga from http://www.africafederation.net/SCRAMBLE_KATANGA.htm Copyrignt 2001 Christine Meuris, Turbulences WEB Editions.

Miller, R. Mc. G., 1983: The Pan-African Damara orogeny of South West Africa/Namibia. In: Miller, R. Mc. G. (Ed.), Evolution of the Damara orogeny, South West Africa/ Namibia. Special Publication Geological Society of South Africa, v. 11, pp. 431-515.

Muchez, P., Brems, D., Clara, E., de Cleyn, A., Lammens, L., Boyce, A., Sikazwe, O., 2010: Evolution of Cu-Co mineralizing fluids at Nkana Mine, Central African Copperbelt, Zambia. *Journal ofAfrican Earth Sciences, 58*(3), 457-474.

Munter, R. C., 1988: Laboratory factors affecting the extractability of nutrients. p. 8-10. In W. C. Dahnke (ed.) Recommended chemical soil test procedures for the North Central Region. North Dakota Agric. Exp. Stn. Bull. 499.

Oosterbosch, R., 1962. Les mineralizations dans le système de Roan au Katanga. In: Lombard, J., Nicolini, P. (Eds.), Gisements stratiformes de cuivre en Afrique. Association des Services Géologiques Africains, pp. 71–136.

Porada, H., 1989: Pan-African rifting and orogenesis in southern to equatorial Africa and Eastern Brazil. Precambrian Research, 44 (2), 103-136.

Porada, H. and Berhorst, V., 2000. Towards a new understanding of the Neoproterozoic-Early Palaeozoic Lufilian and northern Zambezi Belts in Zambia and the Democratic Republic of Congo. Journal of African Earth Sciences, 30(3), 727-771.

Rainaud, C., Armstrong, R. A., Master, S., and Robb, L. J., 1999: A fertile Palaeoproterozoic magmatic arc beneath the Central African Copperbelt. Mineral Deposits: Processes to Processing, Stanley et al. (eds)

Ramsay, C. R., Ridgeway, J., 1986: A provisional Metamorphic Map of Zambia-Explanatory Notes. *Journal of African Earth Sciences (1983)*, vol. 5, no.5, pp. 441-446.

Reedman, J., 1979: Techniques in Mineral Exploration. *Applied Science Publishers.*

Robert, 1956: Géologie et Géographie du Katanga y compris l'étude des ressources et de la mise en valeur. Hayez, Bruxelles, 620p.

Sanfo, Z., 2006: Multi-Element Geochemistry in Mineral Exploration. *Geochemistry workshop, Ouagadougou.*

Schmandt, D., Broughton, D., Hitzman, M. W., Plink-Bjorklund. P., Edwards, D. and Humphrey, J., 2013: The Kamoa Copper Deposit, Democratic Republic of Congo: Stratigraphy, Diagenetic and Hydrothermal alteration, and Mineralization. *Society of economic Geologists, Inc.*

Schneider, J., Melcher, F. and Brauns, M., 2007: Concordant ages for the giant Kipushi base metal deposit (DR Congo) from direct Rb-Sr and Re-Os dating of sulphides. *Mineralium Deposita, 42(7),* 791-797.

Sebagenzi, M.N. and Kaputo, A.K., 2002. Geophysical evidences of continental break up in the southeast of the Democratic republic of Congo and Zambia (Central Africa). EGU Stephan Mueller Spec. Publ. Series, 2(2002), 193-206.

Selley, D., Broughton, D., Scott, R., Hitzman, M., Bull, S., Large, R., Mc-Goldrick, P., Croaker, M., Pollington, N. and Barra, F., 2005: A new look at the geology of the Zambian Copperbelt. Society of Economic Geologists, Inc. 100$^{th}$ Anniversary Volume, p. 965-1000.

Sillitoe, R. H., 2012: Copper Provinces: Society of Economic Geologists, Special Publication 16, p.1-18.

Sinclair, A., 1991: A fundamental approach to threshold estimation in exploration geochemistry: Probability plots revisited. *Journal of Geochemical Exploration, 41(1),* 1-22.

Soltanpour, P. N., Khan, A., and Lindsay, W. L., 1976: Factors affecting DTPA-extractable Zn, Fe, Mn and Cu from soils. Commun. Soil Sci. Plant Anal. 7:797-821.

Sweeney, M. A. and Binda, P. L., 1994: Some constraints on the formation of the Zambian Copperbelt deposits. *Journal of African Earth Sciences, 19(4), 303-313.*

Swenson, J.B., Person, M., Raffensperger, J.P., Cannon, W.F., Woodruff, L.G., and Berndt, M.E., 2004: A hydrogeologic model of stratiform copper mineralization in the Midcontinent Rift System, northern Michigan, USA: Geofluids, v. 4, p. 1–22.

Thien, S. J., Whitney, D. A. and Karlen, D. L., 1978: Effect of microwave radiation drying on soil chemical and mineralogical analysis. Commun. Soil. Sci. Plant Anal. 9: 231-241.

Tillberg, M., 2012: Ore-forming processes and tectonic control of the sediment-hosted Cu-Co deposits in the Central African Copperbelt. *Dept. of Earth Sciences, University of Gothenburg. C92 Project*

Unrug, R., 1988: Mineralization controls and source of metals in the Lufilian Fold Belt, Shaba-Zaire, Zambia, and Angola. Economic Geology, 83 (6), 1247-1258.

Van Den Brande, P., 1932b: Le Conglomerat de la Serie de Mwashya. Annales du Service des Mines, Comite Special du Katanga, t.III, 72-78.

Wendorff, M., 2000: Genetic aspects of the Katangan megabreccias: Neoproterozoic of Central Africa. Journal of African Earth Sciences, 30(3), 703-715.

Wendorff, M., 2000: Revision of the stratigraphical position of the 'Roches Argilo-Talqueuses (R.A.T.) in the Neoproterozoic Katangan Belt, South Congo. Journal of African Earth Sciences, 30, 717-726.

Wendorff, M., 2005: Evolution of Neoproterozoic–Lower palaeozoic Lufilian Arc, Central Africa: A new model based on syntectonic conglomerates. Journal of the Geological Society, 162(1), 5-8.

Wendorff, M., 2011: Tectonosedimentary expressions of the evolution of the Fungurume foremand basin in the Lufilian Arc, Neoproterozoic-Lower Palaeozoic, Central Africa. Geological Society of London, Special Publications, 357, 69-83.

Wilson, T. J., Grunow, A. M. and Hanson, R. E., 1997: Gondwana assembly: The view from Southern Africa and East Gondwana. Journal of Geodynamics, v. 23, no 263-286.

www.intertek.com | www.genalysis.com.au : Schedule of services and charges 2011. South Africa & Namibia.